



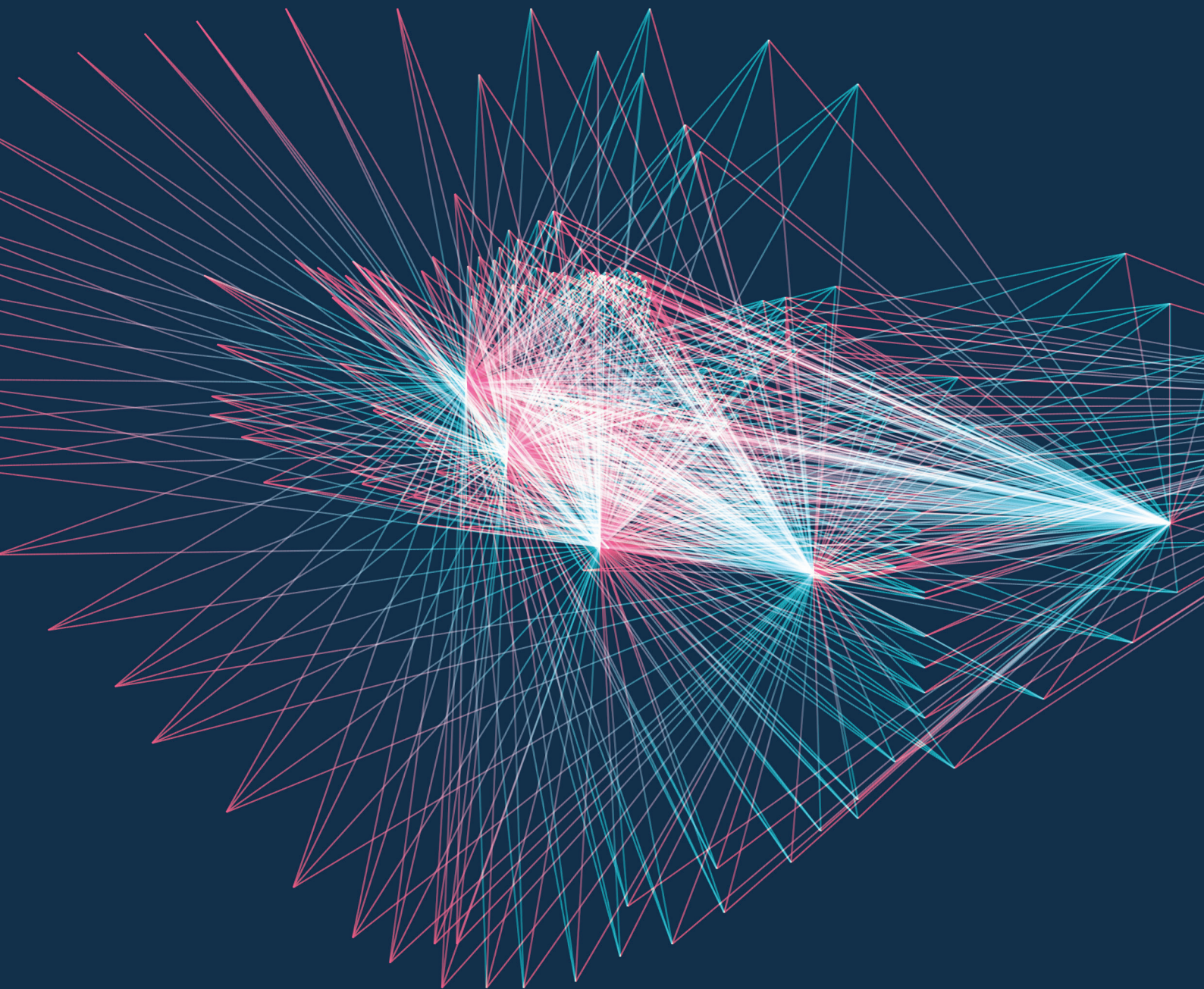
ISSN: xxxx-xxxx (Online)

OSR Oral Sciences Reports

Vol.44 No.3

September-December 2023

www.dent.cmu.ac.th/cmdj



Chiang Mai University's Faculty of Dentistry publishes academic research articles in the newly titled - **Oral Sciences Reports**, which was previously known as *Chiang Mai Dental Journal (CMDJ)*. The journal was originally established for the purposes of publishing academic research articles by the Faculty of Dentistry at Chiang Mai University in 1977. In the current report, editors and experts in their respective fields review articles received from authors prior to being published to ensure that the content of all articles is up-to-date, universal, logical, and in accordance with academic principles so the reader can apply knowledge and cite works in the development of dentistry for the purposes of advancing future research while being beneficial to patients and society.

At present, Oral Sciences Reports openly receives all submissions through an online journal review process system. The new online system also allows reviewers and researchers an ability to read 3 issues each year.

Aim and Scope of the journal

To compile research and content that is up to date and usable to all branches of dentistry and related fields. The articles in Oral Sciences Reports are fundamental research work, including original articles, review articles, case reports/series, short communications, and letters to the editor.

Policy

Accepted articles will be fairly reviewed by the editors and experts with full transparency through the following process.

1. The articles must be correct according to academic principles and not duplicate works that have been previously published.
2. The articles will be considered and reviewed through a non-bias process by concealing the names of authors and related persons in the considered documents while also concealing the names of the experts and reviewers who review the articles (double-blind review).
3. The review process can be tracked online. The article authors can review the status of their article and are able to follow up on the article evaluation through the online process. The duration of each step is closely monitored so that the articles can be published on time.
4. Authors of articles are responsible to review and verify the accuracy of the text, images, tables in the articles before publication.
5. Articles published in Oral Sciences Reports are the copyright of Oral Sciences Reports, which forbids anyone from duplicating published articles for any purpose without explicit permission from Oral Sciences Reports.

Indexing

Thai Journal Citation Index Centre (TCI) Tier 1
Asian Citation Index (ACI)
Google Scholar

Editorial Board

Editor-in-Chief

Anak Iamaroon, Chiang Mai University, Chiang Mai, Thailand
anak.ia@cmu.ac.th

Associate Editors

Awiruth Klaisiri, Thammasat University, Thailand

dentton@tu.ac.th

Papimon Chompu-Inwai, Chiang Mai University, Thailand

papimon.c@cmu.ac.th

Pimduen Rungsiyakull, Chiang Mai University, Thailand

pimduen.rungsiyakull@cmu.ac.th

Pinpinut Wanichsathong, Chiang Mai University, Thailand

pinpinut.w@cmu.ac.th

Sorasun Rungsiyanont, Srinakharinwirot University, Thailand

Sorasun@g.swu.ac.th

Tanida Srisuwan, Chiang Mai University, Thailand

tanida.srisuwan@cmu.ac.th

Wannakamon Panyarak, Chiang Mai University, Thailand

wannakamon.p@cmu.ac.th

Editorial Board

Alex Forrest, The University of Queensland, Australia

alexander.forrest@uq.edu.au

Atiphan Pimkhaokham, Chulalongkorn University, Thailand

atiphan.p@chula.ac.th

Daraporn Sae-Lee, Khon Kaen University, Thailand

darsae@kku.ac.th

Evelina Kratunova, University of Illinois at Chicago, USA

evelina.kratunova@dental.tcd.ie

Han Dong Hun, Seoul National University, Republic of Korea

dhhan73@gmail.com

Keiichi Sasaki, Tohoku University, Japan

keiichi.sasaki.e6@tohoku.ac.jp

Komkham Pattanaporn, Mae Fah Luang University, Thailand

komkham.pat@mfu.ac.th

Korakot Nganvongpanit, Chiang Mai University, Thailand

korakot.n@cmu.ac.th

Mansuang Arksornnukit, Chulalongkorn University, Thailand

mansuang@yahoo.com

Marnisa Sricholpech, Srinakharinwirot University, Thailand

marnisa@g.swu.ac.th

Ming-Lun Allen Hsu, National Yang Ming University, Taiwan

mlhsu@ym.edu.tw

Pasuk Mahakkanukrauh, Chiang Mai University, Thailand

pasuk.m@cmu.ac.th

Piamkamon Vacharotayangul, Harvard School of Dental Medicine, USA

pvacharotayangul@bwh.harvard.edu

Qing Li, The University of Sydney, Australia

qing.li@sydney.edu.au

Rawee Teanpaisan, Prince of Songkhla University, Thailand
rawee.t@psu.ac.th

Siriporn Chattipakorn, Chiang Mai University, Thailand
siriporn.c@cmu.ac.th

Teekayu Plangkoon Jorns, Khon Kaen University, Thailand
teepla@kku.ac.th

Toru Chikui, Kyushu University, Japan
chikui@rad.dent.kyushu-u.ac.jp

Wai Keung Leung, The University of Hong Kong, Hong Kong
ewkleung@hku.hk

Yuniardini Wimardhani, University of Indonesia, Indonesia
yuniardini@ui.ac.id

Types of Submission

Oral Sciences Reports invites the following submissions:

1. Original Articles Original contributions of research reports or unpublished recent academic research to the development and applications in dentistry and related fields. The original article must not exceed 4000 words in length and must contain no more than 10 figures and tables in total.
2. Review Articles Comprehensive reviews of special areas of focus in dentistry and related fields. Articles that contain important collected data from numerous books or journals and from the writer's experience. Information should be described, reviewed, compared, and analyzed. The review article must not exceed 4000 words in length and must contain no more than 10 figures and tables in total.
3. Systematic Reviews Clearly formulated reviews that uses systematic and reproducible methods to identify, select and critically appraise all relevant research, and to collect and analyze data from the studies that are included in the review.
4. Case Reports/Series Original findings that highlight novel technical and/or clinical aspects in dentistry and related fields which include clinical symptoms, diagnosis, patient care, treatment, follow-up, and evaluation. The report must not exceed 2500 words in length and must contain no more than 5 figures.
5. Letters to the Editor Commentaries on published papers in the journal and other relevant matters that must not exceed 1000 words in length
6. Short Communications Original contributions describing new developments of high impact that justify expedited review. The report must not exceed 2000 words in length and must contain no more than 3 figures.

Submission Checklist

Authors should ensure to prepare the following items for submission. Failure to complete the required items may contribute to the delay of publication process. Please check the relevant section in this guideline for more details.

1. Title page Must include title of the article, author names and affiliations. One author has been designated as the corresponding author with contact details (e-mail address and full postal address) (see 'Title page' section for more information and an example)

- | | |
|---------------------------------------|---|
| 2. CRediT Contribution | Author will be asked to provide CRediT Contributions as well as their degree of contribution at the time of the original submission. CRediT Contribution is a high-level classification of the diverse roles performed in the work leading to a published research output in the sciences. Its purpose to provide transparency in contributions to scholarly published work, to enable improved systems of attribution, credit, and accountability. |
| 3. Abstract | Must not exceed 250 words. Relevant keywords (up to five keywords) must be included at the end of the abstract. (see the 'Abstract' section for more details) |
| 4. Main Manuscript | Author details and affiliation must not be included. (see 'Manuscript' section for more details) |
| 5. Figures | Should include relevant captions. (see the 'Figures' section for more details) |
| 6. Tables | Should include titles, description, and footnotes. (see the 'Tables' section for more details) |
| 7. Supplementary data (if applicable) | |

Additional considerations the author should confirm before submission:

1. Manuscript must be 'spell-checked', 'grammar-checked', and 'plagiarism-checked'.
2. All figures, tables, and references mentioned in the text should match the files provided.
3. Permission must be obtained for use of copyrighted material from other sources (including the internet).
4. Authors must provide conflicts of interest statement, even if there is no conflict of interests to declare.

Ethical Guidelines

Authors must acknowledge to the following ethical guidelines for publication and research.

A. Authorship and Author Contributions

The policy of Oral Sciences Reports that only ONE corresponding author is accepted. Where there is any uncertainty regarding authorship, the editor of the journal reserves the right to contact the corresponding author of the study for further information. Authors must acknowledge that the manuscript has been read and approved by all authors and that all authors agree to the submission of the manuscript to the Journal. Authors are required to identify the contributions for which they are responsible. Author will be asked to provide CRediT Contributions as well as their degree of contribution at the time of the original submission. CRediT Contribution is a high-level classification of the diverse roles performed in the work leading to a published research output in the sciences. Its purpose to provide transparency in contributions to scholarly published work, to enable improved systems of attribution, credit, and accountability.

Authors are expected to carefully consider the list and order of authors before submitting their manuscript and provide the definitive list of authors at the time of the original submission. Any addition, deletion, or rearrangement of author names in the authorship list should be made only before the manuscript has been accepted and only if approved by the editor of the journal. To request such a change, the editor must receive the following from the corresponding author:

- (a) The reason for the change in the author list
- (b) Written confirmation (e-mail, letter) from all authors that they agree with the addition, removal, or rearrangement.

In case of addition or removal of authors, these must be confirmed from the author being added or removed. Please be informed that changes of the authorship cannot be made in any circumstances after the manuscript has been accepted.

B. Ethical Considerations

All studies using human or animal subjects should include an explicit statement in the Material and Methods section identifying the review and ethics committee's approval for each study. Experimentation involving human subjects will only be published if such research has been conducted in full accordance with the World Medical Association Declaration of Helsinki (version 2008) and the additional requirements or with ethical principles of the country where the research has been carried out. Manuscripts must be accompanied by a statement that the experiments were undertaken with the understanding and written consent of each subject and according to the above-mentioned principles.

Experimentation involving animal subjects should be carried out in accordance with the guidelines laid down by the National Institute of Health (NIH) in the USA or with the European Communities Council Directive of 24 November 1986 (86/609/EEC) and in accordance with local laws and regulations. Editors reserve the right to reject papers if there is doubt as to whether appropriate procedures have been used.

C. Clinical Trials

All clinical trials must register in any of the following public clinical trials registries:

- Thai Clinical Trials Registry (TCTR)
- NIH Clinical Trials Database
- EU Clinical Trials Register
- ISRCTN Registry

The clinical trial registration number and name of the trial register should be included in Materials and Methods of the manuscript. For epidemiological observational trials, authors of epidemiological human observations studies are required to review and submit a 'strengthening the reporting of observational studies in Epidemiology' (STROBE) checklist and statement. Compliance with this must be detailed in Materials and Methods.

D. Systematic Review

The abstract and main body of the systematic review should be reported using the PRISMA for Abstract and PRISMA guidelines respectively. Authors submitting a systematic review should register the protocol in one of the readily-accessible sources/databases at the time of project inception and not retrospectively (e.g. PROSPERO database, OSF registries). The protocol registration number, name of the database or journal reference should be provided at the submission stage in Materials and Methods. A PRISMA checklist and flow diagram (as a Figure) should also be included in the submission material.

E. Conflicts of Interest

All authors must disclose any financial and personal relationships with other people or organizations that could inappropriately influence (bias) their work. Potential sources of conflict of interest include (but are not limited to) patent or stock ownership, membership of a company board of directors, membership of an advisory board or committee for a company, and consultancy for or receipt of speaker's fees from a company. If there are no interests to declare, please state 'The authors declare no conflict of interest'. Authors must disclose any interests in the section after acknowledgments.

F. Submission Declaration and Verification

Submission of an article implies that the work described has not been published previously (except in the form of an abstract, a published lecture or academic thesis), that it is not under consideration for publication elsewhere, that its publication is approved by all authors and tacitly or explicitly by the responsible authorities where the work was carried out, and that, if accepted, it will not be published elsewhere in the same form, in English or in any other language, including electronically without the written consent of the copyright-holder. The conference proceedings are allowed to be part of the article if the contents do not exceed 70% of the article.

G. Copyright

As an author, you have certain rights to reuse your work. Subscribers may reproduce tables of contents or prepare lists of articles including abstracts for internal circulation within their institutions. Permission of the Publisher is required for resale or distribution outside the institution and for all other derivative works, including compilations and translations. If excerpts from other copyrighted works are included, the author(s) must credit the source(s) in the article.

Manuscript Preparation

All texts in the submitted manuscript are required to be inclusive language throughout that acknowledges diversity, conveys respect to all people, is sensitive to differences, and promotes equal opportunities. Authors should ensure that writing is free from bias, for instance by using 'he or she', 'his/her' instead of 'he' or 'his', and by making use of job titles that are free of stereotyping (for instance by using 'chairperson' instead of 'chairman' and 'flight attendant' instead of 'stewardess'). Articles should make no assumptions about the beliefs or commitments of any reader, should contain nothing which might imply that one individual is superior to another on the grounds of race, sex, religion, culture, or any other characteristic.

A. Title page

The title page will remain separate from the manuscript throughout the peer review process and will not be sent to the reviewers. It should include these following details:

- Title should be concise, information-retrieval, and not exceed 30 words. Please avoid abbreviations and formulae where possible.
- Author names and affiliations. Please clearly indicate the given name(s) and family name(s) of each author are accurately spelled. Present the authors' affiliation addresses (where the actual work was done) below the names. Indicate all affiliations with a lower-case superscript number immediately after the author's name and in front of the appropriate address. Provide the full postal address of each affiliation, including the country name and the e-mail address of each author.
- Corresponding author will handle correspondence at all stages of refereeing and publication, also post-publication. This responsibility includes answering any future queries about Methodology and Materials. Please ensure that the e-mail address and contact details given are kept up to date by the corresponding author.

B. Abstract

Abstract must not exceed 250 words with concise and informative explanations about the article. Authors must prepare an abstract separately from the main manuscript using Microsoft Word processing software (.doc or .docx). Please avoid references and uncommon abbreviations, but if essential, abbreviations must be defined at their first mention in the abstract itself. Abstract structure of the original articles must consist of 'Objectives, Methods, Results, and Conclusions'.

Abstract of other types of submitted articles should be summarized in one paragraph. Up to five keywords relevant to the articles must be provided and arranged in alphabetical order.

C. Manuscript

Oral Sciences Reports adheres to a double-blinded review. The main body of the paper (including the references, figures, tables and any acknowledgements) must not include any identifying information, such as the authors' names. The layout of the manuscript must be as simple as possible with double-spaced, single column format with Sans Serif font and uploaded as an editable Microsoft Word processing file (.doc or .docx). Complex codes or hyphenate options must be avoided, but the emphatic options such as bold face, italics, subscripts, and superscripts, etc. are encouraged.

1. Original article

- *Introduction* should include literature reviews of previous studies, research questions, and the rationale for conducting the study. The Introduction should not be too long and should be easy to read and understand while avoiding a detailed literature survey or a summary of the results.

- *Methods* should provide sufficient details in a logical sequence to allow the work to be reproduced by an independent researcher. Methods that are already published should be summarized and indicated by a reference. If quoting directly from a previously published method, use quotation marks and cite the source. Any modifications to existing methods should also be described.

- *Results* should show the data gained from the study's design in text, tables and/or illustrations, as appropriate, and be clear and concise.

- *Discussion* is criticism, explanation, and defense of the results from the standpoint of the author, and comparison with other peoples' reports. The discussion can include criticism of materials, methods and study results, problems, and difficulties, pointing out the benefits of adoption and providing feedback where appropriate. Discussions should explore the significance of the results of the work, not repeat them. Avoid extensive citations and discussion of published literature.

- *Conclusions* refers to a summary of the study or research results.

- *Acknowledgments*: Please specify contributors to the article other than the authors accredited. Please also include specifications of the source of funding for the study.

Formatting of funding source:

This work was supported by the 1st organization name [grant numbers xxxx]; the 2nd organization name [grant number yyyy]; and the 3rd organization name [grant number zzzz].

If no funding has been provided for the research, please include the following sentence:

This research did not receive any specific grant or funding from funding agencies in the public, commercial, or not-for-profit sectors.

- *References* should be confined to documents relating to the author's article or study. The number should not exceed 80, placed in order and using numbers which are superscripted and put in parentheses, starting with number 1 in the article and in reference document's name. (see 'References' section for more information regarding reference formatting)

2. Review articles should be divided into Introduction, Review and Conclusions. The Introduction section should be focused to place the subject matter in context and to justify the need for the review. The Review section should be divided into logical sub-sections in order to improve readability and enhance understanding. Search strategies must be described, and the use of state-of-the-art evidence-based systematic approaches is expected. The use of tabulated and illustrative material is encouraged. The Conclusion section should reach clear conclusions and/or recommendations on the basis of the evidence presented.

3. Systematic review

- Introduction should be focused to place the subject matter in context and to justify the need for the review.
- Methods should be divided into logical sub-sections in order to improve readability and enhance understanding (e.g. details of protocol registration, literature search process, inclusion/exclusion criteria, data extraction, quality assessment, outcome(s) of interest, data synthesis and statistical analysis, quality of evidence).

- Results should present in structured fashion (e.g. results of the search process, characteristics of the included studies, results of primary meta-analysis, additional analysis, publication bias, quality of evidence).
- Discussion should summarize the results, highlighting completeness and applicability of evidence, quality of evidence, agreements and disagreements with other studies or reviews, strength and limitations, implications for practice and research.
- Conclusion(s) should reach clear conclusions and/or recommendations on the basis of the evidence presented.

4. Case reports/series should be divided into Introduction, Case report, Discussion and Conclusions. They should be well illustrated with clinical images, radiographs and histologic figures and supporting tables where appropriate. However, all illustrations must be of the highest quality.

There are some necessary considerations which should be comprehended and consistent throughout the article:

1. Abbreviations: define abbreviations at their first occurrence in the article: in the abstract and in the main text after it. Please ensure consistency of abbreviations throughout the article.

2. Mathematical expressions: the numbers identifying mathematical expressions should be placed in parentheses after the equation, flush to the right margin; when referring to equations within text, use the following style: Eq. (5), Eqs. (3-10), [see Eq. (4)], etc.

3. Nomenclature: abbreviations and acronyms should be spelled out the first time they are used in the manuscript or spelled out in tables and figures (if necessary). Units of measure and time require no explanation. Dental nomenclature in the manuscript should be complete words, such as maxillary right central incisor. Numbering of teeth from pictures or tables should follow the FDI two-digit system.

4. Units: use the international system of units (SI). If other units are mentioned, please give their equivalent in SI.

5. Product identification: all products mentioned in the text should be identified with the name of the manufacturer, city, state, and country in parentheses after the first mention of the product, for example, The ceramic crown was cemented on dentin surface with resin cement (RelyX™ U200, 3M ESPE, St. Paul, MN, USA)...

D. Figures

Figures should be prepared and submitted separately from the main manuscript. Color artworks are encouraged at no additional charge. Regardless of the application used other than Microsoft Office, when the electronic artwork is finalized, please 'save as' or 'export' or convert the images to **EPS, TIFF, or JPEG format with the minimum resolution of 300 dpi**. Keep the artwork in uniform lettering, sizing, and similar fonts. Please do not submit graphics that are too low in resolution or disproportionately large for the content. Authors must submit each illustration as a separate file.

Please ensure that each illustration has a caption according to their sequence in the text and supply captions separately in editable Microsoft Word processing file (.doc or .docx), not attached to the figure. A caption should comprise a brief title (not on the figure itself) and a description of the illustration. Keep text in the illustrations themselves to a minimum but explain all symbols and abbreviations used.

E. Tables

Please submit tables as editable Microsoft Word processing files (.doc or .docx), not as images, and avoid using vertical rules and shading in table cells. Each table should be placed on a separate page, not next to the relevant text in the article. Number tables consecutively in accordance with their appearance in the text and place any table notes below the table body while ensuring that the data presented in them does not duplicate results described elsewhere in the article.

F. References

Citation in text

Any citations in the text should be placed in order and using numbers which are superscripted and put in parentheses. Please ensure that all citations are also present in the reference list consecutively in accordance with their appearance in the text.

Reference style

All references should be brought together at the end of the paper consecutively in accordance with their appearance in the text and should be in the Vancouver reference format. Please follow these examples of correct reference format below:

1. *Journal article*

1.1. One to six authors

Author(s) – Family name and initials. Title of article. Abbreviated journal title. Publication year;volume (issue);pages.

Example:

Parvez GM. Pharmacological activities of mango (*Mangifera Indica*): A review. *J Pharmacognosy Phytother.* 2016;5(3): 1-7.

Or

Choi YS, Cho IH. An effect of immediate dentin sealing on the shear bond strength of resin cement to porcelain restoration. *J Adv Prosthodont.* 2010;2(2):39-45.

Or

Firmino RT, Ferreira FM, Martins CC, Granville-Garcia AF, Fraiz FC, Paiva SM. Is parental oral health literacy a predictor of children's oral health outcomes? Systematic review of the literature. *Int J Paediatr Dent.* 2018;28(5):459-71.

1.2. More than six authors

Author(s) – Family name and initials of the first six authors, et al. Title of article. Abbreviated journal title. Publication year;volume(issue);pages.

Example:

Vera J, Siqueira Jr JF, Ricucci D, Loghin S, Fernández N, Flores B, et al. One-versus two-visit endodontic treatment of teeth with apical periodontitis: a histobacteriologic study. *J Endod.* 2012;38(8):1040-52.

1.3. Article in press

Authors separated by commas – Family name and initials. Title of article. Abbreviated journal title in italics. Forthcoming - year of expected publication.

Example:

Cho HJ, Shin MS, Song Y, Park SK, Park SM, Kim HD. Severe periodontal disease increases acute myocardial infarction and stroke: a 10-year retrospective follow-up study. *J Dent Res.* Forthcoming 2021.

2. *Books*

2.1. Book with author (s)

Author(s) – Family name and initials (no more than 2 initials with no spaces between initials)– Multiple authors separated by a comma. After the 6th author add - "et al". Title of book. Edition of book if later than 1st ed. Place of publication: Publisher name; Year of publication.

Example:

Sherwood IA. Essentials of operative dentistry. Suffolk: Boydell & Brewer Ltd; 2010.

Or

Abrahams PH, Boon JM, Spratt JD. McMinn's clinical atlas of human anatomy. 6th edition. Amsterdam: Elsevier Health Sciences; 2008.

2.2. Book with no author

Title of book. Edition of book if later than 1st ed. Place of publication: Publisher name; Year of publication.

Note: Do not use anonymous. Please begin a reference with the title of the book if there is no person or organization identified as the author and no editors or translators are given.

Example:

A guide for women with early breast cancer. Sydney: National Breast Cancer; 2003.

2.3. Chapter in a book

Author(s) of chapter - Family name and initials, Title of chapter. In: Editor(s) of book - Family name and initials, editors. Title of book. edition (if not first). Place of publication: Publisher name; Year of publication. p. [page numbers of chapter].

Example:

Rowlands TE, Haine LS. Acute limb ischaemia. In: Donnelly R, London NJM, editors. ABC of arterial and venous disease. 2nd ed. West Sussex: Blackwell Publishing; 2009. p. 123-140.

3. *Thesis/dissertation*

3.1. Thesis in print

Author - family name followed by initials. Thesis title [type of thesis]. Place of publication: Publisher; Year.

Example:

Kay JG. Intracellular cytokine trafficking and phagocytosis in macrophages [dissertation]. St Lucia, Qld: University of Queensland; 2007.

3.2. Thesis retrieved from full text database or internet

Author - family named followed by initials. Thesis title [type of thesis/dissertation on the Internet]. Place of publication: Publisher; Year [cited date – year month day]. Available from: URL

Example:

Pahl KM. Preventing anxiety and promoting social and emotional strength in early childhood: an investigation of risk factors [dissertation on the Internet]. St Lucia, Qld: University of Queensland; 2009 [cited 2017 Nov 22]. Available from: <https://espace.library.uq.edu.au/view/UQ:178027>

4. *Webpage*

4.1. Webpage with author

Author/organization's name. Title of the page [Internet]. Place of publication: Publisher's name; Publication date or year [updated date - year month day; cited date - year month day]. Available from: URL

Example:

American Dental Association. COVID-19 and Oral Health Conditions [Internet]. Chicago: American Dental Association; 2021 Feb 12 [updated 2021 Feb 12; cited 2021 Jun 24]. Available from: <https://www.ada.org/en/press-room/news-releases/2021-archives/february/covid-19-and-oral-health-conditions>

4.2. Webpage with no authors

Title [Internet]. Place of publication (if available): Publisher's name (if available); Publication date or year [updated date (if available); cited date]. Available from: URL

Example:

Dentistry and ADHD [Internet]. 2019 Jan 15 [updated 2019 Jan 15; cited 2020 Apr 8]. Available from: <https://snoozedentistry.net/blog/dentistry-and-adhd/>

4.3. Image on a webpage

Author/organization. Title [image on the Internet]. Place of publication: Publisher's name; Publication date or year [updated date; cited date]. Available from: URL

Note: If the image does not have a title - give the image a meaningful title in square brackets.

Example:

Poticny DJ. An Implant-Supported Denture Offers a Number of Advantages [image on the Internet]. Texas: Office of Dan Poticny; 2018 Nov 21 [updated 2018 Nov 21; cited 2019 Aug 30]. Available from: <https://www.dfwsmiledoc.com/blog/post/an-implant-supported-denture-offers-a-number-of-advantages.html>

5. *Government publications/reports*

5.1. Reports and other government publications

Author(s). Title of report. Place of publication: Publisher; Date of publication – year month (if applicable). Total number of pages (if applicable eg. 24 p.) Report No.: (if applicable)

Example:

Australian Institute of Health and Welfare. Oral health and dental care in Australia: key facts and figures trends 2014. Canberra: AIWH; 2014.

5.2. Government reports available online

Author(s). Title of report. Report No.: (if applicable). [Internet]. Place of publication: Publisher or Institution; Publication date or year [updated date - year month day; cited date - year month day]. Available from: URL

Example:

World Health Organization. WHO mortality database [Internet]. Geneva: World Health Organization; 2019 Dec 31 [updated 2019 Dec 31; cited 2021 Mar 29]. Available from: <https://www.who.int/data/mortality/country-profile>

6. *Tables/Figures/Appendices*

Follow the format of book, journal or website in which you found the table/figure/appendix followed by: table/figure/image/appendix number of original source, Title of table/figure/appendix from original source; p. Page number of table/figure/appendix from original source.

Note: each reference to a different table/figure within the same document requires a separate entry in the Reference list. Please provide permission documents from the original sources.

Example:

Smith J, Lipsitch M, Almond JW. Vaccine production, distribution, access, and uptake. *Lancet* 2011;378(9789):428-438. Table 1, Examples of vaccine classes and associated industrial challenges; p. 429.

7. *Journal abbreviation source*

Journal names should be abbreviated according to the Web of Science - Journal Title Abbreviations.

Peer-review Process

Oral Sciences Reports follows a double anonymized review process. Each manuscript will be assigned to at least three expertises for consideration. The identities of both reviewers and authors are concealed from each other throughout the review to limit reviewer bias. To facilitate this, please ensure that the manuscript keeps anonymity before submission such as affiliation, author's gender, country or city of origin, academic status, or previous publication history. Our peer review process is confidential and identities of reviewers are not released. Letters and technical comments are sent to the authors of the manuscript on which they comment for response or refutation, but otherwise are treated in the same way as other contributions with respect to confidentiality.

Submission Procedures

A manuscript must be submitted electronically on the OSR ScholarOne submission site. When entering the submission page for the first time, you will be asked to create an account with your e-mail and password followed by your personal data.

Our online submission system guides you stepwise through the process of entering your article details and uploading your files. Please follow the submission process carefully. The system converts your article files to a single PDF file used in the peer-review process. Editable Microsoft word processing files are required to typeset your article for final publication. All correspondence, including notification of the Editor's decision and requests for revision, is sent to your registered e-mail.

Contact Us

We are grateful to answer all inquiries. Please visit our official website or contact the administrative office at:

Educational Service, Research Administration and Academic Service Section

Faculty of Dentistry, Chiang Mai University

Suthep Road, Suthep sub-district, Mueang, Chiang Mai, THAILAND 50200

Telephone number: +66(0)53-944429

Website: <https://www.dent.cmu.ac.th/cmdj/>

Email address: cmdj.dent@cmu.ac.th



Editor:

Awiruth Klaisiri,
Thammasat University, Thailand.

Received: July 11, 2022

Revised: August 19, 2022

Accepted: February 2, 2023

Corresponding Author:

Dr. Pornpot Jiangkongkho,
Department of Restorative Dentistry,
Faculty of Dentistry, Naresuan
University, Phitsanulok 65000,
Thailand.
E-mail: Jiangkongkho@hotmail.com

The CAD/CAM Technology and Digital Smile Design for Fabricated Ceramic Veneers

Pimchanok Osotprasit¹, Sasipin Lauvahutanon², Pornpot Jiangkongkho³

¹Lamplaimat Hospital, Thailand.

²Department of Prosthodontics, Faculty of Dentistry, Chulalongkorn University, Thailand.

³Department of Restorative, Faculty of Dentistry, Naresuan University, Thailand.

Abstract

Nowadays, the application of digital technologies and devices are widely used in dentistry. The explanation of the innovative and advanced digital technology for designing and fabricating the provisional restorations transfers to final restorations. Computer-aided design/computer-aided manufacturing (CAD/CAM) in digital dentistry has numerous advantages and greater efficiency and accuracy over the conventional techniques. The digital smile design (DSD) is used for esthetic dentistry especially in case of veneer and can be improved the effectiveness and efficiency of dentist to patient and dentist to technician communication. However, the applications of DSD and CAD/CAM require an understanding of the principal concept and digital technology to create the precise and esthetic outcome of the final restoration.

Keywords: computer-aided design/computer-aided manufacturing, digital smile design, veneer

Introduction

Computer-aided design and computer-aided manufacturing (CAD/CAM) systems are used in dentistry to design and fabricate dental restorations such as inlays, onlays, veneers, crowns, fixed partial dentures, implant abutments and full-mouth reconstruction. CAD/CAM systems typically consist of three main components.⁽¹⁻³⁾ First, digital data collecting from the patient's mouth or data from stone models by the conventional impression of the patient's teeth and surrounding structures which using intraoral scanners to create a digital model. Second, CAD software for designing the virtual restoration on a virtual working cast and calculating the milling parameters needed to fabricate the restoration. Third, computerized milling devices and additive manufacturing systems are used to fabricate the restoration by following the milling parameters that are calculated in the design phase of CAD software to shape the material into the desired restoration. The CAD/CAM systems can be classified into laboratory systems and chairside systems which the chairside CAD/CAM system is further divided into two categories: systems with their own milling units including the scanners and systems with their own only scanners without designing capabilities, therefore, to create a product or design the restoration they need to be connected to an opened lab scanner.^(1,3,4) Additionally, CAD/CAM systems may be classified into opened and closed systems based on data communication. Closed systems provide completely CAD/CAM processes including data gathering, virtual design and manufacture for fabricating the restorations, performed by the same company. All processes are in closed systems, therefore, systems from the various vendors cannot be used interchangeably. Whereas, opened systems are enable the original digital data by CAM devices from several manufacturers and CAD software.^(1,5,6) The laboratory CAD systems always are opened systems as the data must be stored in an STL file (STereoLithography or Standard Tessellation Language). For this reason, the different data formats from many companies that will not be compatible with each other can be sent to an opened laboratory CAM system, which supports the type of STL file from the laboratory CAD system, so the restoration will be fabricated.⁽¹⁾

For fabricating the restoration, there are two primary methods, subtractive (milling and grinding) and additive manufacturing. Milling technology is a type of restoration

fabrications that utilizes subtraction manufacturing from the large solid blocks.⁽¹⁾ The milling manufacturing is categorized into dry and wet milling. Wet milling process uses the milling diamond or carbide cutter that protected by spray of cool liquid against overheating within the milled of the milled material. To prevent heat-related damage, this type of processing is required for all metals and glass ceramic materials.^(1,3) In dry milling process, the blocks or banks of resin material are placed into a computer-controlled milling machine, using rotary cutting tools to remove material from the blocks to create the desired shape. Dry milling process mostly uses for the fabrication of zirconia crowns from zirconium oxide blanks (ZrO_2) or milling resin material blanks such as PMMA (polymethyl methacrylate) banks for temporary crown restoration.⁽⁷⁾

Additive manufacturing is defined by the American Society for Testing and Materials (ASTM) as “the process of joining materials to make objects from 3D (three-dimensional) model data, usually layer upon layer, as opposed to subtractive manufacturing methodologies”.^(1,8) After the 3D model designed by CAD software is completed, it is segmented into multislice images.⁽¹⁾ Typically, in each millimeter of material, there are 5-20 layers in which the machine lays down successive layers of liquid or powder material that are fused to create the final shape.^(1,9) There are several different technologies used in additive manufacturing and the varying specific processes depend on the type of 3D printer. Some technologies are commonly used in additive manufacturing such as Direct Metal Laser Sintering (DMLS), StereoLithography (SLA), Scan, Spin and Selectively Photocuring (3SP), PolyJet, and Direct Light Projection (DLP).^(1,8) Printing a digital 3D model is more accurate than milling and conventional plaster models.⁽¹⁰⁾ Moreover, additive manufacturing facilitates the production of complex geometries with fine details that cannot be reproduced by other methods.⁽¹¹⁾

In dentistry, CAD/CAM was the favorable technique to fabricate fixed restoration especially veneers. Veneers have been used to improve the aesthetic and protection of teeth. One of the most common materials that used to fabricate laminate veneers is ceramic. The translucency of material results in color appearance of natural teeth. Ceramic veneers are used to correct many factors such as tetracycline staining, fluorosis, amelogenesis imperfecta and aging. The others are restoring fractured or worn teeth, abnormal tooth morphology and correction of minor

malposition. However, the patients with parafunctional habits, edge to edge relation, and poor oral hygiene should be concern to the limitation of ceramic veneers.⁽¹²⁻¹⁴⁾ The longevity and survival rate of ceramic veneers were reported for 5 years (98%), 10 years (96%), 15 years (91%) and 20 years (91%).⁽¹⁵⁾ The survival rate of ceramic veneers depends on the remaining enamel and bonding systems. Therefore, the conservative preparation and cementation technique are required to ensure predictable outcome of ceramic veneers.^(16,17)

There are four different designs of teeth preparations.⁽¹²⁻¹⁴⁾ The first, window preparation (Figure 1A); the incisal edge of the tooth is preserved. This technique is favorable in case of slight correction of malposition and non-adjustment position of the incisal edge. Window preparation provides more than one path of insertion. Second, feather preparation (Figure 1B); the incisal edge of the tooth is prepared labio-palatal, but the incisal length is not reduced. This technique is favorable in case of slight correction of malposition and discolored teeth. Feather preparation provides more than one path of insertion. The third, bevel preparation (Figure 1C); the incisal edge of the tooth is prepared labio-palatal and the length of the incisal edge is slightly reduced (0.5-1.0 mm). This technique is favorable in case of correction of malposition, discolored teeth and provided one path of insertion. The last, incisal overlap preparation (Figure 1D); the incisal edge of the tooth is prepared labio-palatal, and the length is reduced (about 2.0 mm), so the veneer is extended to the palatal aspect of the tooth. The incisal overlap preparation technique is favorable in case of correction of malposition, discolored teeth and provided one path of insertion. This preparation created the most stability of restoration. Two millimeters of reduction is enough to create an opalescence effect of the restoration.

CAD/CAM materials for veneers

The conventional technique for fabricated feldspathic ceramic veneer requires a skilled and experienced of dental technician. In addition, feldspathic ceramic veneers are weaker and easily chip or crack more than other materials such as lithium disilicate ceramic and zirconia.^(17,18)

CAD/CAM ceramic materials for manufacturing veneers can be classified into glass-matrix ceramics and resin-matrix ceramics. Resin-matrix ceramics include resin-based composites and polymer infiltrated ceramic

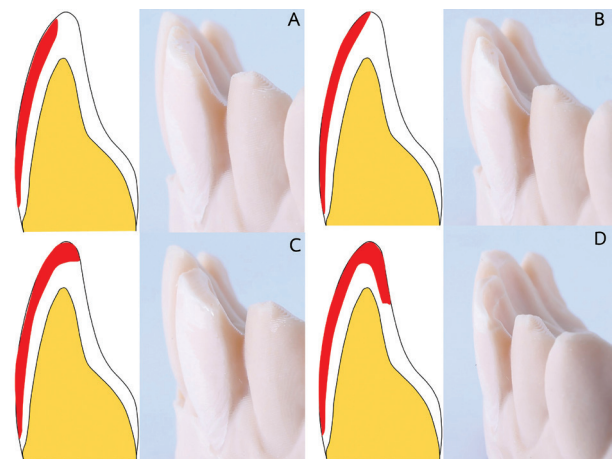


Figure 1: Representative type of preparation. (A) Window preparation. (B) Feather preparation. (C) Bevel preparation. (D) Incisal overlap preparation.

networks (PICNs).⁽¹⁹⁾ Glass-matrix ceramic materials include feldspar ceramics, the first CAD/CAM fine-structure feldspar ceramics (VITABLOCKS[®] Mark II, VITA Zahnfabrik, Bad Säckingen, Baden-Württemberg, Germany) have developed from conventional feldspathic ceramics and are still used in clinical^(19,20), leucite reinforced glass ceramics (IPS Empress[®] CAD, Ivoclar vivadent[®], Schaan, Liechtenstein) are improved from early generations of CAD/CAM blocks containing leucite crystals up to 40% embedded in feldspathic glass-ceramic⁽²¹⁾, lithium disilicate ceramics (IPS e.max[®] CAD, Ivoclar vivadent[®], Schaan, Liechtenstein) the strength was significantly increased with a glass-ceramic by precipitating lithium disilicate crystals⁽¹⁵⁾ and zirconia-reinforced lithium silicate glass-ceramics (VITA SUPRINITY[®] PC, VITA Zahnfabrik, Bad Säckingen, Baden-Württemberg, Germany), Celtra (Celtra Duo, Dentsply Sirona, Bensheim, Hessen, Germany).⁽¹⁹⁻²¹⁾ The success of CAD/CAM ceramic veneers depends on many factors such as the case planning, the ceramics selecting, methods of cementation and preparation of teeth.⁽¹⁵⁾ Moreover, the patient's occlusion and function must be taken into consideration when selecting the material.⁽¹⁵⁻¹⁷⁾

Lithium disilicate glass ceramic is the favorable material for CAD/CAM veneers because of the advantage of their significantly higher strength, which can be more than five times stronger than feldspathic porcelain.^(17,19,20) The disadvantage is these veneers milled out of a single block of material, which limits the variation in achievable color. This can be modified by the external stain.^(22,23)

Another problem is time consumption. One veneer takes thirty minutes for milling while the heat press technique can be achieved more than 6 veneers within 2 hours. Moreover, the CAD/CAM lithium disilicate discs can be used for multiple veneers to reduce costs and time. The alternative technique uses 3D printing of castable resin following the conventional heat press technique. The result is veneers can be as accurate than conventional heat press technique. In addition, using cut-back then hand layering ceramic over the surface to create better esthetics, especially the opalescence effect at an incisal edge area.^(21,23,24)

CAD/CAM procedure for veneers

The digital smile design (DSD) concept aims to help clinicians by improving the esthetic visualization of the patient's concern, giving an understanding of the possible solution therefore educating and motivating them about the benefits of the treatment and increasing the case acceptance.^(17,25) DSD is a digital mode software in CAD systems that helps us to create the new smile design by attaining a simulation and pre-visualization of the ultimate result of the proposed treatment. A design created digitally involves the participation of the patients on the designing process of their self-smile design, leading to customization of smile design as per individual needs and desires that complements with the morpho-psychological characteristics of the patient, relating the patient to an emotional level, increasing their confidence in the process and better acceptance of the anticipated treatment.^(25,26)

The design is accomplished into a complete digital drawing on DSD software on a computer. This can easily be edited to achieve the final design balancing patients' aesthetic and functional requirements.^(25,26) Therefore, the advantages of DSD software include simplifying the smile design, stepping through the gap between conventional and digital workflows especially ensuring that provisional restoration and final restoration serves both the functional and patient esthetic requirement.^(27,28) The DSD can representative the predictably result, accordingly, reduce chairside time in dental clinic.⁽²⁸⁾

DSD technology is carried out by digital equipment already prevailing in current dental practice like a computer with one of the DSD software, a digital SLR camera or even a smart phone. A digital intraoral scanner for digital impression, a 3D printer and CAD/CAM are additional

tools for complete digital 3D workflow. An accurate photographic documentation is essential as complete facial and dental analysis rests on preliminary photographs on which changes and designing is formulated, a video documentation is required for dynamic analysis of teeth, gingiva, lips and face during smiling, laughing and talking in order to integrate facially guided principles to the smile design.^(28,29) The intraoral scanners have become significantly better, faster, and smaller, with more intuitive design software surfaces. This virtual workflow with on-screen designing and computer-assisted production of prototyping, such as milling or the 3D printing, allows for the fabrication of various restorations without any conventional models.^(20,29)

Case report

A female patient aged 31 years old reported to the dental department of Lamplimat Hospital with a chief complaint of esthetic concern. She gave a history of spacing between anterior teeth 11/12 from orthodontics. Her major concern was an unesthetic appearance when smiling from the reverse curve of the left and right upper canine and she desired to close the gap between 11/12 teeth in a manner that resulted in a natural look. The patient had a healthy medical history and no drug allergies. Her oral hygiene was at a good level. The treatment began with a clinical examination, and a series of pre-operative intra and extra-oral photographs were taken. These photographs were used to determine and treatment planning about the smile design, gingiva zeniths, occlusal planes, tooth shape and color.

CAD for digital smile design (DSD)

All DSD software allows for aesthetic designing through the drawing of reference lines and shapes on extra- and intraoral digital photographs. Although the inclusions of aesthetic parameters are different in each DSD software, basic procedure of smile designing remains the same as follow.

1. The following photographic views in fixed head position are necessary:

Two frontal views:

- Full face with a full smile and the teeth apart. (Figure 2)
- Frontal view of the full maxillary and mandibular arch with teeth apart. (Figure 3)

2. Facial analysis is developed using the reference lines and parameters for the frontal view of the face. The horizontal reference line is the inter-pupillary that delivers a balance and horizontal overview in the aesthetically pleasing face. The vertical reference line includes the facial midline, passing the glabella, nose, and chin (Figure 4), and the canine line which indicated the total length of upper anterior teeth.

3. The boundary of upper and lower lip at smile position was located (Figure 5).

4. Figure 4 and Figure 5 from above mention were aligned with 2 corresponding points on each photo (Figure 6). The facial photograph with a wide smile and the teeth apart is moved behind superimposition with a retracted view of the full maxillary and mandibular arch to determine the ideal horizontal plane and vertical midline which permits a comparative analysis of the teeth and face.

5. Three vertical lines are marked on the teeth, two vertical lines drawn from the base of the nose to the canine, and one vertical line drawn from the midline to adjacent central incisors. Two horizontal lines represent the boundary of the upper and lower lips (Figure 7). This support reproducing the cross of the reference inter-pupillary, canine line and facial midline on the face onto the intraoral view.

6. The length of the upper lip at the smile is checked to determine the gingival display. A smile curve is established by correlating the curvature of the incisal edges of the maxillary anterior teeth. The longer incisal edge position is shown in Figure 7A. After adjusting the position of the incisal edge to above 1.0-2.0 mm from the lower lip was created smile curve (Figure 7B-C).

7. The ideal size of dental width to length ratio can be incorporated by any one of the published theories which include Golden proportion, Pound's theory, Recurring aesthetic dental proportion, Dentogenic theory, or Visagism. The adjustment is carried out with a digital ruler (Figure 8) which can be calibrated on the photograph by measuring the width of the central incisors in the study model. The tooth design can be modified, decreased, or adapted to different situations, depending on the aesthetic requirement and individual needs of the patient (Figure 9).

8. After the new smile design is attained it can be digitally presented to the patient to evaluate the appreciation and feedback (Figure 10). This digitally approved smile design at this stage can be used to create a physical

mockup that can be tested aesthetically in the patient's mouth. The mock-up allows for not only visualization of the shape integrated into the gingiva, lips and face, but also phonetics during the evaluation period. Finally, the patient may evaluate, provide an opinion and approve the final shape of the new smile before any irreversible procedures are performed.



Figure 2: Full face with a full smile and the teeth apart.



Figure 3: Frontal view of the full maxillary and mandibular arch with teeth apart.

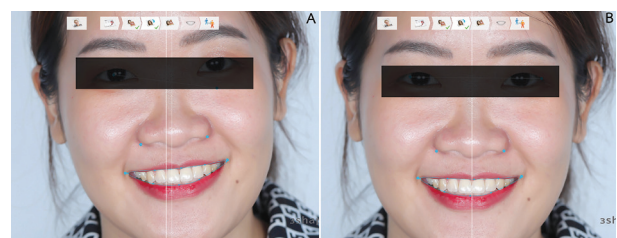


Figure 4: Representative the vertical reference line includes the facial midline, passing the glabella, nose, and chin. (A) Non-adjustment inter-pupillary line. (B) Adjustment inter-pupillary line.

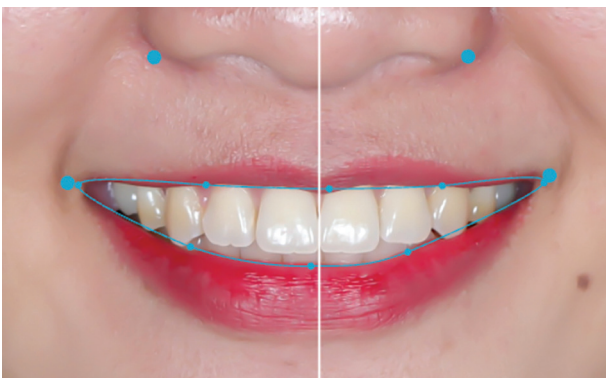


Figure 5: The boundary of upper and lower lip at smile position (blue line).



Figure 6: Two photo were aligned with 2 corresponding points on each photo.

Advantage of DSD⁽²⁹⁻³¹⁾

1. Digital smile imaging and designing help patients visualize the expected final result before treatment starts, enhancing the treatment's predictability.
2. The dentist can realize patients' concerns by showing digitally the final outcome, motivating and educating them about the benefits of the treatment.
3. Digital imaging improves dentist diagnosis and treatment plan by aesthetic visualization of patient's problem through digital analysis of facial, gingival and dental parameters that will analyze the smile and the face in an objective and standardized manner.

Limitation of DSD⁽²⁹⁻³¹⁾

1. The treatment plan depends on photographic documentation, inadequacy of them may distort the reference image and may result in an incorrect diagnosis and planning.
2. For complete digital workflow, software with updates, intraoral scanner, 3D printer and CAD/CAM are required which makes it economically expensive.

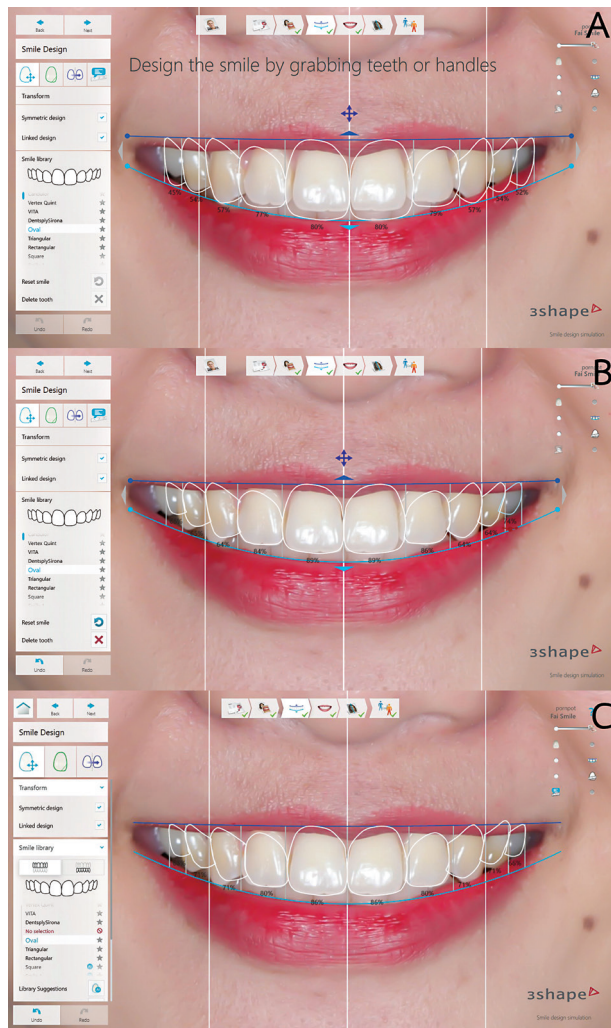


Figure 7: Representative digital smile design: three vertical lines are marked on the teeth, two vertical lines drawn from the base of the nose to the canine and one vertical line drawn from the midline to adjacent central incisors. (A) Before adjustment. (B) Adjustment the position of the incisal edge above 1.0-2.0 mm from the lower lip to create a smile curve. (C) Adjustment the proportion by decreasing in width of the anterior teeth.



Figure 8: Representative a digital ruler by measuring the width of the central incisors.

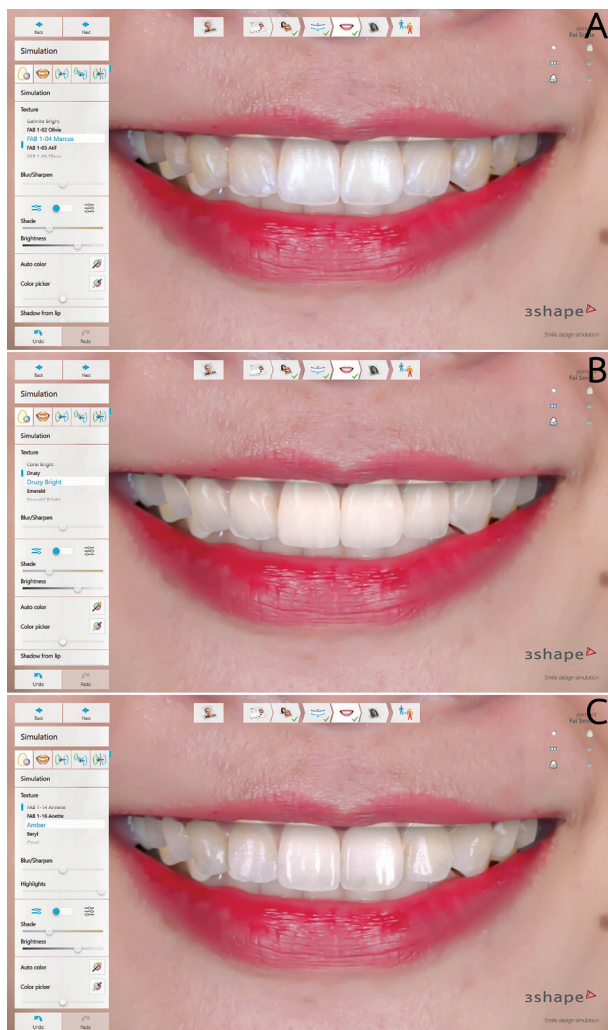


Figure 9: Representative the simulation of different surface texture styles on teeth depending on the aesthetic requirement and individual needs of the patient. (A) Fab 1. (B) Druzy Bright. (C) Amber.

3. Training for understanding software is necessary, which further increases chair time.

CAD procedure for provisional veneers

Digital impression for virtual diagnostic wax-up was performed using an intraoral scanner (Trios4, 3Shape/TRIOS®, Copenhagen, Denmark). In this case, level of the upper canine top cusp, is below the anterior plane. This results in a reverse anterior curve and represents sadness smile (Figure 11). The extraoral image indicated that the upper canine and first premolar submerge into the lower lip (Figure 12). CAD (3Shape Dental System 2020) was used to create a virtual diagnostic wax-up. The DSD image was used to superimposition and created the final virtual diagnostic wax-up (Figure 13-14). After design upper canine cusp tip was repositioned over the anterior plane.



Figure 10: Representative final shape of the new smile design in full face.

The upper maxillary teeth simultaneously elevated with the lower lip when smiling and turned to a smile curve.

A 3D printing machine (Asiga MAX, Asiga, Sydney, New South Wales, Australia) was used for building a virtual diagnostic wax-up digital model (Asiga Denta-MODEL, Asiga, Sydney, New South Wales, Australia) (Figure 15). The clear acrylic sheet (Bioplast®, Scheu Dental GmbH, Iserlohn, Germany) was used to create a provisional veneer template. The hole at the incisal edge was created with cylinder steel bur (Figure 16).

Adaptation of the putty silicone (Amcoflexplus, Amcorp, Hamburg, Germany) over the facial, occlusal, lingual surfaces, and palatal area on a digital model. Three horizontal slices (incisal, middle, cervical) and one vertical releasing incision on only one side. This silicone index was used as a preparation guide (Figure 17). Then, tooth preparation for upper maxillary 8 veneers using 3 designs of veneer preparations. Place the silicone index into the prepared abutment, resting it on the palate and the molars, and use an occlusal mirror to check the preparations. Each horizontal slice incisal, middle and cervical was used verify the amount of preparation on the incisal, middle, and cervical region respectively (Figure 18).

A digital impression for prepared abutment was performed using an intraoral scan (Figure 19). The provisional veneer was created with flowable composite resin (Filtek™ Supreme Flowable restorative, 3M ESPE, St. Paul, MN, USA) using a clear acrylic template (Figure 20) and evaluation as follows: First, level of incisal edge should be below upper lip 1-2 mm at rest position. Second, level of incisal edge should be above lower lip at smile position. Third, plane of anterior teeth should be parallel to inter pupil line. Finally, midline should be straight or parallel to mid face (mid-nose).

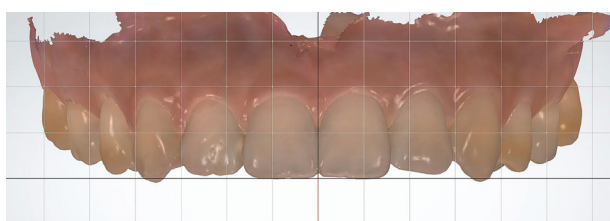


Figure 11: Digital impression showed level of upper canine cusp tip below anterior plane.



Figure 12: Extraoral image indicated that upper canine and first premolar submerge into lower lip.

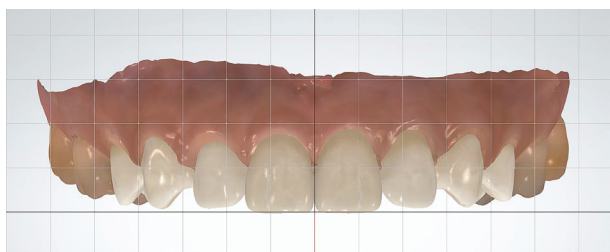


Figure 13: Representative virtual diagnostic wax-up.

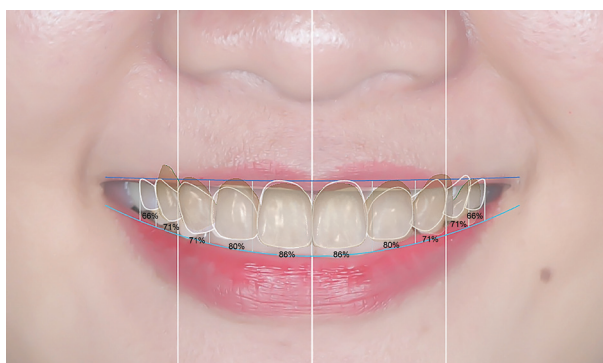


Figure 14: Representative digital smile design image superimposition with final design.

CAD procedure for veneers restorations

A digital impression for provisional veneer was created using intra oral scan. (Figure 21). CAD procedure for veneers was created using 3shape Dental System (3Shape Dental System 2020). Superimposition of the scan of provisional veneer and scan of the prepared abutment was completely created using 3 markers (16, 26, 27 mesio-lingual cusp tip) (Figure 22). All information from a scan of the provisional veneer was used for the design of the final veneer. The position of incisal edge, axis, alignment and contour, was simultaneous with a scan of the provisional veneer. The transparency mode of the final design indicated adequate clearance between preparation abutment and final design. The superimposition between the front view smile image and the final design was used for esthetic assessment (level of incisal edge, anterior plane, midline) (Figure 23). Then, the final design of the final veneer was exported in the STL file.

CAM procedure for veneers restorations

Additive manufacturing is used by the 3D printing machine for building castable resin (Asiga DentaCAST, Asiga, Sydney, New South Wales, Australia) (Figure 24). After building castable resin was cleaned using ultrasonic in isopropyl alcohol (PROPAN-2-OL, RCI Labscan Limited, Bangkok, Thailand). Post polymerization with light-curing machine unit for 3D printing material (Hi-Lite® power 3D, Kulzer GmbH, Berlin, Germany) was created for 20 minutes.

Procedure for fabricate veneers restorations

The castable resin was sprueing on the investment ring (Figure 25). Investment (IPS® PressVEST Premium

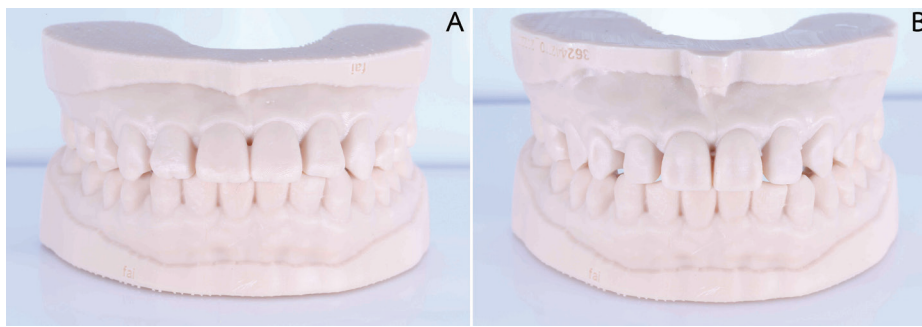


Figure 15: Representative: (A) Study digital model. (B) Virtual diagnostic wax-up digital model.

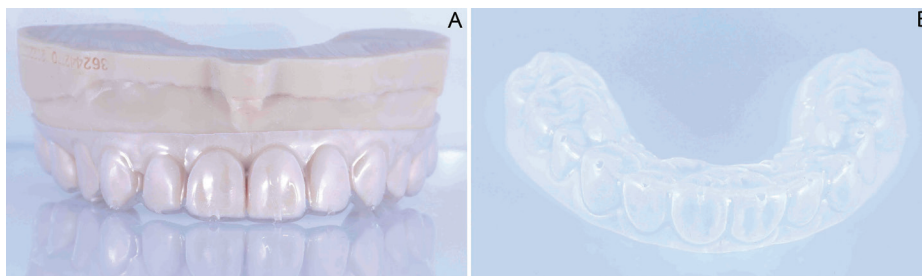


Figure 16: Representative: (A) Provisional veneer template in study digital model. (B) Provisional veneer template with hole for injection of flowable composite resin.

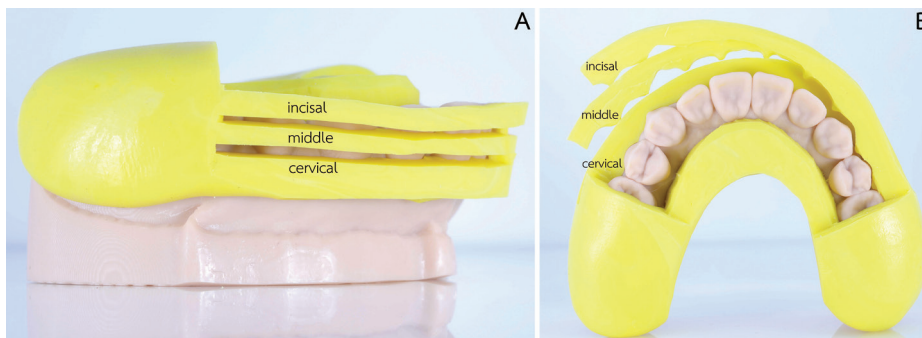


Figure 17: Representative silicone index. (A) Lateral view. (B) Top view



Figure 18: Representative silicone index for verify amount of preparation. (A) Incisal, (B) Middle, (C) Cervical



Figure 19: Digital impression.



Figure 20: Provisional veneer was created with flowable composite resin.



Figure 21: Digital impression for the provisional veneer.

Speed, Ivoclar vivadent[®], Schaan, Liechtenstein) is carried out in a silicone ring for 30 minutes. After setting the time of the investment material, the investment ring is prepared for preheating at 850°C for 60 minutes. Then, remove the investment ring from the preheating furnace immediately after completion of the preheating cycle. Place the lithium disilicate ingot (IPS e.max[®] Press, Ivoclar vivadent[®], Schaan, Liechtenstein) and alox plunger into the investment ring. Place the loaded investment ring in the center of the hot press furnace. After the end of the press cycle, divest the investment ring with polishing beads at 4 bars (Figure 26). Finally, clean the veneer with Al₂O₃ at 2 bars following a steam jet. In the cut-back layering technique, layering materials (IPS e.max Ceram, Ivoclar vivadent[®], Schaan, Liechtenstein) are applied. The anatomical shape is completed and the individual esthetic appearance is achieved. Place the layered veneer on the firing tray and fire. Finish the veneer with diamonds and heatless stone (Figure 27). The stain firing is conducted with color (IPS Ivocolor Shade Kit[®], Ivoclar vivadent[®], Schaan, Liechtenstein) and special color (IPS Ivocolor Essence Kit[®], Schaan, Liechtenstein), then glaze firing (IPS Ivocolor Glaze Paste, Ivoclar vivadent[®], Schaan, Liechtenstein) (Figure 28).

Porcelain veneers have become increasingly popular as a method for restoring diastema, discolored, fractured and worn teeth. For several years, conventional feldspathic ceramics have been considered as one of the materials in providing aesthetic outcomes. Nowadays, lithium disilicate glass ceramics have been commonly recommended for porcelain laminate veneers because of their

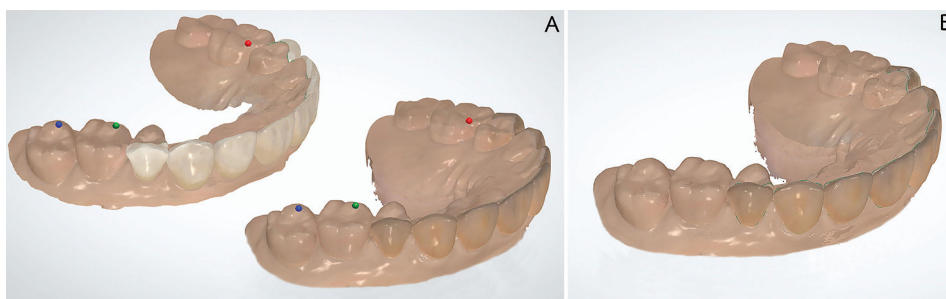


Figure 22: Representative: (A) Superimposition of the scan of provisional veneer and the scan of prepared abutment were completely created using 3 markers (16, 26, 27 mesio-lingual cusp tip). (B) After superimposition.

high flexural strength, excellent esthetics and can be fabricated with either a CAD/CAM or heat pressed technique.⁽³²⁾ Major advantages of the CAD/CAM technology over the conventional technique are faster in design, patient's preferences and the most important thing is excellent

marginal and internal fit of fixed restoration.^(32,33) Due to the application of homogeneous blocks and heat press of castable resin, fewer material failures are likely to occur during fabrication and clinical application.⁽²⁴⁾ In comparison with hand-built materials, CAD/CAM blocks and heat press of castable resin reveal a decreased presence of flaws and pores, resulting in increased reliability.^(33,34) In addition, DSD helps the dentist create and plan a treatment course by providing a virtual simulation of the result, especially in the predictability of final plan results or the final esthetic result. Besides, it is a tool that facilitates improved communication and discussion between the dental team, dental laboratory technicians, and patients.^(26,29,34)

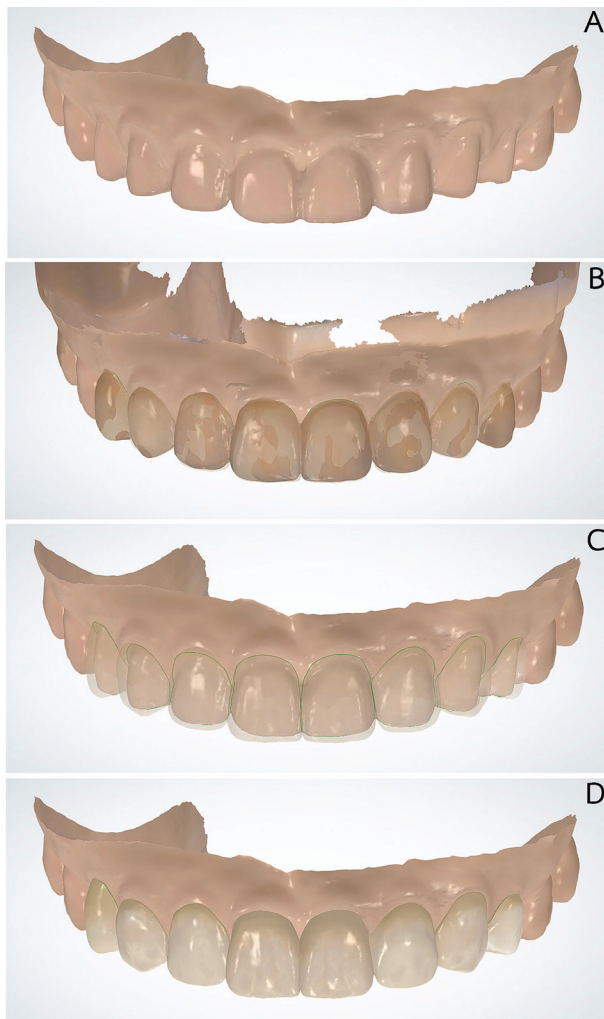


Figure 23: Representative: (A) Digital impression. (B) Superimposition of the scan of provisional veneer and final design. (C) Transparency mode of final design. (D) Final design in surface texture mode.

Conclusions

Digital dentistry is now developing rapidly and many more systems. Consequently, these new technologies should be up to date, adequately understanding and fully educated in order to return the excellent outcome for your patients. DSD utilizes photographic information to create an esthetic treatment plan and then, the castable resin veneer serves as confirmation and demonstration of the final porcelain veneer restorations. The combination of DSD and castable resin veneer for diagnosis and treatment planning has positive results in the esthetic of the anterior teeth. When used in combination, these techniques offer predictable results and highly satisfactory results.

Acknowledgment

Thank you Faculty of Dentistry Naresuan University and NU dental lab for fabricated restoration.

Conflicts of Interest

The authors declare no conflicts of interest.



Figure 24: Castable resin from 3d printing.



Figure 25: Representative: (A) The castable resin spruing on investment ring. (B) Pouring investment.

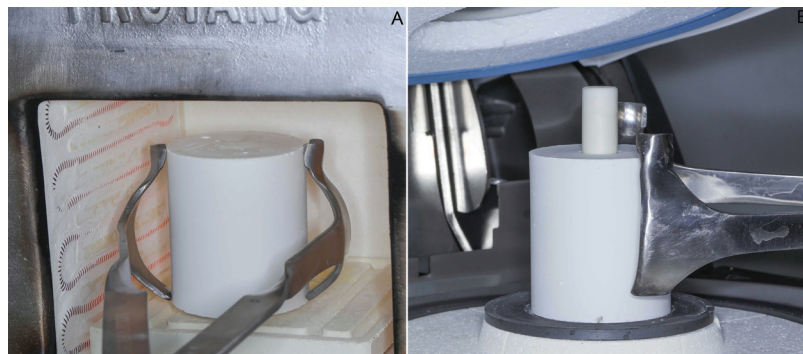


Figure 26: Representative: (A) Preheating investment ring in furnace. (B) Place the loaded investment ring in the press furnace.

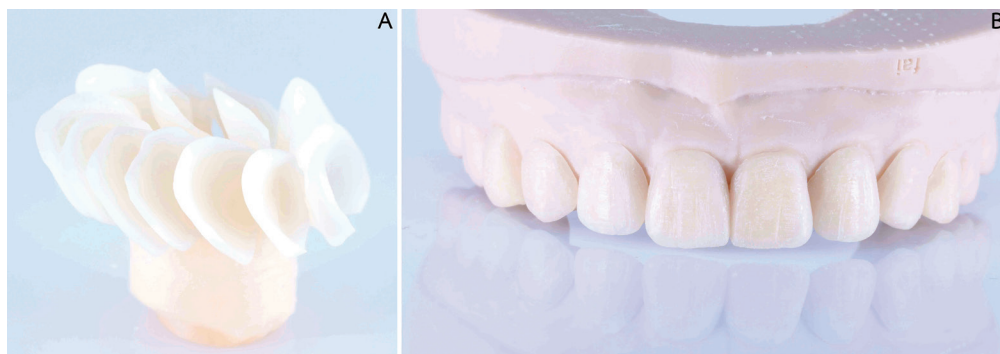


Figure 27: Representative: (A) After sandblast with Al_2O_3 following a steam jet. (B) After anatomical shape.



Figure 28: Representative final restorations after staining and glazing.

References

- Alghazzawi TF. Advancements in CAD/CAM technology: options for practical implementation. *J Prosthodont Res.* 2016;60(2):72-84.
- Antov H, Jablonski RY, Keeling A, Nixon P. CAD/CAM techniques for the conservative and efficient management of tooth wear. *Br Dent J.* 2019;227(9):791-6.
- Beuer F, Schweiger J, Edelhoff D. Digital dentistry: an overview of recent developments for CAD/CAM generated restorations. *Br Dent J.* 2008;204(9):505-11.
- Zimmermann M, Mehl A, Mörmann W, Reich S. Intraoral scanning systems-a current overview. *Int J Comput Dent.* 2015;18(2):101-29.
- Tapiea L, Lebonb N, Mawussic B, Chabouisd HF, Durete F, Attalf J. Understanding dental CAD/CAM for restorations—the digital workflow from a mechanical engineering viewpoint. *Int J Comput.* 2015;18(1):21-44.
- Abdel-Azim T, Zandinejad A, Metz M, Morton D. Maxillary and mandibular rehabilitation in the esthetic zone using a digital impression technique and CAD/CAM-fabricated prostheses: a multidisciplinary clinical report. *Oper Dent.* 2015;40(4):350-6.
- Jassim ZM, Majeed MA. Comparative evaluation of the fracture strength of monolithic crowns fabricated from different all-ceramic CAD/CAM materials (an *in vitro* study). *Biomed Pharmacol J.* 2018;11(3):1689-97.
- Methani MM, Revilla-León M, Zandinejad A. The potential of additive manufacturing technologies and their processing parameters for the fabrication of all-ceramic crowns: a review. *J Esthet Restor Dent.* 2020;32(2):182-92.
- Abdulla MA, Ali H, Jamel RS. CAD-CAM technology: a literature review. *Al-Rafidain Dent J.* 2020;20(1):95-113.
- Kim JH, Kim KB, Kim WC, Kim JH, Kim HY. Accuracy and precision of polyurethane dental arch models fabricated using a three-dimensional subtractive rapid prototyping method with an intraoral scanning technique. *Korean J Orthod.* 2014;44(2):69-76.
- Uçar Y, Aysan-Meriç İ, Ekren O. Layered manufacturing of dental ceramics: fracture mechanics, microstructure, and elemental composition of lithography-sintered ceramic. *J Prosthet Dent.* 2019;28(1):e310-8.
- Kallala R, Daly MS, Gassara Y, Dakhli R, Touzi S, Hadyaoui D, *et al.* Rationalizing indication of ceramic veneers: a systematic review. *EAS J Dent Oral Med.* 2021;3(2):51-8.
- Alothman Y, Bamasoud MS. The success of dental veneers according to preparation design and material type. *Open Access Maced J Med Sci.* 2018;6(12):2402-8.
- Sisler ZS. Preparation guides: 10 steps to maximize success for veneer preparation. *J Cos Dent.* 2020;35(4):26-33.
- AlJazairy YH. Survival rates for porcelain laminate veneers: a systematic review. *Eur J Dent.* 2021;15(2):360-8.
- Durán OG, Henríquez GI, Guzmán MÁ, Báez RA, Tisi LJP. A step-by-step conservative approach for CAD-CAM laminate veneers. *Case Rep Dent.* 2017;2017:1-6.
- Li RWK, Chow TW, Matinlinna JP. Ceramic dental biomaterials and CAD/CAM technology: state of the art. *J Prosthodont Res.* 2014;58(4):208-16.
- Marchesi G, Camurri PA, Nicolin V, Turco G, Di LR. Chair-side CAD/CAM materials: current trends of clinical uses. *Biology (Basel).* 2021;10(11):1-11.
- Su Y, Xin M, Chen X, Xing W. Effect of CAD-CAM ceramic materials on the color match of veneer restorations. *J Prosthet Dent.* 2021;126(2):255.e1-7.
- Spitznagel FA, Boldt J, Gierthmuehlen PC. CAD/CAM ceramic restorative materials for natural teeth. *J Dent Res.* 2018;97(10):1082-91.
- Höland W, Schweiger M, Watzke R, Peschke A, Kappert H. Ceramics as biomaterials for dental restoration. *Expert Rev Med Devices.* 2008;5(6):729-45.
- Bona DA, Nogueira AD, Pecho OE. Optical properties of CAD-CAM ceramic systems. *J Dent.* 2014;42(9):1202-9.
- Alghazzawi TF, Lemons J, Liu PR, Essig ME, Janowski GM. Evaluation of the optical properties of CAD-CAM generated yttria-stabilized zirconia and glass-ceramic laminate veneers. *J Prosthet Dent.* 2012;107(5):300-8.
- Belli R, Wendler M, Ligny Dd, Cicconi MR, Petschelt A, Peterlik H, *et al.* Chairside CAD/CAM materials: part 1. measurement of elastic constants and microstructural characterization. *Dent Mater.* 2017; 33(1):84-98.
- Us Y, Yüzbasioğlu E, Albayrak B, Özdemir G. Digital smile design: predictable results. *J Exp Clin Med.* 2021;38(3):123-8.
- Jreige CS, Kimura RN, Segundo ÂR, Coachman C, Sesma N. Esthetic treatment planning with digital animation of the smile dynamics: a technique to create a 4-dimensional virtual patient. *J Prosthet Dent.* 2022;128(2):130-8.
- Zarina R, Jaini J, Raj R. Evolution of the software and hardware in CAD/CAM systems used in dentistry. *Int J Prev Clin Dent Res.* 2017;4(4):284-91.
- Chochlidakis KM, Paspaspyridakos P, Geminiani A, Chen CJ, Feng IJ, Ercoli C. Digital versus conventional impressions for fixed prosthodontics: systematic review and meta-analysis. *J Prosthet Dent.* 2016;116(2):184-90.
- Coachman C, Georg R, Bohner L, Rigo LC, Sesma N. Chairside 3D digital design and trial restoration workflow. *J Prosthet Dent.* 2020;124(5):514-20.
- Veneziani M. Ceramic laminate veneers: clinical procedures with a multidisciplinary approach. *Int J Esthet Dent.* 2017;12(4):426-48.
- Lee S, Kim JE. Evaluating the precision of automatic segmentation of teeth, gingiva and facial landmarks for 2D digital smile design using real-time instance segmentation network. *J Clin Med.* 2022;11(3):1-12.

32. Yuce M, Ulusoy M, Turk AG. Comparison of marginal and internal adaptation of heat-pressed and CAD/CAM porcelain laminate veneers and a 2-year follow-up. *J Prosthet Dent.* 2019;28(5):504-10.
33. Gallardo YR, Bohner L, Tortamano P, Pigozzo MN, Lagana DC, Sesma N. Patient outcomes and procedure working time for digital versus conventional impressions: a systematic review. *J Prosthet Dent.* 2018;119(2):214-9.
34. Zhang Y, Kelly JR. Dental ceramics for restoration and metal veneering. *Dent Clin North Am.* 2017;61(4):797-819.



Editor:
Sorasun Rungsiyanont,
Srinakharinwirot University, Thailand.

Received: June 12, 2023
Revised: August 9, 2023
Accepted: August 29, 2023

Corresponding Author:
Dr. Jirayu Saepoo,
Department of Oral Diagnostic
Sciences, Faculty of Dentistry, Prince
of Songkla University, Songkhla 90112,
Thailand.
E-mail: jirayu.sa@psu.ac.th

Malignant Transformation in Oral Lichen Planus and Lichenoid Reactions in Southern Thai Population

Jirayu Saepoo¹, Duangporn Kerdpon¹, Kanokporn Pangsomboon¹

¹Department of Oral Diagnostic Sciences, Faculty of Dentistry, Prince of Songkla University, Thailand.

Abstract

Objectives: This study aimed to determine the prevalence of malignant transformation (MT) and the incidence rate of oral squamous cell carcinoma (OSCC) in oral lichen planus (OLP) and oral lichenoid reaction (OLR) patients from southern Thailand.

Methods: This hospital-based retrospective cohort study comprised OLP/OLR patients who were treated between January 2016 and December 2022. Data on the general characteristics, clinical manifestations and laboratory investigations were obtained from the hospital records and analyzed. Descriptive and analytical statistics were performed to assess the demographic data, clinical profiles of the patients and the prevalence and incidence rate of MT.

Results: A total of 117 patients were included in the study; 103 (88%) were diagnosed with OLP, and 14 (12%) were diagnosed with OLR. The median follow-up time was 15.6 months (interquartile range; 6.1-46.0). The overall prevalence of MT in OLP/OLR was 1.71% (2/117 patients); specifically, MT in OLP was 1.94% (2/103 patients). The overall annual incidence rate of MT into OSCC was 0.0060 (95% confidence interval, 0.0015-0.0240).

Conclusions: These findings suggest that OLP is a potentially malignant disorder with an MT incidence of 1.94% in the southern Thai population. OLP patients must be regularly followed-up and advised about the risk of MT.

Keywords: lichen planus, lichenoid reactions, oral squamous cell carcinoma, Southeast Asian people

Introduction

Oral lichen planus (OLP) is a chronic inflammatory and immune-mediated disease of the oral mucosa. A recent meta-analysis revealed that the global prevalence of OLP is 1.01%, with a remarkable difference based on the geographic location. Furthermore, the prevalence of OLP is known to increase with age, especially after the age of 40.⁽¹⁾ In the Thai population, OLP predominantly affects females with a 1:4 male-to-female ratio.⁽²⁾ The clinical manifestations of OLP include white reticules, white patches, atrophic mucosa, and ulcerative areas.^(3,4) Furthermore, OLP and oral lichenoid lesions (OLL) have been recently classified as oral potentially malignant disorders (OPMDs), which can transform into oral squamous cell carcinoma (OSCC). Additionally, OLP showed a cancer development rate of approximately 1-2%.⁽³⁾

However, the malignant transformation (MT) of OLP remains controversial. The rate of MT in OLP ranges from 0% to 12.5% across the world.⁽⁵⁾ Previous studies, including systematic reviews and meta-analyses, have reported the following rates of MT for the OPMDs: 0.44%–2.28% for OLP, 1.88%–3.80% for OLL and 1.71% for OLR.⁽⁶⁻¹⁰⁾ A multicenter study in Thailand reported an MT rate of 0.2% in Thai patients, based on data gathered from all regions, except southern Thailand.⁽²⁾ In addition, a recent clinical study on OLP patients from northern Thailand found that none of the patients developed OSCC.⁽¹¹⁾ To the best of our knowledge, there are no reports on the MT of OLP in the southern Thai population. Therefore, this study aimed to raise awareness about this issue and provide supporting evidence by investigating the prevalence of MT and the annual incidence rate of OSCC associated with MT in OLP/OLR patients in the southern Thai population.

Materials and Methods

Study population and data collection

All patients diagnosed with OLP/OLR and treated between 2016 and 2022 at the Dental Hospital, Faculty of Dentistry, Prince of Songkla University, Thailand were identified via a hospital database search using the International Classification of Diseases, version 10- ICD-10 (L430-8). Patients with a biopsy report indicating OLP/OLR and the necessary follow-up records were included in the study. The OLP patients were diagnosed according to the clinical and histopathological criteria of van der

Meij and van der Waal in 2003.⁽¹²⁾ The diagnosis of OLR patients relied on the patient's history, clinical correlation with causative agents, and histopathological reports reviewed by clinicians. The clinicians in this setting did not use the term “OLL” in the retrospective hospital records, which means that the study population in this present study was defined only as “OLP” or “OLR. Furthermore, OLP/OLR with epithelial dysplasia was recorded and included to the study population as Gonzalez-Moles and Ramos-García's recommendation.⁽¹³⁾

After recruiting eligible participants, the hospital records were reviewed to extract the following information: general characteristics, clinical characteristics of OLP/OLR, review of biopsy report and laboratory investigations. Data on the general characteristics included sex, age, medical history, alcohol consumption, smoking, betel quid chewing, and total follow-up time. The clinical characteristics of the patients included the type of OLP/OLR, location of OLP/OLR and corticosteroid prescription, while the laboratory investigations included the presence of hepatitis C (HCV) and *Candida* superinfection. The following criteria were used to ascertain the primary outcomes⁽¹⁴⁾: (a) clinically and histopathologically verified OLP diagnosis; (b) development of OSCC at the site of OLP/OLR; and (c) follow-up at least 6 months prior to OSCC transformation.

Ethical Approval

This study was approved by the Human Research Ethics Committee (HREC) of the Faculty of Dentistry, Prince of Songkla University-EC6503-016 (amendment version). HREC is certified in full compliance with the international Guideline for Human Research Protection—the Declaration of Helsinki, the Belmont Report, CIOMS guidelines and the International Conference on Harmonization in Good Clinical Practice (ICH-GCP). HREC was approved for waiver of informed consent according to retrospective study design.

Statistical analysis

The STATA software, version 16.0 (Stata Corp, College Station, TX, USA), was used for data analysis. The general characteristics, clinical characteristics of OLP/OLR and laboratory investigations were analyzed using descriptive statistics. Categorical data were described as frequencies/percentages and continuous data were described as mean/

standard deviation or median/interquartile range (IQR), depending on the data distribution. The prevalence of MT and the overall annual incidence of OSCC among the patients was determined across the study population with recorded follow-up time. The findings were reported with a 95% confidence interval (CI; $\alpha=0.05$).

Results

A total of 207 patients with ICD 10 (L430-8) were selected, out of which 90 patients (43.5%) were excluded according to no histopathological diagnosis (50 patients), no follow-up data (16 patients), loss of dental records (12 patients) and biopsies showed as other conditions/diseases (7 patients), respectively. As a result, a total of 117 (56.5%) patients met the eligibility criteria and were included in the study (Figure 1).

Among the 117 patients, 103 (88.0%) were diagnosed with OLP, while the remaining 14 (12%) were diagnosed with OLR. Two patients (1.7%) had OLP with mild epithelial dysplasia and none of OLP with epithelial dysplasia patients developed OSCC during the follow-up periods of 21.7 and 60.2 months. The median follow-up time for the study population was 15.6 months, with an IQR of 6.1-46.0 months.

The general characteristics of the OLP/OLR patients are summarized in Table 1. OLP/OLR was predominant in females with a male-to-female ratio of 1: 3.9. The mean age of the OLP patients at diagnosis was 55.4 ± 11.1 years. Sixty-one patients (53.0%) had underlying systemic diseases (generally more than one disease). Hypertension (29.9%) and dyslipidemia (24.8%) were the most common systemic diseases in these patients. Assessment of the risk factors revealed that 7.7% (9/117) of the patients had a smoking habit, 6.0% (7/117) consumed alcohol, and 0.9% (1/117) chewed betel quid. However, the risk assessment was not performed in all the OLP/OLR patients due to missing data (Table 1).

The clinical characteristics of the patients are summarized in Table 2. The majority of patients presented with OLP/OLR lesions at multiple sites (76.9%) with multiple clinical manifestations (66.7%) in the oral cavity. The most common affected site was the buccal mucosa (83.8%), followed by the gingiva (67.5%) and tongue (20.5%). Reticular patterns were most commonly seen (89.7%), followed by the presence of desquamative gingivitis (41%) and atrophic lesions (35%). A variety of

corticosteroids were prescribed during the follow-up period, the most common being a 0.1% fluocinolone acetonide oral paste (56.4%), followed by a 10% triamcinolone acetonide (TA) mouthwash (31.6%) and a 0.1% TA oral paste (29.9%; Table 2). The clinicians usually started with high-potency steroids and subsequently changed to other lower-potency topical steroids depending on the severity of the lesions. Of the 117 patients, 5 (4.3%) were positive for HCV; the relevant data were missing in 82.9% of the patients. Of the two patients (1.7%) positive for HBV, one was co-infected with both HCV and HBV. Furthermore, *Candida* superinfection was detected in 42 patients (35.9%).

The overall prevalence of MT in the OLP/OLR patients was 1.71% (2/117 patients; 95% CI, 0.21-6.03). Specifically, the prevalence was 1.94% (2/103 patients; 95% CI, 0.24-6.84) in the OLP patients and 0% in the OLR patients. The overall annual incidence rate of OSCC, related to the MT of OLP/OLR, was estimated at 0.0060 (95% CI, 0.0015-0.0240). The general and clinical characteristics of patients who developed OSCC in this study are described in Table 3. Both patients developed OSCC at the site of the OLP lesion and other sites in the oral cavity were verified to be free of any cancer cases. One patient, who presented with red/ulcerative lesions, had a smoking habit and experienced an HCV infection, developed OSCC within a short time during the follow-up period (6.3 years). The other patient developed OSCC 17.5 years after being diagnosed with OLP.

Discussion

The overall prevalence of MT in OLP and OLR patients was 1.71%, and it was observed only in the OLP patients (prevalence, 1.94%). It is noteworthy that this study was the first to investigate the MT in OLP and OLR in the southern Thai population. The finding is consistent with previous studies, which reported MT rates ranging from 0.44 to 2.28%.^(9,10,14) However, the MT in the present study is slightly higher than those reported previously in Asian populations, such as Iran, Taiwan, China and Japan (range, 0.07-0.7%).⁽¹⁵⁻¹⁸⁾ A multicenter study, which investigated the prevalence of MT in all the regions of Thailand, except the southern region, reported an MT rate of 0.2% in the population.⁽²⁾ Alternatively, another study reported no incidence of MT in OLP in the northern region of Thailand; however, one case of MT in

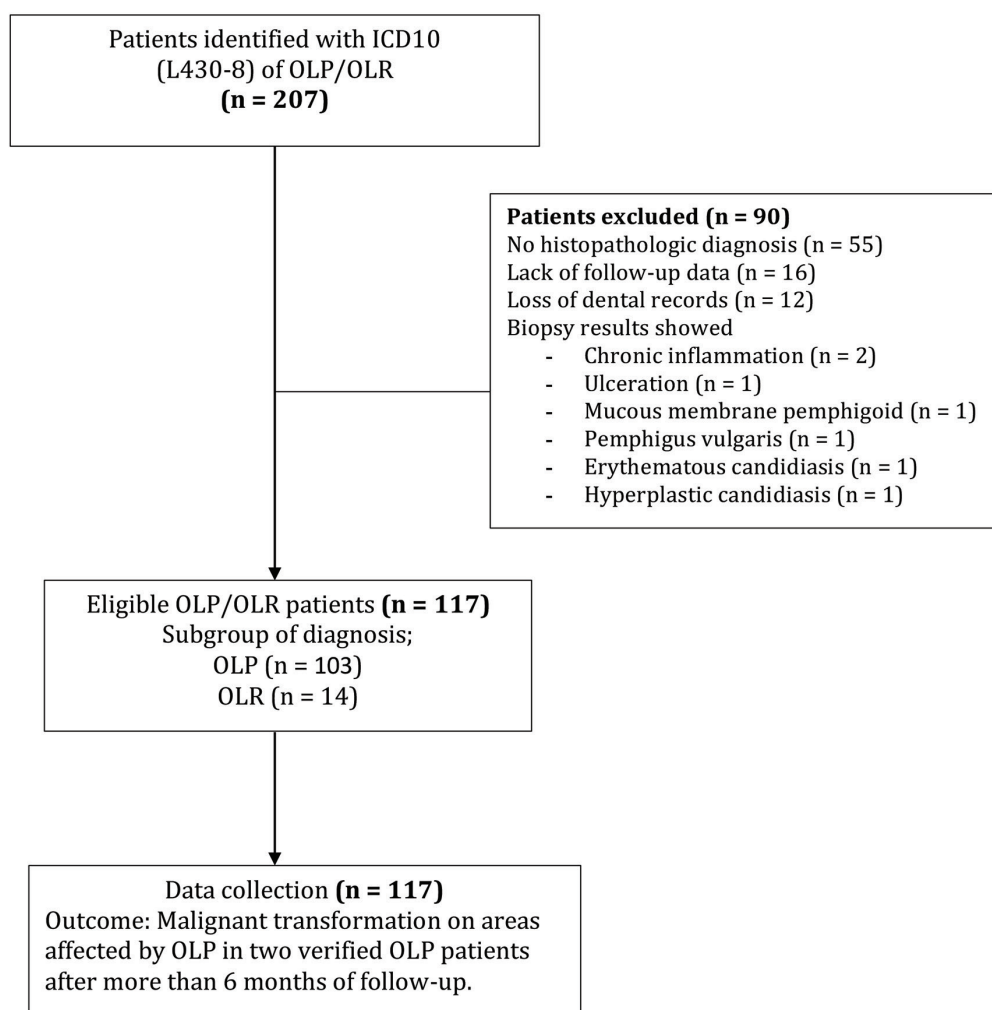


Figure 1: Study flowchart with inclusion and exclusion criteria

OLP was subsequently reported in the same population during the COVID-19 crisis.^(11,19) The discrepancy in the MT rates observed in this study and other studies, which revealed a higher malignization rate compared to other regions of Thailand or Asian populations, may be due to differences in diagnostic criteria or the exclusion of epithelial dysplasia as a diagnostic criterion. Therefore, its inclusion or exclusion of study criteria can affect the MT rates observed in studies. Furthermore, although previous studies have suggested that OLL and OLR lesions have a slightly higher malignant potential than OLP lesions⁽⁶⁻¹⁰⁾, no study has specifically determined the potential for MT in OLL and OLR in the Thai population. Although the study found no cases of MT in OLR patients, the findings may be considered as inconclusive owing to the limited number of OLR patients in this study (n=14). Further multicenter studies in Thailand are necessary to investigate the prevalence of MT in OLR and OLL

patients, highlighting the need for calibrated diagnostic criteria for OLP, OLR and OLL. Therefore, based on the study's result and previous studies in Thailand^(2,19), OLP is considered a potentially malignant disorder (OPMD) with an overall MT rate ranging from 0.2 to 1.94% in the Thai population.

Certain risk factors can increase the malignant potential in OLP, OLL and OLR patients. Previous studies have suggested that clinically red/erosive forms, the location of the lesion, smoking and alcohol consumption and HCV infection are associated with an increased risk of MT in OLP patients^(7,10,20), which odd ratio (OR) and risk ratio (RR) were reported OR=2.70 and RR=2.80-4.09 for red/erosive, OR=2.0-4.62 and RR=1.98 for smoking, OR=3.22-3.52 and RR=2.28 for alcohol consumption, and OR=5 and RR=3.77-4.46 for HCV infection, respectively.⁽¹⁰⁾ In the present study, two OLP patients demonstrated MT to OSCC; one patient had presented

Table 1: General characteristics of the study population.

General characteristics	OLP/OLR (n=117)
Gender (n, %)	
Female	92 (78.6%)
Male	25 (21.4%)
Age (years; mean±SD)	
Female	56.0±11.0
Male	53.2±11.2
Systemic diseases (n, %)	
Hypertension	35 (29.9%)
Dyslipidemia	29 (24.8%)
Diabetes mellitus	11 (9.4%)
Thyroid diseases	5 (4.3%)
Allergic rhinitis	3 (2.6%)
Hepatitis B infection	2 (1.7%)
Arthritis	2 (1.7%)
Asthma	1 (0.9%)
Liver cirrhosis	1 (0.9%)
HIV	1 (0.9%)
Osteoporosis	
Risk factors for OSCC (n, %)	
Smoking	9 (7.7%)
Alcohol	7 (6.0%)
Betel quid chewing	1 (0.9%)

*Smoking, alcohol, and betel quid chewing had missing data of about 24.8%, 24.8%, and 60.9%, respectively.

Abbreviations: OLP/OLR, oral lichen planus/oral lichenoid reaction; HIV, human immunodeficiency virus; OSCC, oral squamous cell carcinoma

with the red/ulcerative forms of OLP, while the other had the white form of the disease. The patient with the red/ulcerative form was a heavy smoker (10 packs/year) and had an HCV infection. During the follow-up, the OLP transformed into OSCC within a short period of 6.3 years. However, the other patient with the white form of OLP had no remarkable risk factors and the transformation to OSCC occurred over several years (17.5 years). These findings agree with those of previous studies, which show that the clinical forms, smoking habits and presence of HCV infection can influence and increase the potential for MT in OLP.

OLP with epithelial dysplasia was observed in 1.7% (2/117) of the patients in the current study. This finding was consistent with a previous study which reported a prevalence of 1.7% (9/533 patients) in Thai patients.⁽²⁾ The presence of epithelial dysplasia was associated with an increased rate of MT.^(10,18,21) Gonzalez-Moles and Ramos-García proposed that the presence of dysplasia should be included while investigating the prevalence of

MT in OLP; such cases should be defined as 'OLP with epithelial dysplasia', which was different from the van der Meij and van der Waal criteria that they did not consider epithelial dysplasia in histopathological criteria.⁽¹³⁾ Gonzalez-Moles and Ramos-García also pointed out that there is no current literature proving that OLP lesion itself cannot progress to epithelial dysplasia.^(12,13) In contrast, a model indicating that dysplastic changes could occur in OLP before transforming into OSCC due to chronic inflammation was introduced in the past⁽²²⁾ and there was a previous study suggested that OLP lesions with dysplasia could indicate early-phase MT in OLP.⁽²³⁾ The model was summarized that the presence of dysplasia or development oral cancer in OLP cases resulted from cell DNA damages, loss of epithelial integrity due to inflammatory cytokines, or oxidative stress.⁽²²⁾ However, detecting epithelial dysplasia remains challenging. As expressed in a recent publication, the evaluation of epithelial dysplasia, especially mild forms of dysplasia in OLP, is controversial and requires experienced pathologists.⁽²⁴⁾ Because, it is

Table 2: Clinical characteristics of the study population.

Clinical characteristics	OLP/OLR (n=117)
Follow-up (months; median with IQR)	15.6 with an IQR of 6.1-46.0
Clinical manifestations (n, %)	
Reticular type	105 (89.7%)
Desquamative gingivitis	48 (41.0%)
Atrophic type	41 (35.0%)
Erosive type	22 (18.8%)
Plaque type	
Clinical sites (n, %)	
Buccal mucosa	98 (83.8%)
Gingiva	79 (67.5%)
Tongue	24 (20.5%)
Lip	19 (16.2%)
Alveolar ridge	16 (13.7%)
Floor of the mouth	8 (6.8%)
Palate	7 (6.0%)
Labial mucosa	6 (5.1%)
Corticosteroid prescription (n, %)	
0.1% FA oral paste	66 (56.4%)
10% TA mouthwash	37 (31.6%)
0.1% TA oral paste	35 (29.9%)
10% Dexamethasone mouthwash	24 (20.5%)
0.05% CP oral paste	2 (1.7%)
Systemic prednisolone	5 (4.3%) with a range of 10-40 mg/day
HCV investigation (n, %)	
Negative	15 (12.8%)
Positive	5 (4.3%)
Missing data	97 (82.9%)
Presence of <i>Candida</i> Superinfection (n, %)	42 (35.9%)

Abbreviations: OLP/OLR; oral lichen planus/oral lichenoid reaction; IQR, interquartile range; FA, fluocinolone acetonide; TA, triamcinolone acetonide; CP, clobetasol propionate; HCV, hepatitis C virus

Table 3: General and clinical characteristics of patients who developed oral squamous cell carcinoma.

Case	Demographics and Risk factors	Site of OLP malignization and time to MT	Staging and treatment
1	Male, 58 years with liver cirrhosis, diabetes mellitus, and hypertension Risk factors: Hepatitis C and smoking 10 packs/year	Right buccal mucosa (Previous red/ulcerative clinical form of OLP) Time to MT: 75.2 months (6.3 years)	T3N1M0; He underwent wide excisional surgery with a right modified radical neck dissection and immediate reconstruction with a right pectoralis major myocutaneous flap followed by chemoradiotherapy.
2	Female, 64 years with unremarkable medical history Risk factors: None	Lower anterior labial gingiva/ vestibule (Previous white lesion site of OLP) Time to MT: 209.9 months (17.5 years)	Not applicable: She was referred to a tertiary hospital for further investigations and treatment, which were covered by her health insurance.

Abbreviations: OLP, oral lichen planus; MT, malignant transformation; TNM, Tumor-Node Involvement-Metastasis staging

crucial to differentiate the actual epithelial dysplasia from reactive epithelial atypia that responds to inflammatory stimuli, which is common in OLP lesion.

The present study found no MT in OLP with epithelial dysplasia (2/117 patients) during the current study's follow-up periods (1.8 and 5 years). This is in concordance with other expert experiences that epithelial dysplasia even high grade may not progress to malignancy.⁽²⁵⁾ On the other hand, this lack of MT may be due to the limited sample size of the OLP with epithelial dysplasia population and the short follow-up periods. Nonetheless, it is necessary to monitor patients with OLP/OLL/OLR with epithelial dysplasia in the long term, as previous studies have recommended.

This study has some limitations. The sample size was relatively small, and there was an issue that should be addressed, as shown in Figure 1. Of 207 patients, a high proportion of excluded patients (55/90 patients; 61.1%) had been diagnosed with OLP based on the clinical findings only. According to previous study, both clinical and histopathological examinations are essential to confirm a diagnosis of OLP/OLL/OLR⁽¹³⁾ and ascertain the actual MT of OLP. Furthermore, it is also important to rule out other OPMDs that clinically resemble OLP. Previous studies have shown that lesions resembling early-stage OLP could develop into proliferative verrucous leukoplakia (PVL), or that the clinicopathological features of OLL could be similar to those of PVL.⁽²⁶⁻²⁸⁾ Therefore, we recommend that patients with clinical signs of OLP undergo an incisional biopsy to determine the definitive diagnosis, assess the presence of epithelial dysplasia as a potential risk for MT and plan appropriate treatment accordingly. Furthermore, the assessment of risk factors was not possible in all patients in the current study due to missing data on smoking, alcohol consumption, betel quid chewing and HCV testing. Comprehensive clinical records for OLP, OLL and OLR should be used to ascertain the effect of these risk factors on MT in the Thai population. Additional multicenter studies must be conducted using appropriate criteria for histopathological diagnosis that clearly discriminate among OLP, OLL and OLR across all regions of Thailand. This will aid in determining the rate of MT and raise awareness about its potential in patients with these lesions.

Conclusions

The prevalence of MT in OLP was 1.94% with the overall annual incidence rate was estimated at 0.0060 in the southern Thai population, based on the study. We recommend that all OLP/OLR patients undergo regular follow-ups; a comprehensive history of the patient, including the cancer risks, must be taken to enable the early detection of OSCC transformation. Furthermore, OLP patients should be counseled about the potential for MT, even if the symptoms are controlled.⁽²⁹⁾ Therefore, clinicians should communicate with OLP patients, inform them about the risks and address the importance of long-term follow-up.

Acknowledgments

This research did not receive any specific grant or funding from funding agencies in the public, commercial, or not-for-profit sectors.

Conflicts of Interest

The authors declare no conflicts of interest.

Data Availability Statement

The data are available from the corresponding author upon reasonable request.

References

- González-Moles M, Warnakulasuriya S, González-Ruiz I, González-Ruiz L, Ayén Á, Lenouvel D, *et al.* Worldwide prevalence of oral lichen planus: a systematic review and meta-analysis. *Oral Dis.* 2021;27(4):813-28.
- Thongprasom K, Youngnak-Piboonratanakit P, Pongsirivet S, Laothumthut T, Kanjanabud P, Rutchakitprakarn L. A multicenter study of oral lichen planus in Thai patients. *J Investig Clin Dent.* 2010;1(1):29-36.
- Warnakulasuriya S, Kujan O, Aguirre-Urizar JM, Bagan JV, González-Moles M, Kerr AR, *et al.* Oral potentially malignant disorders: a consensus report from an international seminar on nomenclature and classification, convened by the WHO collaborating centre for oral cancer. *Oral Dis.* 2021;27(8):1862-80.
- Warnakulasuriya S, Johnson NW, van der Waal I. Nomenclature and classification of potentially malignant disorders of the oral mucosa. *J Oral Pathol Med.* 2007;36(10):575-80.
- Gonzalez-Moles MA, Scully C, Gil-Montoya JA. Oral lichen planus: controversies surrounding malignant transformation. *Oral Dis.* 2008;14(3):229-43.

6. Giuliani M, Troiano G, Cordaro M, Corsalini M, Gio-co G, Lo Muzio L, *et al.* Rate of malignant transformation of oral lichen planus: a systematic review. *Oral Dis.* 2019;25(3):693-709.
7. González-Moles M, Ruiz-Ávila I, González-Ruiz L, Ayén Á, Gil-Montoya JA, Ramos-García P. Malignant transformation risk of oral lichen planus: a systematic review and comprehensive meta-analysis. *Oral Oncol.* 2019;96:121-30.
8. Iocca O, Sollecito TP, Alawi F, Weinstein GS, Newman JG, De Virgilio A, *et al.* Potentially malignant disorders of the oral cavity and oral dysplasia: a systematic review and meta-analysis of malignant transformation rate by subtype. *Head Neck.* 2020;42(3):539-55.
9. González-Moles MÁ, Ramos-García P, Warnakulasuriya S. An appraisal of highest quality studies reporting malignant transformation of oral lichen planus based on a systematic review. *Oral Diseases.* 2021;27(8):1908-18.
10. Ramos-García P, González-Moles MÁ, Warnakulasuriya S. Oral cancer development in lichen planus and related conditions-3.0 evidence level: a systematic review of systematic reviews. *Oral Diseases.* 2021;27(8):1919-35.
11. Kaomongkolgit R, Daroonpan P, Tantanapornkul W, Palasuk J. Clinical profile of 102 patients with oral lichen planus in Thailand. *J Clin Exp Dent.* 2019;11(7):e625-9.
12. Van Der Meij EH, Van Der Waal I. Lack of clinicopathologic correlation in the diagnosis of oral lichen planus based on the presently available diagnostic criteria and suggestions for modifications. *J Oral Pathol Med.* 2003;32(9):507-12.
13. González-Moles M, Ramos-García P. Oral lichen planus and related lesions. What should we accept based on the available evidence? *Oral Dis.* 2023;29(7):2624-37.
14. Idrees M, Kujan O, Shearston K, Farah CS. Oral lichen planus has a very low malignant transformation rate: a systematic review and meta-analysis using strict diagnostic and inclusion criteria. *J Oral Pathol Med.* 2021;50(3):287-98.
15. Pakfetrat A, Javadzadeh-Bolouri A, Basir-Shabestari S, Falaki F. Oral lichen planus: a retrospective study of 420 Iranian patients. *Med Oral Patol Oral Cir Bucal.* 2009;14(7):e315-8.
16. Tsushima F, Sakurai J, Uesugi A, Oikawa Y, Ohsako T, Mochizuki Y, *et al.* Malignant transformation of oral lichen planus: a retrospective study of 565 Japanese patients. *BMC Oral Health.* 2021;21(1):298.
17. Xue JL, Fan MW, Wang SZ, Chen XM, Li Y, Wang L. A clinical study of 674 patients with oral lichen planus in China. *J Oral Pathol Med.* 2005;34(8):467-72.
18. Wang YY, Tail YH, Wang WC, Chen CY, Kao YH, Chen YK, *et al.* Malignant transformation in 5071 southern Taiwanese patients with potentially malignant oral mucosal disorders. *BMC Oral Health.* 2014;14:99.
19. Chompunud Na Ayudhya C, Kaomongkolgit R. Malignant transformation of oral lichen planus during COVID-19 crisis. *Oral Dis.* 2022;2:doi: 10.1111/odi.14423.
20. Aghbari SMH, Abushouk AI, Attia A, Elmaraezy A, Menshawy A, Ahmed MS, *et al.* Malignant transformation of oral lichen planus and oral lichenoid lesions: a meta-analysis of 20095 patient data. *Oral Oncol.* 2017;68:92-102.
21. Shearston K, Fateh B, Tai S, Hove D, Farah CS. Oral lichenoid dysplasia and not oral lichen planus undergoes malignant transformation at high rates. *J Oral Pathol Med.* 2019;48(7):538-45.
22. Georgakopoulou EA, Achartari MD, Achartaris M, Foukas PG, Kotsinas A. Oral lichen planus as a preneoplastic inflammatory model. *J Biomed Biotechnol.* 2012;2012:759626. doi: 10.1155/2012/759626.
23. Lodi G, Scully C, Carrozzo M, Griffiths M, Sugerman PB, Thongprasom K. Current controversies in oral lichen planus: report of an international consensus meeting. part 2. clinical management and malignant transformation. *Oral Surg Oral Med Oral Pathol Oral Radiol Endod.* 2005;100(2):164-78.
24. González-Moles M, Warnakulasuriya S, González-Ruiz I, Ayén Á, González-Ruiz L, Ruiz-Ávila I, *et al.* Dysplasia in oral lichen planus: relevance, controversies and challenges. a position paper. *Med Oral Patol Oral Cir Bucal.* 2021;26(4):e541-8.
25. Aguirre-Urizar JM, Warnakulasuriya S. The significance of oral epithelial dysplasia in the clinical management of oral potentially malignant disorders. *Int J Oral Maxillofac Surg.* 2023;52(4):510-1.
26. Barba-Montero C, Lorenzo-Pouso AI, Gándara-Vila P, Blanco-Carrión A, Marichalar-Mendía X, García-García A, *et al.* Lichenoid areas may arise in early stages of proliferative verrucous leukoplakia: a long-term study of 34 patients. *J Oral Pathol Med.* 2022;51(6):573-81.
27. McParland H, Warnakulasuriya S. Lichenoid morphology could be an early feature of oral proliferative verrucous leukoplakia. *J Oral Pathol Med.* 2021;50(2):229-35.
28. Garcia-Pola MJ, Llorente-Pendás S, González-García M, García-Martín JM. The development of proliferative verrucous leukoplakia in oral lichen planus. a preliminary study. *Med Oral Patol Oral Cir Bucal.* 2016;21(3):e328-34.
29. Greenberg MS. AAOM clinical practice statement: subject: oral lichen planus and oral cancer. *Oral Surg Oral Med Oral Pathol Oral Radiol.* 2016;122(4):440-1.



Editor:

Wannakamon Panyarak,
Chiang Mai University, Thailand.

Received: March 28, 2023

Revised: May 18, 2023

Accepted: September 20, 2023

Corresponding Author:

Associated Professor
Marasri Chaiworawitkul,
Department of Orthodontics and
Pediatric Dentistry, Faculty of Dentistry,
Chiang Mai University, Chiang Mai
50200 Thailand.

E-mail: dr.marasri@gmail.com

Comparison of the Upper Pharyngeal Airway in Thai Children With or Without Unilateral Cleft Lip and Palate in the Supine Position

Prang Wiwattanadittakul¹, Marasri Chaiworawitkul², Nuntigar Sonsuwan³,
Sangsom Prapayasatok⁴

¹Postgraduate Student in Residency Training Program of Department of Orthodontics and Pediatric Dentistry, Faculty of Dentistry, Chiang Mai University, Thailand

²Department of Orthodontics and Pediatric Dentistry, Faculty of Dentistry, Chiang Mai University, Thailand

³Department of Otolaryngology, Faculty of Medicine, Chiang Mai University, Thailand

⁴Department of Oral Biology and Diagnostic Sciences, Faculty of Dentistry, Chiang Mai University, Thailand

Abstract

Objectives: This study aimed to evaluate differences in the upper pharyngeal airway morphology between Thai children with repaired unilateral cleft lip and palate (UCLP) and Thai non-cleft children.

Methods: This prospective study used cone beam computed tomography (CBCT) and polysomnography (PSG) studies. The subjects were 34 children with UCLP (21 males and 13 females; mean age 8.94±1.87); and 32 non-cleft children (20 males and 12 females; mean age 10.03±1.91). The Dolphin imaging software measured the volume and the most constricted cross-sectional airway (version 11.7 premium).

Results: An independent sample t-test showed that the differences between groups were significant. The means of oropharyngeal ($p=0.003$), hypopharyngeal ($p=0.020$), and total volume ($p=0.013$) in UCLP children were lower than those in non-cleft children. Furthermore, the most constricted axial area of the oropharyngeal airway in UCLP children was narrower than that in non-cleft children ($p=0.004$).

Conclusions: The volume and most constricted axial area of the upper pharyngeal airway in Thai UCLP children were significantly smaller than those in Thai non-cleft children.

Keywords: cleft lip and palate, cone-beam computed tomography, upper pharyngeal airway lumen, upper pharyngeal airway volume

Introduction

Orofacial clefts are the most common congenital defect in head and neck regions.⁽¹⁾ Studies in newborn infants in the northern Thai population have shown a prevalence of 1.6 per 1000 newborn children.⁽²⁾ These defects can significantly impact facial growth, particularly in the midface, pharyngeal airway, and maxilla.^(3,4) Moreover, medical conditions such as respiratory constriction, sleep problems, obstructive sleep apneas (OSAS), adenoid hypertrophy and velopharyngeal insufficiency⁽⁵⁻⁷⁾ have been reported in children with cleft lip and palate (CLP), significantly affecting their quality of life.⁽⁸⁾

Sleep disorder breathing (SDB) encompasses various conditions characterized by snoring and resistance while breathing during sleep, the range of it was from just primary snoring (PS) to upper airway resistance syndrome and apnea (OSAS, Central Sleep Apnea, and Mixed Sleep Apnea).⁽⁹⁾ According to the American Thoracic Society, OSAS in children is defined as a disorder of breathing during sleep characterized by prolonged partial upper airway obstruction and/or intermittent complete obstruction (obstructive apnea) that disrupt normal ventilation during sleep and normal sleep pattern.⁽¹⁰⁻¹²⁾ OSAS is associated with various risk factors, including obesity (defined as a body mass index (BMI) greater than 22 kg/m²), hypertrophy of the adenoid and enlargement of the tonsil glands.^(11,13,14) Polysomnography (PSG) is a fundamental tool for diagnosis and treating sleep disorders. It is considered the gold standard for diagnosing sleep-related breathing disorders, including OSAS.⁽¹¹⁾ PSG data, including parameters such as apnea-hypopnea index (AHI), desaturation index (DI) and oxygen saturation levels, are utilized for diagnosing SDB.⁽¹⁵⁾ In children, a normal AHI is one event per hour of total sleep time (hrTST), mild OSA is AHI one to five, moderate OSA is five to ten and severe OSA is more than ten.⁽¹¹⁾ Severe OSAS patients often use continuous positive air pressure machines (CPAP) to keep their airway open during sleep.⁽¹⁶⁾

The pharyngeal airway has been identified as a fundamental risk factor of OSAS in children. Previous studies have attempted to clarify the differences in the upper pharyngeal airway between CLP and non-cleft patients, using lateral cephalogram for calculation and estimation.⁽¹⁷⁾ Nowadays, 3-dimensional (3D) cone-beam computed tomography (CBCT) images are considered more precise for evaluating the airway.^(18,19) Software, such as the

Dolphin imaging program, has been tested and proven accurate and reliable in evaluating both the volume and axial areas of the upper pharyngeal airway compared to other digital software programs.^(20,21)

Muntz *et al.*,⁽¹⁾ Oosterkamp *et al.*,⁽²²⁾ and Celikoglu *et al.*⁽²³⁾ explained that cleft patients have a smaller pharyngeal airway size and volume compared to normal children. However, controversially, Ceilo *et al.*⁽²⁴⁾ and Rana *et al.*⁽²⁵⁾ found no difference in the upper pharyngeal airway between normal and abnormal children. Several studies have been conducted to evaluate the upper pharyngeal airway in an upright position^(25,26), while sleep problems are typically identified during sleep or in the supine position.⁽⁵⁾ To date, reports on the upper pharyngeal airway in growing unilateral CLP (UCLP) patients in the supine position using 3D radiographs are scarce, with none comparing cleft and non-cleft conditions.⁽²⁷⁾ Therefore, this prospective study focused on comparing the sizes of the most constricted axial area and volume of the upper pharyngeal airway using CBCT in the supine position between groups, controlling for demographics and PSG findings.

Materials and Methods

This study was conducted prospectively, enrolling subjects from patients who visited Chiang Mai University Hospital and the Faculty of Dentistry, Chiang Mai University, during the period from 2019 to 2021. The study received ethical approval from the Human Experimental Committee of the Faculty of Dentistry, Chiang Mai University, Thailand (No. 59/2019). Prior to participation, patients and their caregivers provided informed consent for the release of their CBCT scans, polysomnography reports, and medical information to the researchers.

Participants

The study included Thai children aged 5 to 12 years who visited the hospital and the Faculty of Dentistry during the period from 2019 to 2021. A total of 66 children who met the criteria for undergoing CBCT scans of their orofacial regions were divided into two groups.

The first group comprised of thirty-four children diagnosed with UCLP, without any additional orofacial cleft deformities. All participants in this group had undergone cheiloplasty and palatoplasty procedures at the appropriate times. The second group, consisting of

thirty-two children, had no orofacial cleft conditions.

All participants with adenotonsillar hypertrophy were undergoing medication treatment for six weeks. However, those with a history of continuous positive airway pressure therapy, suspected or diagnosed with central sleep apnea or mixed sleep apnea, as well as participants and parents who did not agree to participate in the research project, were excluded from the study.

Measurements

Participants provided their personal information, including age, sex, weight and height. Body mass index (BMI) of each patient was calculated. A thorough medical evaluation of each child's tonsil glands and adenoid size was conducted by a physician. The physical examination of tonsil size used the Brodsky scale, which classifies tonsillar gland enlargement into five grades (0-4), with higher grades indicating more severe enlargement⁽²⁸⁾ (Figure 1). Adenoid hypertrophy was clinically evaluated using the adenoid-to-choanal opening ratio as a percentage, divided into three groups: groups 1-3 represented adenoid tissue occupying more than 50%, 50–75%, and more than 75%, respectively.⁽²⁹⁾ Overnight portable PSG type 4 (SOMNOlab-2, Hamburg, Germany) was conducted for all participants. A pediatric otolaryngologist with 12-year of expertise analyzed the PSG data to determine the AHI, DI, minimum oxygen saturation and average oxygen saturation.

CBCT scans of the samples were obtained using the MobiiScan scanner, following a standard protocol with specific settings (90 kV, 6 mA, 16 cm×16.8 cm FOV, 0.4 mm voxel size and 26 s scanning time).⁽³⁰⁾ The patients were positioned in the supine position on the machine bed, maintaining maximum intercuspation occlusion. The supine position was established using the machine's laser guide. During image acquisition, the subjects were instructed not to swallow or change positions.

Subsequently, CBCT DICOM raw files were exported and analyzed using the Dolphin imaging software (version 11.7 premium, Dolphin Imaging & Management Solutions, Chatsworth, CA, USA). A clinician identified the boundaries of the upper pharyngeal airway prior to assessing airway volume using specific tools in the program. (Figure 2)

According to Rana *et al.*⁽²⁵⁾ assessment methods, we had calibrated the orientation of the images by using

the manual option in the Dolphin imaging program. The midsagittal plane from Ricketts's analysis was adjusted in the frontal plane as illustrated in Figure 3. In cases of asymmetry, patients' conditions were assessed at the discretion of their attending physician. The sagittal planes were then adjusted using the Frankfort horizontal plane, a plane extending from left Orbitale to both Porion points. Using Dolphin 3D analysis, the clinician measured the volume and the most constricted axial area of the upper pharyngeal airway⁽²⁵⁾, employing the same anatomical landmarks as in 2D images as illustrated in Figure 4 and Figure 5. The definitions of all anatomical landmarks are described in Table 1. The linear axial slice 2D images of the pharyngeal airway were segmented into three planes for each part of the upper pharyngeal airway: the nasopharyngeal area, the oropharyngeal area and the hypopharyngeal area.

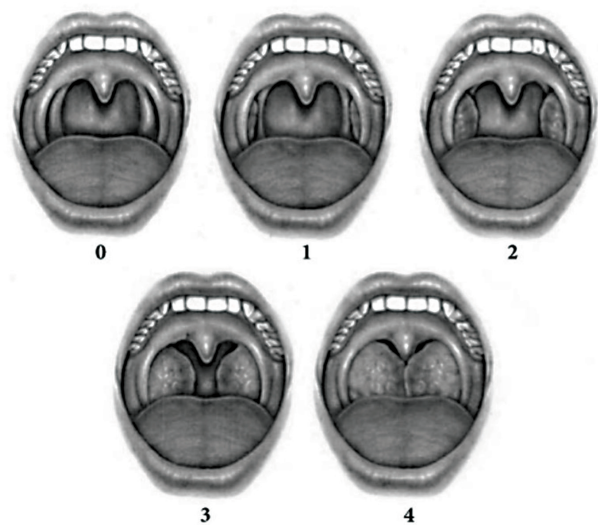


Figure 1: The tonsil grading scale from Brodsky grading scale as described in Cahali *et al.*⁽²⁶⁾

Data Analysis

The Statistical Package for Social Sciences (SPSS) version 26.0 for Windows (IBM Corp., Armonk, New York, USA) was used for data analysis. Data normality was assessed using the Shapiro-Wilks test. Analysis of Variance (ANOVA) was employed to evaluate the differences in age, baseline characteristics and PSG findings between the groups.

To ensure accuracy and minimize errors in measurement and digital programming, each value was measured three times, and the mean was calculated. Intra-examiner

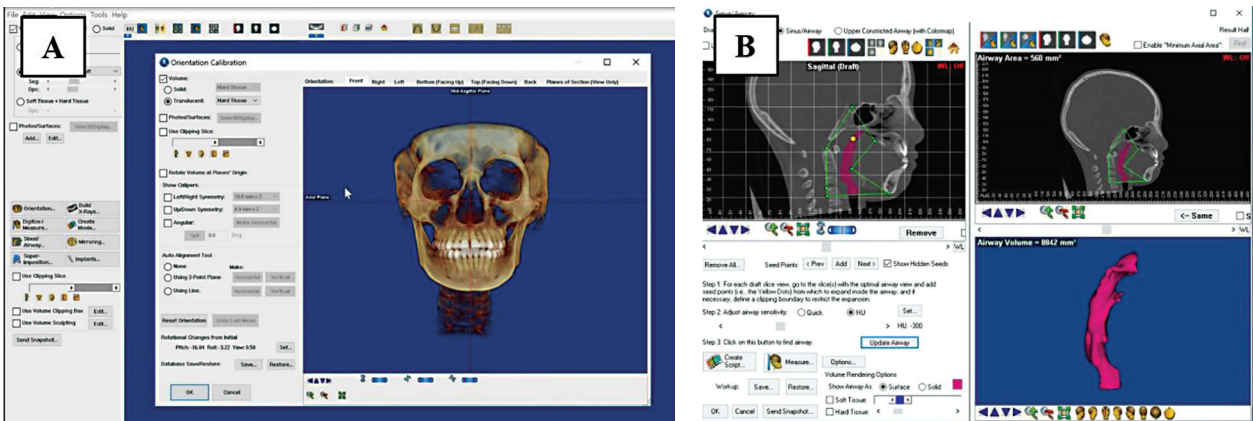


Figure 2: Screenshots of the Dolphin software, showing the manual option: (A) The orientation calibration (B) Airway measurement

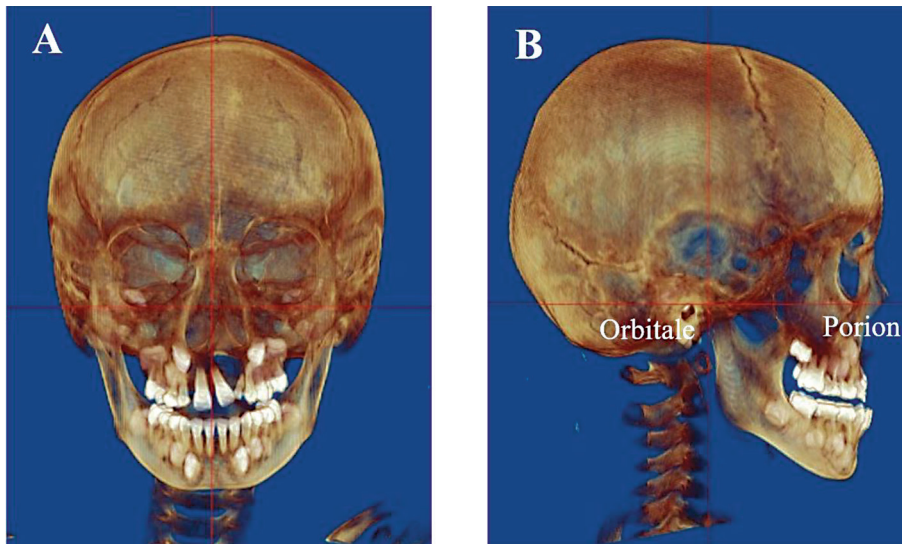


Figure 3: Adjusting the orientations of the images in two views prior to conducting measurements. (A) Frontal view was perpendicular to sagittal view and (B) Sagittal view with Frankfort horizontal plane (porion-orbitale).

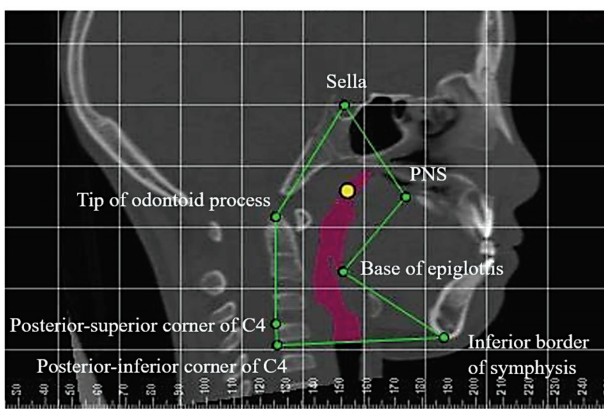


Figure 4: The anatomical landmarks identified in Dolphin 3D images. Labels in the form of green dots were strategically located to indicate the location of each major landmark. The images showed the upper pharyngeal airway spaces as the pink area.

assessment involved repeating the airway assessment on 10 radiographs, conducted three times within one week and then once more after one month from the initial assessment. For inter-examiner reliability, the assessments of 10 radiographs were compared with those of an expert. Additionally, an independent sample t-test was used to assess mean differences between the UCLP and non-cleft groups. *P*-value of less than 0.05 was considered as statistical significance.

Results

The demographic data for the study participants are presented in Table 2. The chronological ages of all patients ranged from 5.00 to 12.00 years, with a mean age of 9 ± 2 years for the UCLP group and 10 ± 2 years for the non-

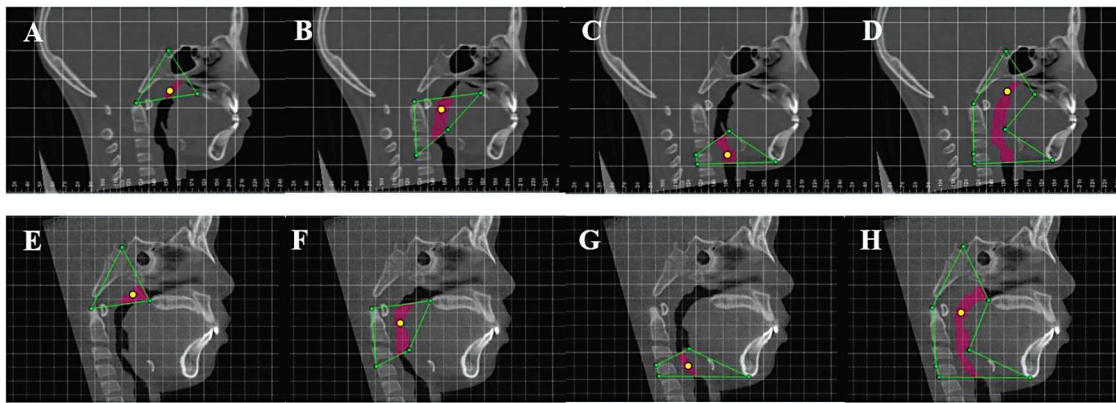


Figure 5: Assessment in sagittal view from CBCT in Dolphin software: (A) - (D) images were example images from UCLP subject, and (E) - (F) images were example images from non-cleft subject. (A) and (E); The image of nasopharyngeal airway (Sella-PNS-tip of odontoid process), (B) and (F); The images of oropharyngeal airway (tip of odontoid process - PNS - base of epiglottis - posterior-superior corner of C4), (C) and (G); The images of hypopharyngeal airway (posterior-superior corner of C4 - base of epiglottis - inferior border of symphysis - posterior-inferior corner of C4), and (D) and (H); The images of total upper pharyngeal airway spaces (all landmarks were used to construct the areas).

Table 1: The definition of CBCT anatomic landmarks as described in Rana S *et al.*⁽²⁵⁾

Region	Anterior boundary	Posterior boundary	Superior boundary	Inferior boundary
Nasopharyngeal	Line extending from Sella (S) to the posterior nasal spine (PNS)	Line extending from Sella (S) to the tip of the odontoid process		Line extending from the PNS to tip of the odontoid process
Oropharyngeal	Line extending from the PNS to the base of the epiglottis	Line extending from the tip of the odontoid process to the posterior-superior border of cervical vertebra 4 (C4)	Line extending from the PNS to the tip of the odontoid process	Line extending from the base of the epiglottis to the posterior-superior border of C4
Hypopharyngeal	Line extending from the base of the epiglottis to the inferior border of the symphysis	Line extending from the posterior-superior corner of C4 to the posterior-inferior corner of C4	Line extending from the base of the epiglottis to the posterior-superior corner of the C4	Line extending from the posterior-inferior corner of C4 to the inferior border of the symphysis

cleft group. Within the UCLP group, there were 21 males and 13 females, while the non-cleft group consisted of 19 males and 13 females.

The average BMI of all subjects was below 22.9 kg/m², indicating that the sample was not considered obese. Both groups exhibited similar baseline demographics, adenotonsillar hypertrophy index, and polysomnographic findings.

Comparison between UCLP and non-cleft groups

The reliability tests conducted for intra- and inter-examiner measurements showed strong correlations (r=0.999, r=0.998), demonstrating a high level of reproducibility in the measurements. Analysis using the inde-

pendent t-test revealed significant differences between the UCLP and non-cleft subjects in oropharyngeal volume (p=0.003), hypopharyngeal volume (p=0.020), total volume (p=0.013) and the most constricted axial area of the oropharyngeal airway (p=0.004). Furthermore, Figure 6 and 7 display the averages of the upper pharyngeal airway parts' volume and the corresponding most constricted cross-sectional areas.

Discussions

In this study, we aimed to compare the upper pharyngeal airway in Thai children with and without Unilateral Cleft Lip and Palate (UCLP) in the supine position. Orofacial clefts are common congenital defects that can

Table 2: The baseline demographics and polysomnographic findings

Variables		UCLP (n=34)	Non-cleft (n=32)	p-value
Demographic				
Sex	cases	male, 21; female, 13	male, 19; female, 13	0.020 ^a
Age (years)	mean±SD	8.94±1.87	10.03±1.91	0.002 ^a
Weight (kg)	mean±SD	30.01±9.57	40.90±17.21	0.003 ^a
Height (cm)	mean±SD	130.38±12.08	141.02±15.52	0.032 ^a
Body mass index (kg/m ²)	mean±SD	17.32±3.63	19.87±5.35	
Adenotonsillar hypertrophy index				
Tonsil size				
Brodsky scale 0	cases	8	7	
Brodsky scale 1	cases	11	3	
Brodsky scale 2	cases	8	14	0.102 ^b
Brodsky scale 3	cases	7	7	
Brodsky scale 4	cases	0	1	
Adenoid-to-choanal opening ratio	percentage	55.85±22.83	45.16±22.41	0.059 ^a
Polysomnographic findings				
Apnea-hypopnea index	per hour	2.23±3.05	2.53±3.93	0.733 ^a
Desaturation index	per hour	3.78±3.27	4.63±5.80	0.463 ^a
Minimum oxygen saturation	percentage	79.03±8.38	80.34±8.84	0.538 ^a
Average oxygen saturation	percentage	97.52±0.87	96.93±1.12	0.019 ^a

UCLP=unilateral cleft lip and palate; ^aOne-way ANOVA; ^bFisher’s Exact test; * indicates statistical significance: *p*<0.01

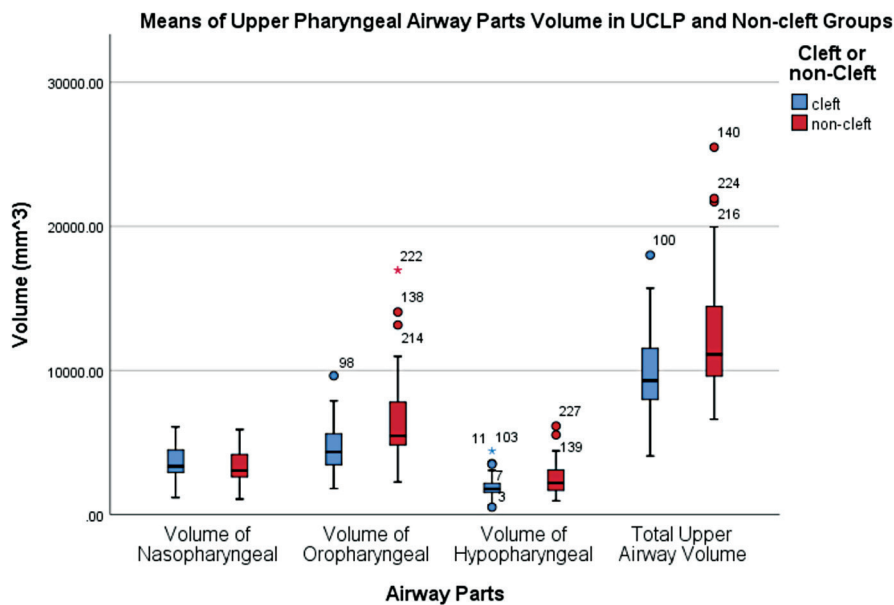


Figure 6: Box plots for the comparisons of the means volume of upper pharyngeal airway between UCLP and non-cleft groups.

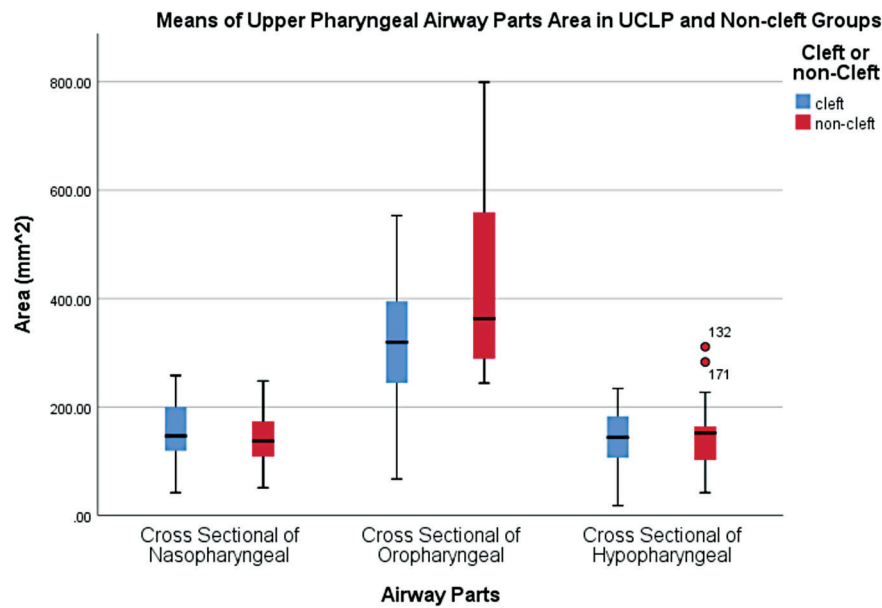


Figure 7: Box plots for the comparisons of the means of the most constricted cross-sectional area in each airway (mm²) between two groups.

impact facial growth and lead to medical conditions such as obstructive sleep apneas. The upper pharyngeal airway has been identified as a crucial risk factor for sleep-related breathing disorders in these children. To achieve this comparison, we used 3D cone beam computed tomography (CBCT) and polysomnography data. The findings from this study contribute to a better understanding of the airway differences in children with UCLP, potentially aiding in the development of targeted interventions for better respiratory health and improved quality of life.

The results of this study revealed that the mean total volume of the upper pharyngeal airway in non-cleft patients was significantly larger compared to the UCLP groups. This finding is supported by Celikoglu *et al.*⁽²³⁾ and Karia *et al.*⁽³¹⁾, who also reported decreased volumes and cross-sectional areas of the oropharyngeal and total upper airways in UCLP patients.

Regarding the nasopharyngeal airway, the mean volume and the most constricted cross-sectional area were larger in the UCLP group than in the non-cleft group, although the difference was not statistically significant, as supported by Rana *et al.*⁽²⁵⁾ Notably, despite palatoplasty surgery being performed in cleft patients, the percentage of adenoid glands in each group was quite similar to that in non-cleft patients. This could imply that the surgical deformities may have induced larger spaces in the nasopharyngeal airway. Additionally, it is important to consider that the use of PNS points as one of the landmarks

for nasopharyngeal airway measurement could influence these values⁽³⁾, as noted by Trindade *et al.*⁽³²⁾ who found anteriorly located nasal constriction in repaired cleft sides. In this study, we observed a significant difference in the mean volume of the hypopharyngeal airway between UCLP patients and non-cleft patients. Specifically, the hypopharyngeal airway volume in UCLP patients was found to be considerably smaller compared to the non-cleft group. This finding aligns with previous research by Yoshihara *et al.*⁽⁴⁾ and Mattos *et al.*⁽³³⁾, who also reported a significantly larger mean volume of the oropharyngeal airway in the non-cleft group compared to the UCLP group. This reduction volume of the oropharyngeal airway in UCLP patients may be contributed to scar contraction resulting from the reparative procedures for the orofacial deformities.⁽³⁴⁾

Moreover, our study found that the tongue positions in cleft patients were lower than those in non-cleft patients, primarily due to the smaller maxilla and the asymmetric anatomical shape of the dorsum of the tongue. Cleft patients also exhibited a higher number of muscle fibers in their tongues compared to normal children.⁽³⁵⁾ These unique characteristics of cleft patients might contribute to the observed differences in airway volume, particularly in the hypopharyngeal area, leading to a reduction in the hypopharyngeal airway volume in UCLP patients. However, our study found that the most constricted areas of the hypopharyngeal airway showed no

significant difference between the two groups.

The mean total volume of the upper pharyngeal airway was significantly lower in children with UCLP children compared to non-cleft children, possibly due to the deformities resulting from the surgical procedures. Despite using CBCT images with a voxel size of 0.4 mm, previous research reported no significant differences in measurement accuracy between voxel sizes of 0.2 mm and 0.4 mm.⁽³⁶⁾ Taking a CBCT in the supine position, akin to sleeping, is relevant as gravity has been shown to influence airway shape and volume in different body positions.^(27,37) However, it is worth noting that CBCT measurements of the minimum axial area and cross-sectional area at the level of vallecula in the pharyngeal airway may be subject to unreliability, as mentioned by Mattos *et al.*⁽³³⁾ Additionally, the study was limited in its inability to control for craniocervical inclination during CBCT scans, which could influence the alteration of the pharyngeal airway space⁽³⁸⁾ due to constraints with the MobiiScan system. On the other hand Rana *et al.*⁽²⁵⁾ suggested that using landmarks based on bony structures and soft tissue anatomy in the sagittal view of 2D cephalometric radiograph could minimize inaccuracies in measurements and allow reproducibility by other specialists. However, in UCLP patients with severe palate malformations, the shorter PNS points were more challenging to accurately mark.⁽³⁾

An additional limitation of the research is related to the postoperative deformities observed in UCLP children following cheiloplasty and palatoplasty procedures. These deformities have the potential to impact the anatomical structure and function of the participants. To mitigate of individual growth variations, subjects with dramatically different baseline demographics and measures were excluded.

Conclusions

In conclusion, this study provided comparison results of the upper pharyngeal airway in Thai children with and without UCLP in the supine position. We found that the volume and most constricted cross-sectional areas of the nasopharyngeal airway did not significantly differ between the UCLP and non-cleft groups. However, the oropharyngeal airway in the UCLP group exhibited significantly smaller volume compared to the non-cleft group, as did the hypopharyngeal airway. The total volume of the

upper pharyngeal airway was also significantly less in the UCLP group. These findings highlight the importance of assessing the pharyngeal airway in children with UCLP, as it may have implications for their respiratory health and overall quality of life.

Acknowledgments

The authors extend their sincere gratitude to the Princess Sirindhorn IT Foundation Craniofacial Center, Chiang Mai University, and the Cleft Center of the Faculty of Dentistry, Chiang Mai University, Thailand, for providing patient data. We would also like to express our thanks to NECTEC for their support in providing the MobiiScan machine for the study. Special appreciation is given to Prof. Dr. Chairat Neruntarat for his valuable comments and insights. Additionally, we acknowledge Dr. Chin Osathanunkul for conducting the statistical analysis. Their contributions have been instrumental in the successful completion of this research.

Conflicts of Interest

The authors declare no conflicts of interest.

Funding Statement

This study was funded by the Research Fund, Faculty of Dentistry, Chiang Mai University, Thailand to Chaiworawitkul M.

Reference

1. Muntz H, Wilson M, Park A, Smith M, Grimmer F. Sleep disordered breathing and obstructive sleep apnea in the cleft population. *Laryngoscope*. 2008;118(2):348-53.
2. Chaiworawitkul M. Incidence, etiology, and prevention of cleft lip and/or palate. *CM Dent J*. 2012;33(2):45-55.
3. Dec W, Olivera O, Shetye P, Cutting CB, Grayson BH, Warren SM. Cleft palate midface is both hypoplastic and displaced. *J Craniofac Surg*. 2013;24:89-93.
4. Yoshihara M, Terajima M, Yanagita N, Hyakutake H, Kanomi R, Kitahara T, *et al.* Three-dimensional analysis of the pharyngeal airway morphology in growing Japanese girls with and without cleft lip and palate. *Am J Orthod Dentofacial Orthop*. 2012;141(4 Suppl):S92-101.
5. Carlson AR, Sobol DL, Pien IJ, Allori AC, Marcus JR, Watkins SE, *et al.* Obstructive sleep apnea in children with cleft lip and/or palate: results of an epidemiologic study. *Dent Oral Craniofac Res*. 2017;3(4):1-7.

6. Cielo CM, Taylor JA, Vossough A, Radcliffe J, Thomas A, Bradford R, *et al.* Evolution of obstructive sleep apnea in infants with cleft palate and micrognathia. *J Clin Sleep Med.* 2016;12(7):979-87.
7. MacLean J, Fitzmons D, Fitzgerald D, Waters K. Comparison of clinical symptoms and severity of sleep-disordered breathing in children with and without cleft lip and/or Palate. *Cleft Palate Craniofac J.* 2017;54(5):523-9.
8. Aslan BI, Gülşen A, Tirank ŞB, Findikçioğlu K, Uzuner FD, Tutar H, *et al.* Family functions and life quality of parents of children with cleft lip and palate. *J Craniofac Surg.* 2018;29(6):1614-8.
9. Robison J, Otteson T. Increased prevalence of obstructive sleep apnea in patients with cleft palate. *Arch Otolaryngol Head Neck Surg.* 2011;137(3):269-74.
10. Society AT. Standards and indications for cardiopulmonary sleep studies in children. *Am J Respir Crit Care Med.* 1996;153(2):866-78.
11. Dehlink E, Tan HL. Update on paediatric obstructive sleep apnoea. *J Thorac Dis.* 2016;8(2):224-35.
12. Marcus CL, Brooks LJ, Draper K, Gozal D. Clinical practice guideline: diagnosis and management of childhood obstructive sleep apnea syndrome. *Pediatrics.* 2002;109(4):704-12.
13. Kaditis A, Kheirandish-Gozal L, Gozal D. Algorithm for the diagnosis and treatment of pediatric OSA: a proposal of two pediatric sleep centers. *Sleep Med.* 2012;13:217-27.
14. Ho ACH, Savoldi F, Wong RWK, Fung SC, Li SKY, Yang Y, *et al.* Prevalence and risk factors for obstructive sleep apnea syndrome among children and adolescents with cleft lip and palate: a survey study in Hong Kong. *Cleft Palate Craniofac J.* 2023;60(4):421-9.
15. Jafari B, Mohsenin V. Polysomnography. *Clin Chest Med.* 2010;31(2):287-97.
16. Marcus CL, Brooks LJ, Draper KA, Gozal D, Halbower AC, Jones J, *et al.* Diagnosis and management of childhood obstructive sleep apnea syndrome. *Pediatrics.* 2012;130(3):e714-55.
17. Sonsuwan N, Suchachaisri S, Chaloeykitti L. The relationships between cephalometric parameters and severity of obstructive sleep apnea. *Auris Nasus Larynx.* 2011;38(1):83-7.
18. Abramson Z, Susarla S, Tagoni J, Kaban L. Three-dimensional computed tomographic analysis of airway anatomy. *J Oral Maxillofac Surg.* 2010;68(2):363-71.
19. Cevidanesa L, Stynerb M, Proffit WR. Image analysis and superimposition of 3-dimensional conebeam computed tomography models. *Am J Orthod Dentofacial Orthop.* 2006;129(5):611-8.
20. Weissheimer A, Menezes L, Sameshima G, Enciso R, Pham J, Grauer D. Imaging software accuracy for 3-dimensional analysis of the upper airway. *Am J Orthod Dentofacial Orthop.* 2012;142(6):801-13.
21. Ghoneima A, Kula K. Accuracy and reliability of cone-beam computed tomography for airway volume analysis. *Eur J Orthod.* 2013;35(2):256-61.
22. Oosterkamp B, Rimmelink H, Pruim G, Hoekema A, Dijkstra P. Craniofacial, craniocervical, and pharyngeal morphology in bilateral cleft lip and palate and obstructive sleep apnea patients. *Cleft Palate Craniofac J.* 2007;44(1):1-7.
23. Celikoglu M, Buyuk S, Sekerci A, Ucar F, Cantekin K. Three-dimensional evaluation of the pharyngeal airway volumes in patients affected by unilateral cleft lip and palate. *Am J Orthod Dentofacial Orthop.* 2014;145(6):780-6.
24. Cielo CM, Marcus CL. Obstructive sleep apnea in children with craniofacial syndrome. *Paediatr Respir Rev.* 2015;16(3):189-96.
25. Rana S, Duggal R, Kharbanda O. Area and volume of the pharyngeal airway in surgical treated unilateral cleft lip and palate patient: A cone beam computed tomography study. *J Cleft Lip Palate Craniofacial Anomalies.* 2015;2(1):27-33.
26. Campos LD, Trindade IEK, Yatabe M, Trindade SHK, Pimenta LA, Kimbell J, *et al.* Reduced pharyngeal dimensions and obstructive sleep apnea in adults with cleft lip/palate and class III malocclusion. *Cranio.* 2021;39(6):484-90.
27. Sutthiprapaporn P, Tanimoto K, Ohtsuka M, Nagasaki T, Lida Y, Katsumata A. Positional changes of oropharyngeal structures due to gravity in the upright and supine positions. *Dentomaxillofac Radiol.* 2008;37(3):130-5.
28. Cahali M, Soares C, Dantas D, Formigoni G. Tonsil volume, tonsil grade and obstructive sleep apnea: is there any meaningful correlation?. *Clinics (Sao Paulo).* 2011;66(8):1347-51.
29. Sharifkashani S, Dabirmoghaddam P, Kheirkhah M, Hosseinzadehnik R. A new clinical scoring system for adenoid hypertrophy in children. *Iran J Otorhinolaryngol.* 2015;27(1):55-61.
30. NECTEC. MobiiScann [Internet]. 2016 Oct 3, [updated 2016 Oct 3; cited 2019 Apr 8]. Available from: <https://www.nectec.or.th/innovation/innovation-hardware-electronics/mobiiscan.html>
31. Karia H, Shrivastav S, Karia A. Three-dimensional evaluation of the airway spaces in patients with and without cleft lip and palate: a digital volume tomographic study. *Am J Orthod Dentofacial Orthop.* 2017;152(3):371-81.
32. Trindade I, Gomes A, Fernandes M, Trindade S, Filho O. Nasal airway dimensions of children with repaired unilateral cleft lip and palate. *Cleft Palate Craniofac J.* 2015;52(5):512-6.
33. Mattos CT, Cruz CV, da Matta TC, Pereira Lde A, Solon-de-Mello Pde A, Ruellas AC, *et al.* Reliability of upper airway linear, area, and volumetric measurements in cone-beam computed tomography. *Am J Orthod Dentofacial Orthop.* 2014;145:188-97.

34. Abdel-Aziz M, Hussien A, Kamel A, Azooz K, Fawaz M. The impact of velopharyngeal surgery on the polysomnographic parameters after cleft palate repair. *J Craniofac Surg*. 2018;29(3):717-9.
35. Starikova NV, Nadtochiĭ AG, Safronova IuA, Fomina GI, Volkova KN. Tongue structure, position and function in cleft lip and palate children assessed by ultrasound examination. *Stomatologĭia (Mosk)*. 2012;91(3):56-60.
36. Fernandes T, Adamczyk J, Poleti M, Henriques J, Friedland B, Garib D. Comparison between 3D volumetric rendering and multiplanar slices on the reliability of linear measurements on CBCT images: an *in vitro* study. *J Appl Oral Sci*. 2015;23(1):56-63.
37. Hsu W, Wu T. Comparison of upper airway measurement by lateral cephalogram in upright position and CBCT in supine position. *J Dent Sci*. 2019;14:185-91.
38. Muto T, Takeda S, Kanazawa M, Yamazaki A, Fujiwara Y, Mizoguchi I. The effect of head posture on the pharyngeal airway space (PAS). *Int J Oral Maxillofac Surg*. 2002;31(6):579-83.



Editor:
Awiruth Klaisiri,
Thammasat University, Thailand.

Received: October 26, 2023
Revised: December 8, 2023
Accepted: December 14, 2023

Corresponding Author:
Dr. Suparaksa Yamockul,
Department of Prosthodontics,
Faculty of Dentistry, Chulalongkorn
University, Bangkok 10330, Thailand
E-mail: nienee23@gmail.com

Comparative Radiopacity Evaluation of Eight Provisional Restoration Materials

Wisarut Prawatvatchara¹, Suparaksa Yamockul¹, Pranpreeya Chaiteerapapkul¹,
Siriporn Arunpraditkul²

¹Department of Prosthodontics, Faculty of Dentistry, Chulalongkorn University, Bangkok, Thailand

²Part-time lecturer, Department of Prosthodontics, Faculty of Dentistry, Chulalongkorn University, Bangkok, Thailand

Abstract

Objectives: The purpose of this study was to evaluate the radiopacity value of eight provisional restorative materials.

Methods: The specimens were divided into 8 groups (n=10) based on commercial product which were UNIFAST Trad, Dentalon Plus, Luxatemp Star, Luxatemp Fluorescence, LuxaCrown, Prottemp 4, SmarTemp X1 and VIPI BLOCK TRILUX. Disc specimens of provisional restoration materials (diameter: 6 mm and thickness: 1 mm) were fabricated by manufacturer's instruction. The samples were digitally radiographed together the aluminium step wedge used as standard for radiologic analysis. The digital radiographic images were performed and analyzed with Image J program. The relationship between the gray value for each specimen and the aluminium step wedge thickness were plotted. Data were analyzed using one-way analysis of variance (ANOVA) and Post hoc Tukey's test at 95% confidence level.

Results: Luxatemp Fluorescence showed the highest radiopacity value ($p<0.05$). While UNIFAST Trad and Dentalon Plus demonstrated the lowest radiopacity value ($p<0.05$) in all group of specimens. Prottemp 4 did not show a statistically significant difference from VIPI BLOCK TRILUX groups ($p>0.05$).

Conclusions: There were statistically significant of radiopaque among eight groups of provisional restoration materials

Keywords: Bis-acryl composite materials, PEMA, PMMA, provisional restoration, radiopacity

Introduction

Before the final restoration, the provisional restoration plays an important part in the treatment procedure for a fixed prosthesis.^(1,2) The provisional restoration protects the pulpal tissue from injuries that could be caused by physical, chemical, or thermal forces. It also ensures the tooth's stability, occlusal function, and periodontal health, and it allows for an evaluation in an area that is highly concerned with esthetics to achieve an acceptable emergence profile.⁽¹⁻⁴⁾

The incidence of aspiration or ingestion of dental appliances and prosthesis materials has often been frequently reported⁽⁵⁻¹⁵⁾, such as removable prostheses^(5-7,10-12), crowns, inlays, orthodontic attachments, provisional crowns⁽¹³⁾, bridges⁽¹⁴⁾, impression materials⁽¹⁵⁾, burs, and clamps. The present symptoms are choking, dyspnea, and dysphagia.⁽⁷⁾ In severe cases, it may cause a harmful complication such as asphyxiation⁽⁸⁾, bleeding from the digestive or airway tract mucosa⁽⁹⁻¹¹⁾, and septicemia.⁽¹²⁾

Many studies have tried to develop a radiopaque material because these materials can be localized to their position in radiographic examination.⁽¹⁶⁻¹⁹⁾ On the other hand, radiolucent materials make it difficult to localize their position, so many studies suggest using radiopaque restorative materials in patients.⁽²⁰⁾ Hence, the provisional restoration materials should not only have an accepted mechanical property but also a desirable radiopaque property because, when they dislodge or fracture, their fragments can be detected in a radiographic image, and they could be removed if they impact the airway or digestive tract. Moreover, evaluating the marginal discrepancy of provisional restoration, which predicts the quality of temporalization and periodontal health.^(3,4)

The International Standards Organization ISO10477: 2018 Dentistry-Polymer-based crown and bridge materials⁽²¹⁾ does not define that radiopacity should be. Various studies propose that the optimal radiopacity for optimal clinical performance should be equal to or higher than the same thickness of aluminium^(22,23), more radiopaque than human dentine^(24,25) or slightly higher radiopaque than enamel.^(26,27)

From the past to the present, polymethyl methacrylate (PMMA), polyethyl methacrylate (PEMA), and Bis-acryl composite materials have been used as provisional restoration materials. They have different strengths

and weaknesses. In terms of radiopacity, many studies evaluated the effect of radiopacified agents such as lithium, barium, zirconium, strontium, zinc, or other metal compounds on dental restoration materials.^(18,28-30) However, there are a few studies that compare the radiopacity of provisional restoration materials, especially between PMMA, PEMA, and Bis-acryl composite materials.

The objective of this study was to investigate the radiopacity of eight groups of provisional restorative materials. The null hypotheses were that the radiopacity of provisional restoration materials was not statistically different from each other.

Material and Methods

The provisional restoration materials used in this study are listed in Table 1. Disc-shaped specimens (n=10) from 8 provisional restoration materials were prepared according to the manufacturer's instructions with a silicone mold (6 mm in diameter and 1.4 mm in height) (Figure 1).

For PMMA materials (UNIFAST Trad), they were prepared following a manufacturer's recommendation. powder/liquid ratio, which measured 1 g of powder to 0.5 ml of liquid. The liquid was then poured into a rubber cup. Next, add the powder, and mix thoroughly for 20-30 seconds with a mixing spatula. When the mixture reaches a dough state, put it into a silicone mold. The silicone mold surface was covered with a glass slide and constantly pressed by the weight of 1000 g for 10 minutes. After setting, remove the specimen from the mold.

For PEMA materials (Dentalon Plus), they were also prepared following a manufacturer's instruction, the powder/liquid ratio, which measured 2 g of powder to 1.2 ml of liquid. The liquid was then poured into a rubber

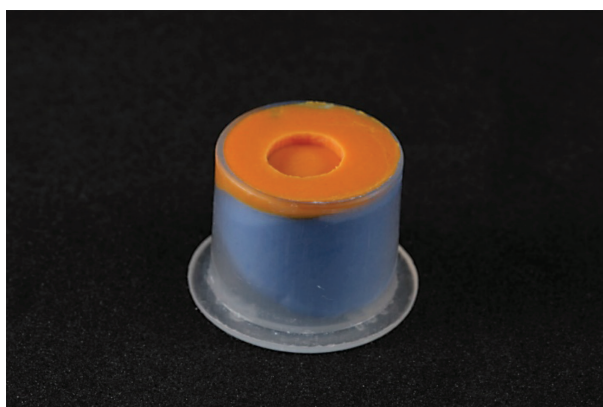


Figure 1: Silicone mold with a hole in the middle.

cup. Next, add the powder, and mix for 40 seconds with a mixing spatula. The process after these is like the PMMA materials previously described.

For Bis-acryl materials (Luxatemp Star, Luxatemp Fluorescence, LuxaCrown, Protemp 4 and SmarTemp X1), they were directly dispensed into silicone mold by using a dispensing gun. The process after these as the similar as PMMA materials that previously described.

For milling PMMA material (VIPI BLOCK TRI-LUX), the block was designed and milled at the bottom part to obtain the shade A3 by a milling machine (VHF CAM 5-S1 Impression, Bimedis, Ternopil Region, Ukraine).

All specimens were polished on both sides with 2000-grit silicon carbide paper (PACE Technologies, Tucson, AZ, USA). A digital vernier caliper (Model CD-6 CS, Mitutoyo Corp., Kanagawa, Japan) was utilized to verify their dimensions of 6 mm in diameter and 1 mm in height, which determined a critical tolerance of 1 ± 0.01 mm and evaluated and excluded the defective specimens with a stereomicroscope (Olympus Stereo Microscopes, SZ61, Tokyo, Japan) at a magnification of $\times 40$. All specimens were cleaned with distilled water using an ultrasonic cleanser for 10 minutes and soaked in distilled water in an incubator (Contherm 160M, Contherm Scientific Ltd., Korokoro, Lower Hutt, New Zealand) for 24 hours before starting the test. The metal step wedge was prepared from 98% pure aluminium (DHEF Inc., Taipei, Taiwan). It had 5 steps, each of which had a thickness of 0.5 mm, a width of 4 mm, and a length of 6 mm (Figure 2).

The specimens from each group were placed on a digital radiograph sensor (3x4 cm Digora Imaging Plate) in two lines at 2 mm distances from each other. The metal step wedge was placed beside these two lines (Figure 3).

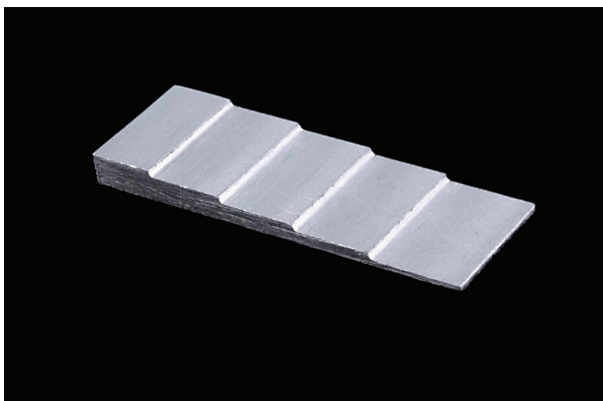


Figure 2: 5-step wedge made from aluminium.



Figure 3: Specimens and aluminium step wedge placed on the sensor.

Two clear acrylic plates were produced for a stabilized base and a fixed, constant distance from the radiation source of 12 mm (Figure 4). Specimens were radiographed by a dental X-ray system (Planmeca Prox machine, Planmeca Oy, Helsinki, Finland) at 60 kV and 7 mA for a 0.211-second exposure time. After that, all 10 digital files of specimens and an aluminium step wedge (Figure 5) were transferred to Image J software (Image J1.41, Wayne Rasband, National Institutes of Health, Bethesda, MD, USA) for analysis in grayscale. The digital analysis area was 60 mm^2 . The mean gray values, which were obtained from 10 gray valves, were calculated into the mean gray value, and plotted for equations and calibration curves: $Y = 92.607\ln(x) + 109.78$ or $x = e^{\frac{y-109.78}{92.607}}$, which was a relation between aluminium thickness (Y) and gray value (x) (Figure 6).

For each specimen, the gray values were obtained from 12.5 mm^2 of specimen area. The mean gray value of each specimen group was obtained from 10 readings per material (n=10). The equation and calibration curves were then used for calculating the mean gray value of the material group and turned into equivalent aluminium thickness values.

The aluminium thickness values of specimens were calculated, and the data were statistically analyzed using one-way analysis of variance (ANOVA) followed by Tukey's test at a significant level of $p < 0.05$.

Results

The equation and calibration curves $Y = 92.607\ln(x) + 109.78$ or $x = e^{\frac{y-109.78}{92.607}}$, which was a relation between aluminium thickness (Y) and gray value (x) (Figure 6) was used for converting the gray values of provisional



Figure 4: Clear acrylic hallow platform which covered the specimens and aluminium step wedge.

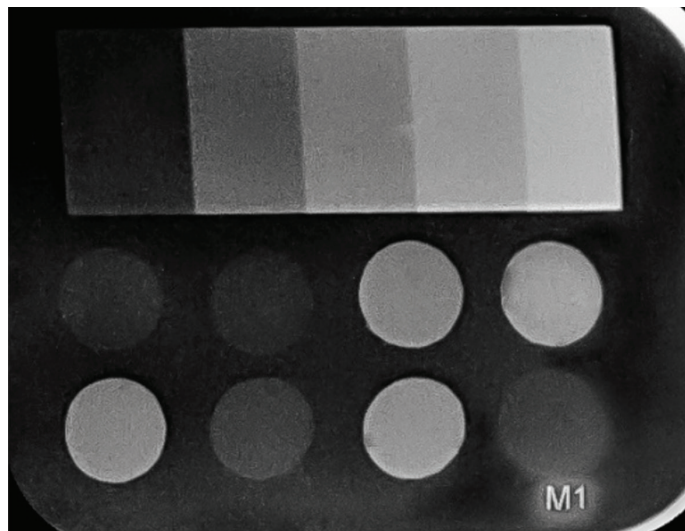


Figure 5: Digital radiograph image of specimens from 8 specimens and aluminium step wedge.

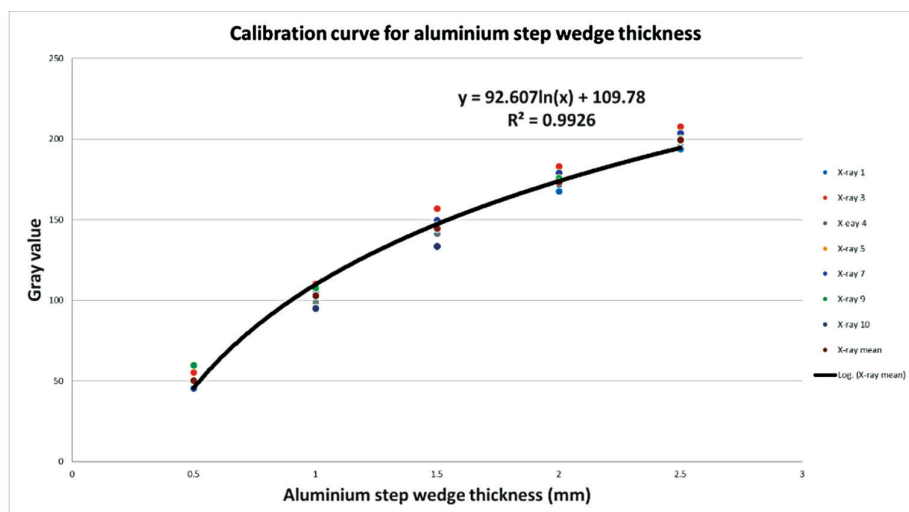


Figure 6: Calibration curve and linear equation related between the gray value (Vertical axis) and aluminium thickness value (Horizontal axis) in millimeter.

Table 1: Description of provisional restoration materials, manufacturer and composition used in this study

Brands, shade and Batch number	Manufacturer	Composition
UNIFAST Trad Ivory Batch number Powder: 1704201 Liquid: 308282	GC America, IL, USA	Powder: poly[(ethyl methacrylate)-co-(methyl methacrylate)] poly(methyl methacrylate), dibenzoyl peroxide, titanium dioxide, iron(III) oxide, cellulose acetate Liquid: Methyl methacrylate, N,N dimethyl-p-toluidine
Dentalon Plus L (light) Batch number Power: K010039 Liquid: K010100	Heraeus Kulzer GmbH, Hanau, Germany	Powder: n-butyl methacrylate, ethyl methacrylate, 2-(2-Hydroxy-3,5-di-tert-pentylphenyl)-2H-benzotriazol Liquid: n-butyl methacrylate, diurethandimethacrylate, ethyl methacrylate, methyltriocylammonium chloride
Luxatemp Star A3 Batch number 212407	DMG, Hamburg, Germany	Glass filler in a matrix of multifunctional methacrylates; catalysts, stabilizers and additives. Free of methyl methacrylate. Total filler volume: 44% wt.% or 24 vol.% (0.02 to 1.5 µm)
Luxatemp Fluorescence A3 Batch number 758441	DMG, Hamburg, Germany	Glass powder and silica, Urethane dimethacrylate, Aromatic dimethacrylate, Glycol methacrylate, catalysts, stabilizers, additives. Free from methyl methacrylate and peroxides. Filler content: 43 wt.-% or 24 vol.-%. (0.02 to 1.5 µm)
Luxacrown A3 Batch number 212209	DMG, Hamburg, Germany	Glass filler material in a matrix of multifunctional methacrylates, catalysts, stabilizers, and additives. Filler content: 46 wt.% = 26 vol.%. (0.02 to 1.5 µm)
Protemp 4 A3 Batch number 3704381	3M ESPE, Seefeld, Germany	Catalyst Paste: Ethanol, 2,2'-[(1-methylethylidene) bis(4,1-phenyleneoxy)] bis-, diacetate, Benzyl-phenyl-barbituric acid, Silane treated silica, Tert-butyl peroxy-3,5,5-trimethylhexanoate Base Paste: dimethacrylate (BISEMA 6), silane-treated amorphous silica, reaction products of 1,6-diisocyanatohexane with 2-[(2-methacryloyl) ethyl] 6-hydroxyhexanoate and 2-hydroxyethyl methacrylate (DESMA), silane-treated silica
SmarTemp X1 A3 Batch number 1913619136	Parkell Dental, Edgewood, New York, USA	Catalyst Paste: 2,4,6(1H,3H,5H)-Pyrimidinetrione, 5-phenyl-1-(phenylmethyl)-, Titanium dioxide Base Paste: Poly(oxy-1,2-ethanediyl), .alpha.,.alpha.'-[(1-methylethylidene) di-4,1-phenylene]bis[.omega.-[(2-methyl-1-oxo-2-propenyl)oxy]-, 2-Propenoic acid, 2-methyl-, (1-methylethylidene)bis[4,1-phenyleneoxy(2-hydroxy-3,1-propanediyl)] ester, 2-Propenoic acid, 2-methyl-, 1,6-hexanediyl ester, Tripropylene glycol diacrylate Copper, bis(2,4-pentanedionato-O,O')
VIPI BLOCK TRILUX Monocolor A3	Dental Vipi Ltda., Pirassununga, SP, Brazil	Polymethyl methacrylate, pigments, Polymerized Ethylene Dimethacrylate (EDMA), Fluorescent

restoration materials to aluminium thickness mean values (Table 2).

This result showed that the radiopacity of provisional restoration material ranged from 0.493 to 1.622 mm aluminium thickness. Luxatemp Fluorescence had the significantly highest aluminium thickness value in all groups of specimens ($p < 0.05$). SmarTempX1 and Luxatemp Star showed significantly higher aluminium thickness values than LuxaCrown ($p < 0.05$). VIPI BLOCK TRILUX had a significantly higher aluminium thickness value than UNIFAST Trad and Dentalon Plus ($p < 0.05$). While Protemp 4 did not show a statistically significant difference from VIPI BLOCK TRILUX groups ($p > 0.05$). Moreover, both UNIFAST Trad and Dentalon Plus had the lowest aluminium thickness values in all groups of specimens ($p < 0.05$).

Discussions

The result of this study revealed that eight provisional restoration materials showed different radiopacity values. Therefore, the null hypothesis of this study was rejected. Today, dental resins are often employed; however, some of them are radiolucent and cannot be scanned with conventional radiographic methods. The detection of these materials may be extremely challenging in cases of unintentional ingestion, aspiration, or traumatic impaction, necessitating invasive procedures or advanced imaging methods. Delays in locating or removing the foreign body could endanger the patient's life. Swallowing or aspirating dental prostheses are relatively uncommon, although it is rare. The bulk of foreign bodies originate through the oral, resulting in frequent injuries and fatalities.⁽³¹⁻³⁴⁾

Consequently, radiopaque properties are essential for dental materials, including temporary restorations, that are used in the oral cavity. Furthermore, the radiopaque properties enable the operator to identify the marginal adaptability of temporary restoration.

In this investigation, a pure aluminium step wedge was utilized since its radiopacity value is more consistent than that of human dentin and enamel, whose values are highly variable.

Human tooth enamel is the hardest and most highly mineralized substance in the human body. It is a bone and not a tissue, which is composed of 92-96% inorganic matter, 1-2% organic material, and 3-4% water in weight.⁽³⁵⁾ Most of the inorganic matter is $\text{Ca}_{10}(\text{PO}_4)_6(\text{OH})_2$, hydroxyapatite, but other atomic elements can be detected as Copper, Potassium, Chloride, Zinc, Iron, Titanium, Strontium, Vanadium, Manganese and Zirconium by using Particle-induced X-ray emission (PIXE) and Particle-induced x-ray emission (PIGE) techniques.⁽³⁶⁾ Regarding a hydrated biological composite, human dentin has a lower inorganic concentration than enamel, and it is made of 70 % inorganic material, 18 % organic matrix, and 12 % water (wt. %).⁽³⁷⁾ This different composition not only affects the mechanical properties of each tooth tissue⁽³⁸⁾ but, since teeth of different animal species may have different composition, the radiodensity of tooth structures are also expected to be influenced. Therefore, many studies reported that the radiopacity of human dentin and enamel was equal to 0.7-1.16 mm and 1.84-2.20 mm thickness of aluminium, respectively.⁽³⁹⁻⁴¹⁾ Although ISO 4049:2019 Dentistry — Polymer-based restorative materials recommended that the radiopacity should be slightly higher than that of dentin radiopacity⁽⁴²⁾, The

Table 2: Means and standard deviations (SD) of gray value and equivalent aluminium step wedge thickness values of the tested materials.

Brands	Gray value (Mean±SD)	Aluminium thickness value (Mean±SD) [#]
UNIFAST Trad	49.104±7.808	0.538±0.045 ^E
Dentalon Plus	51.172±10.609	0.552±0.062 ^E
Luxatemp Star	117.384±5.589	1.315±0.104 ^B
Luxatemp Fluorescence	149.373±5.219	1.536±0.086 ^A
LuxaCrown	111.473±15.770	1.066±0.184 ^C
Protemp 4	75.455±4.291	0.714±0.032 ^D
SmarTempX1	122.981±9.858	1.197±0.128 ^{B^C}
VIPI BLOCK TRILUX	88.723±4.538	0.824±0.040 ^D

Identical letters in the column indicate no statistically significant differences ($p > 0.05$), while non-identical letters in the column indicate statistically significant differences ($p < 0.05$).

result of these studies demonstrated that UNIFAST Trad, Dentalon Plus, and Protemp 4 had lower radiopacity values than dentin. Moreover, their radiopacity values were lower than 1 mm of aluminium thickness, which means that the radiopacity properties of these materials did not meet the requirements of the restorative materials.⁽²²⁾

Nowadays, the radiopacity value of restorative resin used to reconstruct teeth should be distinguished from dentin in accordance with ISO requirements. However, X-rays will locate these materials in the event of an accident (such as one involving the GI tract or airway) but the radiopacity value is still not specified by any standard for these accidental occurrences. Thus, this investigation followed ISO 4049.

The radiopacity of provisional material groups shows significant difference because of radiopaque filler in their composition, as shown in Table 1.

In terms of radiopacity for provisional restoration materials, some of the tested materials were not specific in the type of fillers used in their formulation. But in basic knowledge, it is well known that the high atomic number elements of inorganic filler compounds play an important role in radiopaque value, such as titanium, strontium, yttrium, zirconium, barium, bismuth, and ytterbium. Therefore, many studies endeavored to develop radiopaque polymer-based dental materials^(43,44), but the amount of radiopaque compound was limited by its physical and mechanical properties.^(43,45)

Luxatemp Fluorescence is a material exhibiting fluorescent properties that impacts the optical behavior of provisional restoration in the oral cavity. Fluorescence is a phenomenon that happens when radiation with a shorter wavelength hits a natural tooth and causes it to be absorbed, and then visible light is emitted again. In this study, Luxatemp Fluorescence demonstrated the highest radiopacity because it might be composed of more inorganic filler and rare earth oxide⁽⁴⁶⁾, which are commonly used as fluorescence compounds for simulating natural tooth appearance under ultraviolet rays. The high atomic number of rare earth oxides may participate in the radiopaque of this specimen group. While SmarTempX1 has titanium dioxide and copper, which have a higher atomic number than the silica filler found in Protemp 4, there was no statistically significant difference between the

Dentalon Plus group and UNIFAST Trad group because they might have a few radiopaque compounds.

VIPI BLOCK TRILUX is composed of three layers of PMMA with OMC nanotechnology, which can be used to create prostheses with a natural appearance. In addition, it ensures a high molecular weight as well as superior mechanical, chemical, and abrasion resistance. All this manufacturing claims the possibility of being provisional for long-term use. But it demonstrated a radiopacity value of only 0.824±0.040 mm thickness of aluminium for a haft of Luxatemp Fluorescence (1.536±0.086 mm thickness of aluminium). This may not contain the high-atomic-number element. According to this study, the chemical makeup of various materials causes them to have distinct radiopacities. Without compromising the material's optical and physical properties, radiopacity is primarily produced by adding heavy elements (atomic number>20) to the inorganic filler phase. Due to their potential negative effects on aesthetic materials' translucency and color stability, the addition of radiopacifiers is a process that is controlled by their properties. One of the most popular radiopacifiers is barium, although its inclusion is limited because of how it affects transparency. Because of this, the esthetic provisional materials had low radiopacity. Therefore, it is necessary to develop radiopaque aesthetic temporary materials.

Conclusions

The radiopacity of provisional restoration materials was not more than 2 mm of aluminium thickness. The Bis-acryl composite material groups had a wide range of radiopacity values. Luxatemp Fluorescence showed the highest radiopaque. However, Protemp 4, UNIFAST Trad, and Dentalon Plus demonstrated the lowest radiopaque in this study.

Acknowledgments

This study was supported by the Faculty Research Grant, Faculty of Dentistry, Chulalongkorn University, Thailand.

Conflicts of interest

The authors declare no conflicts of interest.

References

- Burns DR, Beck DA, Nelson SK. A review of selected dental literature on contemporary provisional fixed prosthodontic treatment: Report of the Committee on Research in Fixed Prosthodontics of the Academy of Fixed Prosthodontics. *J Prosthet Dent.* 2003;90(5):474-97.
- Shillingburg HT, Sather DA, Stone SE. *Fundamentals of Fixed Prosthodontics.* 4th ed. Chicago, IL, USA: Quintessence Publishing Co; 2012.
- Nejatidanesh F, Lotfi HR, Savabi O. Marginal accuracy of interim restorations fabricated from four interim autopolymerizing resins. *J Prosthet Dent.* 2006;95(5):364-7.
- Yuodelis RA, Faucher R. Provisional restorations: an integrated approach to periodontics and restorative dentistry. *Dent Clin North Am.* 1980;24(2):285-303.
- Goodacre CJ. A dislodged and swallowed unilateral removable partial denture. *J Prosthet Dent.* 1987;58(1):124-5.
- Kerr AG. Swallowed dentures. *Br Dent J.* 1966;120(12):595-8.
- Hashimi S, Walter J, Smith W. Swallowed partial dentures. *J R Soc Med.* 2004;97(2):72-5.
- Adelman HC. Asphyxial deaths as a result of aspiration of dental appliances: a report of three cases. *J Forensic Sci.* 1988;33(2):389-95.
- Huh JY. Foreign body aspirations in dental clinics: a narrative review. *J Dent Anesth Pain Med.* 2022;22(3):161-74.
- Rajesh PB, Goiti JJ. Late onset tracheo-oesophageal fistula following a swallowed dental plate. *Eur J Cardiothorac Surg.* 1993;7(12):661-2.
- Youngs RP, Gatland D, Brookes J. Swallowed radiolucent dental prostheses: risk of extraluminal oesophageal perforation. *J Laryngol Otol.* 1988;102(1):71-3.
- Hodges ED, Durham TM, Stanley RT. Management of aspiration and swallowing incidents: a review of the literature and report of case. *ASDC J Dent Child.* 1992;59(6):413-9.
- Hisanaga R, Takahashi T, Sato T, Yajima Y, Morinaga K, Ohata H, *et al.* Accidental ingestion or aspiration of foreign objects at Tokyo Dental College Chiba Hospital over last 4 years. *Bull Tokyo Dent Coll.* 2014;55(1):55-62.
- Basoglu OK, Buduneli N, Cagirici U, Turhan K, Aysan T. Pulmonary aspiration of a two-unit bridge during a deep sleep. *J Oral Rehabil.* 2005;32(6):461-3.
- Dent L, Peterson A, Pruett D, Beech D. Dental impression material: a rare cause of small-bowel obstruction. *J Natl Med Assoc.* 2009;101(12):1295-6.
- McCabe JF, Wilson HJ. A radio-opaque denture material. *J Dent.* 1976;4(5):211-7.
- Matsumura H, Sueyoshi M, Atsuta M. Radiopacity and physical properties of titanium-polymethacrylate composite. *J Dent Res.* 1992;71(1):2-6.
- Davy KW, Causton BE. Radio-opaque denture base: a new acrylic co-polymer. *J Dent.* 1982; 10(3):254-64.
- Tsao DH, Guilford HJ, Kazanoglu A, Bell DH. Clinical evaluation of a radiopaque denture base resin. *J Prosthet Dent.* 1984;51(4):456-8.
- Drinnan AJ. Dangers of using radiolucent dental materials. *J Amer Dent Assoc.* 1967;74(3):446-50.
- ISO 10477:2020; Dentistry-Polymer-Based Crown and Veneering Materials. International Organization for Standardization: Geneva, Switzerland, 2020.
- Gu S, Rasimick BJ, Deutsch AS, Musikant BL. Radiopacity of dental materials using a digital x-ray system. *Dent Mater.* 2006;22(8):765-70.
- Watts DC, McCabe JF. Aluminium radiopacity standards for dentistry: an international survey. *J Dent.* 1999;27(1):73-8.
- Attar N, Tam LE, McCamb D. Mechanical and physical properties of contemporary dental luting agents. *J Prosthet Dent.* 2003;89(2):127-34.
- Finger WJ, Ahlstrand WM, Fritz UB. Radiopacity of fiber reinforced resin posts. *Am J Dent.* 2002;15(2):81-4.
- Hara AT, Serra MC, Haiter-Neto F, Rodrigues AL Jr. Radiopacity of esthetic restorative materials compared with human tooth structure. *Am J Dent.* 2001;14(6):383-6.
- Willems G, Noack MJ, Inokoshi S, Lambrechts P, Van Meerbeek B, Braem M, *et al.* Radiopacity of composites compared with human enamel and dentine. *J Dent.* 1991;19(6):362-5.
- Watts DC. Radiopacity versus composition of some barium and strontium glass composites. *J Dent.* 1987;15(1):38-43.
- Taira M, Toyooka H, Miyawaki H, Yamaki M. Studies on radiopaque composites containing ZrO₂-SiO₂ fillers prepared by the sol-gel process. *Dent Mater.* 1993;9(3):167-71.
- Davy KWM, Anseau MR, Berry C. Iodinated methacrylate copolymers as x-ray opaque denture base acrylics. *J Dent.* 1997;25(6):499-505.
- Schneider SS, Roistacher S: Aspiration of denture base materials. *J Prosthet Dent.* 1971;25 (5):493-6.
- Tamura N, Nakajima T, Matsumoto S, Ohyama T, Ohashi Y. Foreign bodies of dental origin in the air and food passages. *Int J Oral Maxillofac Surg.* 1986;15(6):739-51.
- Skok P, Skok K. Urgent endoscopy in patients with "true foreign bodies" in the upper gastrointestinal tract – a retrospective study of the period 1994-2018. *Z Gastroenterol.* 2020;58(3):217-23.
- Adelman HC: Asphyxial deaths as a result of aspiration of dental appliances: a report of three cases. *J Forensic Sci.* 1988;33(2):389-95.
- Gwinnett AJ. Structure and composition of enamel. *Oper Dent.* 1992;5(Suppl):10-7.
- Rizzutto MA, Tabacniks MH, Added N, Liguori Neto R, Acquadro JC, Vilela MM, *et al.* External PIGE-PIXE measurements at the Sao Paulo 8UD tandem accelerator. *Nucl Instrum Methods.* 2002;190(1-4):186-9.
- Mjor IA. Human coronal dentin: structure and reactions. *Oral Surg Oral Med Oral Pathol.* 1972;33(5):810-23.

38. Giannini M, Soares CJ, Carvalho RM. Ultimate tensile strength of tooth structures. *Dent Mater.* 2004;20(4):322-9.
39. Pekkan G, Özcan M. Radiopacity of different resin-based and conventional luting cements compared to human and bovine teeth. *Dent Mater J.* 2012;31(1):68-75.
40. Williams JA, Billington RW. A new technique for measuring the radiopacity of natural tooth substance and restorative materials. *J Oral Rehabil.* 1987;14(3):267-9.
41. Hosney S, Abouelseoud HK, El-Mowafy O. Radiopacity of resin cements using digital radiography. *J Esthet Restor Dent.* 2017;29(3):215-21.
42. ISO 4049:2019 Dentistry- Polymer-based restorative materials; International Organization for Standardization: Geneva, Switzerland, 2019.
43. He J, Söderling E, Lassila LV, Vallittu PK. Preparation of antibacterial and radio-opaque dental resin with new polymerizable quaternary ammonium monomer. *Dent Mater.* 2015;31(5):575-82.
44. Amirouche A, Mouzali M, Watts DC. Radiopacity evaluation of bis-GMA/TEGDMA/opaque mineral filler dental composites. *J Appl Polym Sci.* 2007;104(3):1632-9.
45. Mattie PA, Rawls HR, Cabasso I. Development of a radiopaque, autopolymerizing dental acrylic resin. *J Prosthodont.* 1994;3(4):213-8.
46. Garcia IM, Leitune VCB, Takimi AS, Bergmann CP, Samuel SMW, Melo MA. Cerium dioxide particles to tune radiopacity of dental adhesives: Microstructural and physico-chemical evaluation. *J Funct Biomater.* 2020;11(1):7.



Editor:

Anak Iamaroon,
Chiang Mai University, Thailand.

Received: September 8, 2023

Revised: October 11, 2023

Accepted: December 13, 2023

Corresponding Author:

Assistant Professor Dr. Wannakamon Panyarak, Division of Oral and Maxillofacial Radiology, Department of Oral Biology and Diagnostic Sciences, Faculty of Dentistry, Chiang Mai University, Chiang Mai 50200, Thailand.

E-mail: wannakamon.p@cmu.ac.th

Dental Radiography in Age Determination: Contemporary Methods and Trends

Pornpattra Chulamane¹, Wannakamon Panyarak¹

¹Division of Oral and Maxillofacial Radiology, Department of Oral Biology and Diagnostic Sciences, Faculty of Dentistry, Chiang Mai University, Thailand

Abstract

The determination of an individual's age assumes paramount significance in forensic and legal contexts, necessitating the utilization of diverse techniques. Dental radiography emerges as a non-invasive approach for determining age-related dental changes. This method grants a comprehensive analysis of various dental features to identify an individual's precise age, place them within designated age ranges, or define whether they exceed or subordinate to specific age thresholds. This review summarizes age estimation methodologies using dental radiography and conducts the investigations into contemporary trends by reviewing relevant studies published in Pubmed between 2020 and 2023. Age categorization delineates into three distinct phases: pre-natal, neo-natal, and post-natal; childhood and adolescence; and adulthood. Panoramic radiography becomes the predominant radiographic modality, with the Demirjian method is more commonly known for age estimation in the initial two phases. In contrast, adulthood age estimation relies on anatomical changes. Significantly, artificial intelligence (AI) technology has recently attracted attention for age estimation, yielding promising results. AI demonstrates the potential to enhance the accuracy of conventional methodologies, diminishing human errors and mitigating associated workload burdens, offering inventive ground for future advancements.

Keywords: age estimation, dental imaging, dental radiography, forensic dentistry, forensic odontology

Introduction

Age estimation holds significant importance in both forensic and legal contexts. Numerous methods are employed for this purpose, involving various anatomical markers such as cranial suture closure, pubic symphysis, auricular surface, lumbar vertebrae, acetabulum, bone histomorphometry, and teeth. Among these, teeth stand out as remarkably durable components of the human body, often remaining well-preserved even after disasters or accidents. Their resilience makes them invaluable for post-incident investigations.⁽¹⁻³⁾ Age estimation from dental structures encompasses three distinct categories: morphological methods, such as assessing tooth wear⁽⁴⁻⁶⁾ and root transparency; biochemical methods, including examining aspartic acid racemization and other amino acids within the tooth⁽⁷⁻⁹⁾, and radiological methods, including evaluating tooth development and eruption^(6,10-20), and analyzing pulp size regression due to secondary dentin formation.^(6,21-32) Dental radiography has emerged as a practical, non-destructive technique that significantly aids age estimation.^(6,10-18,21-23,25-33) It is essential to acknowledge that bone and teeth growth rates exhibit variations based on nationality. Employing methods that utilize population-specific databases enhances accuracy in age estimation.^(10-13,16,19,25,29-32)

Additionally, many age estimation models have been manually developed, introducing the potential for human error.^(4,5,10-19,21,22,25,33,34) Addressing this limitation, artificial intelligence (AI) has become a promising approach for creating new age estimation models, as evidenced by previous studies.^(6,20,23,35,36) Deep learning, in particular, has gained prominence in age estimation due to its capacity to reduce human workload, enhance accuracy in detection and decision-making, and, in some cases, even classify genders as part of the age estimation process.^(6,20,35-37)

This review article is to provide a comprehensive overview and critically assess recent trends in age estimation methodologies through the application of dental radiography.

Dental radiography in age estimation

Age estimation stands as a fundamental procedure within the domain of medico-legal investigations. Historical evidence reveals that in the early 19th century, teeth served as pivotal indicators of age, particularly in relation

to child labor regulations. Notably, the English Parliament of 1837 implemented the "Teeth A Test of Age," stipulating that children under the age of nine were prohibited from employment, while those between nine and twelve years old faced restricted working hours based on dental observations related to tooth eruption.⁽³⁸⁾

Furthermore, the utilization of dental structures for age estimation has gained prominence due to their exceptional durability.⁽¹⁻³⁾ Situated within the protective confines of the oral cavity, teeth remain shielded from external environmental factors. Consequently, they exhibit a remarkable resistance to deterioration and a capacity for long-term preservation, establishing them as invaluable assets for age determination in the domains of forensic science, anthropology, and archaeology.

Dental radiography serves as a widely employed, non-invasive methodology for the examination age-related changes within teeth. This involving technique includes various modalities such as intraoral radiography (periapical radiograph), orthopantomography (OPG), cone-beam computed tomography (CBCT), and magnetic resonance imaging (MRI). The non-invasive tooth-based age estimation techniques enhance their appeal, as they eliminate the need for invasive procedures, thereby ensuring minimal disruption to samples and the preservation of invaluable remains.

The process of ascertaining an individual's age through radiological examination involves a comprehensive assessment of multiple features. These encircle the development and mineralization of tooth follicles, root resorption, and completion, and secondary dentin deposition within the pulp cavity. The outcome of this method varies, depending on the specific approach employed, ranging from the estimation of an individual's age, the classification into age groups to the determination of whether an individual falls below or above a precise age cut-off. Age can be stratified into three primary phases based on an individual's age range: pre-natal, neo-natal, and post-natal phase; children and adolescence phase; and adult and elderly phase. Chronological progression of age estimation methods across three age phases is shown in Figure 1 and described in details as follows:

1. Pre-natal, neo-natal, and post-natal phase

The initiation of primary incisor mineralization occurs during the 16th week of intrauterine development.

Prior to the tooth germs mineralization, it is discernible as a radiolucent area in the radiographic images. Subsequently, during the prenatal phase of fetal development, the mineralization of primary teeth manifests as radiopaque structures resembling teeth within radiographs.⁽³⁹⁾

In 1965, Kraus and Jordan⁽⁴⁰⁾ reported the early mineralization of primary teeth and the permanent first molar. This framework comprises ten stages, denoted by Roman numerals I to X, with stage IX further subdivided into three sub-stages and stage X into five sub-stages. This approach, known as the "tooth atlas method," is valuable for age estimation during this developmental phase.

2. Children and Adolescents phase

Age estimation through the observation of tooth development has been widely employed for assessing the age of children and adolescents. This estimation is facilitated through clinical examination and dental radiography, advantaging the precise and stable nature of tooth development. Several methods have been elucidated as follows:

2.1 Tooth development staging method

In 1960, Nolla proposed a method that relies on the observation of calcification in permanent teeth to estimate age. This method involves dividing tooth development into ten stages, including seven maxillary and mandibular teeth on the left side, from the absence of a crypt to complete root formation.⁽⁴¹⁾ The cumulative stages of all teeth provide an estimated age. In 1973, the method of Demirjian in the tooth development staging method was introduced.⁽⁴²⁾ and then in 1976, Demirjian delivered an age estimation method based on the development of seven lower left permanent teeth from the left lower central incisor to the second molar, visible in panoramic radiographs.⁽⁴³⁾ This method presents percentile standards for ages ranging from 2.5 to 17.0 years, separately for each gender. It involves eight stages, denoted A to H, representing the progression from tooth mineralization to the completion of development. Subsequent studies, such as Willems *et al.*⁽⁴⁴⁾, have adapted and modified the Demirjian method to suit their populations. Additionally, many studies have utilized the developmental stage proposed by Demirjian *et al.* to assess the development of third molars and other selected teeth, combined with chronological age, to formulate regression formulas for age estimation.^(10,19,45)

2.2 Atlas of human tooth development and eruption method

The development and eruption of primary and permanent teeth can be assessed through panoramic radiographs, serving as valuable age estimation indicators. The widely used London Atlas by AlQahtani⁽¹⁸⁾ comprehensively illustrates tooth growth and emergence, covering the entire range from ages 1 to 23, including the in-utero period from 30 weeks to birth. Various studies have explored the applicability of this method in their respective populations, yielding promising results.⁽⁴⁶⁻⁴⁸⁾

2.3 Open apices measurement method (Cameriere method)

In 2006, Cameriere introduced an age estimation method centered on measuring open apices of seven mandibular left permanent teeth, ranging from the left mandibular central incisor to the second molar. This method revealed significant and negative correlations between age and open apices in teeth. Additionally, gender and the number of teeth with completely closed root canal apical ends (N0) exhibited significant correlations with chronological age. Utilization of a stepwise multiple regression model, it was demonstrated that a linear relationship exists between open apices, N0, and age.⁽⁴⁹⁾

In instances where the roots of all seven permanent teeth roots are fully closed, attention turns to the third molars, the last teeth to develop. Some studies have indicated that the complete development of third molars can serve as an indicator of adulthood or minority status.⁽⁵⁰⁻⁵³⁾ One notable method in this context is the Third molar maturity index (I3M) proposed by Cameriere.⁽⁵⁰⁾ This index proves valuable in legal contexts to ascertain whether an individual has reached the age of maturity, typically set at 18 years. It is based on the relationship between chronological age and the I3M, defined as the ratio between the sum of two apical pulp widths measured from the inner sides of two open apices and tooth length. If the root development of the third molars is complete, $I3M = 0$, indicating that the individual is at least 18 years old; otherwise, if $I3M < 0.08$, they are classified as below 18 years old, based on the results of a logistic model.⁽⁵⁰⁾

Chronological progression of proposed age estimation methods across three distinct age phases

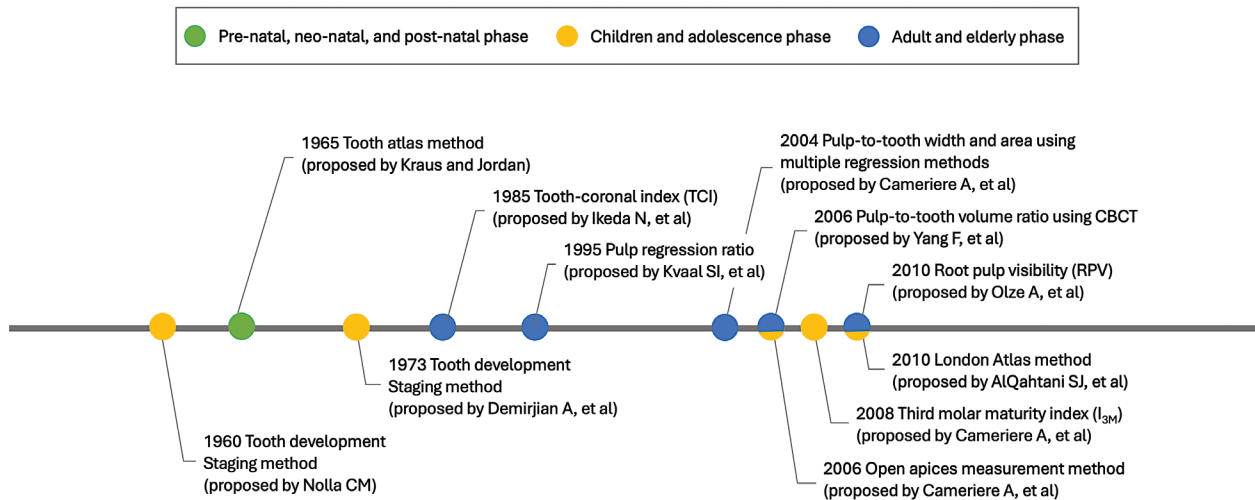


Figure 1: Chronological evolution of proposed age estimation methods across three distinct age phases: prenatal, neo-natal, and post-natal stages; childhood and adolescence stages; and adulthood stages.

3. Adult and elderly phase

3.1 Pulp regression ratio

Age estimation during late adolescence and adulthood presents challenges due to the intricate nature of fully developed permanent teeth. Estimating age based on tooth development in this age group can be inherently challenging or unavailable. Therefore, the assessment of adult age often relies on the examination of changes in secondary dentin. As individuals age, dentin thickens due to the continuous formation of secondary dentin, resulting in a reduction in the pulp cavity size. This correlation between age and the pulp regression ratio serves as a useful tool for estimating age within a specific range.^(27,54,55)

3.2 Linear measurement and ratio

The Kvaal method⁽²⁷⁾ involves the examination of pulp/root length, pulp/tooth length, and pulp/root width, which have shown associations with chronological age. Ratios were calculated to account for potential film distortion at three distinct levels. Regression analysis of these ratios was performed to develop an age estimation formula. This method is particularly valuable for assessing the age of individuals with single-rooted teeth, including the maxillary central incisor, maxillary lateral incisor, maxillary second premolar, mandibular lateral incisor, mandibular canine, and mandibular first premolar. Some studies also incorporate additional teeth, such as the maxillary canine, due to its extensive root length and minimal likelihood of being missing.^(29,32)

Additionally, the tooth-coronal index (TCI) or

coronal pulp cavity index is a widely exploited method that examines the relationship between secondary dentin deposition and age, similar to the Kvaal method. However, TCI calculations are limited to the crown area.^(54,55) The TCI, proposed by Ikeda *et al.*⁽⁵⁴⁾, is determined by measuring the coronal height (CH), defined as the maximum perpendicular distance from the cervical line to the tip of the highest cusp of the tooth. The coronal pulp cavity height (CPCH) denotes the distance from the cervical line to the coronal tip of the pulp chamber. TCI is expressed by $(CPCH \times 100) / CH$ and is analyzed for each tooth, with regression against actual age yielding an age estimation model. Precision in TCI assessment hinges on the accurate identification of reference points, including the cervical line and the mesial and distal cemento-enamel junction points, which demarcate the division between the crown and root.^(54,55)

3.3 Volumetric measurement and ratio

In 2004, Cameriere introduced an age estimation method that relies on the observation of the relationship between pulp and tooth dimensions in single-rooted teeth in panoramic radiographs. This method utilizes ratios such as pulp-tooth width, length ratio, and area ratio, pulp-to-root ratio, and tooth length. A multiple regression model revealed a linear relationship between the pulp-to-root width at the mid-level of root and age, as well as between the pulp-to-tooth area and chronological age.⁽⁵⁶⁾

Subsequently, various studies have explored the assessment of changes in pulp cavity volume using ground

truth data obtained through various radiographic techniques, including CBCT, which offers enhanced accuracy. Yang *et al.*⁽⁵⁷⁾ reported the examination of the relationship between pulp-to-tooth volume ratio and age using CBCT scans of single-rooted teeth. Customized voxel counting software was utilized, revealing a linear relationship between the pulp-to-tooth volume ratio and age.⁽⁵⁷⁾ However, correlations may vary across different genders and populations, emphasizing the importance of utilizing population-specific databases.⁽⁵⁸⁻⁶⁰⁾

3.4 Root pulp visibility (RPV)

Following the completion of tooth formation, the continuous deposition of secondary dentin gradually narrows the pulp canal lumen. This knowledge underpins an age estimation method that assesses the visibility of pulp in radiographic images.

In 2010, Olze *et al.* introduced an age estimation method that focuses on the observation of pulp visibility in fully formed mandibular third molars with apical closure. This method categorizes individuals into four stages based on the visibility of the pulp lumen within the root canals. In Stage 0, the lumen of all root canals is visible to the apex. In Stage 1, the lumen of one root canal is partially obscured. In Stage 2, the lumen of two root canals is partially obscured, or one canal may be virtually invisible its entire length. In Stage 3, the lumen of two root canals is virtually invisible throughout their entire lengths. The study results indicate uncertainty regarding whether the method can accurately determine if someone is younger than 18 when in Stage 0. However, individuals in Stages 1, 2, or 3 were all found to be at least 21 years old.⁽⁶¹⁾

Artificial intelligence aids the age estimation process.

It has become evident that many age estimation models are susceptible to human error, primarily owing to human interpretation, which can introduce variability and bias. However, this challenge finds resolution through the application of automated AI methodologies for the development of novel age estimation models. AI has the capacity to minimize human error and reduce subjectivity in age estimation. It employs standardized algorithms, enhancing the consistency and reliability of age estimations by evaluating a multitude of dental features, from tooth development stages to anatomical changes, facilitating more precise age predictions.

Prior investigations have demonstrated the efficacy of AI-powered age estimation models, guiding in several advantages, including significant cost and resource savings.^(20,62)

While AI assistance in age estimation predominantly revolves around binary or multiple-group age classification, a lesser number of models aspire to achieve numeric age regression. Deep learning has garnered prominence in the ground of age estimation due to its capacity to minimize human intervention while simultaneously enhancing accuracy in the processes of detection and decision-making. Certain studies have exploited deep learning further to classify genders within the context of age estimation.

Numerous studies have embraced fully automatic, deep-learning-based solutions offering two significant advantages. Firstly, these methods require annotation exclusively in terms of expected age, thus reducing the time investment as the traditional process in dental age estimation is mostly manually done and allowing the utilization of expansive datasets comprising thousands of images. Secondly, these approaches circumvent the need for expert identification of specific teeth and bone structures, instead relying on image components that the algorithm deems most relevant to the task at hand.⁽⁶³⁾ Notably, these automatic methodologies maintain functionality even in scenarios involving missing teeth. While these automatic techniques have elevated the performance and utility of dental age estimation methods, there exists room for enhancement in their validation.

The relatively recent emergence of deep learning techniques implies that the automatic methodologies have yet to undergo comprehensive testing across diverse populations or acquisition devices beyond their original contexts. This imparts a degree of uncertainty regarding their generalizability to varied scenarios. Nevertheless, the versatility of these methods enables simplistic adaptation to distinct situations through the employment of specialized domain adaptation techniques, such as transfer learning or fine-tuning.⁽⁶⁴⁾

Current trends of the Radiology-based age estimation

A review of studies published in the Pubmed database in last three-year (2020-2023) was conducted to find the contemporary trends in age estimation via radiology. The

search incorporated the MeSH term “Age Determination by Teeth*/methods” (81 studies) and relevant terms related to dental, age estimation, and radiography, connected with the Boolean operator “AND” (134 studies). The review exclusively considered articles published in English, full-text-accessibility and the usage of human radiography. The 215 collected data on 26 October 2023 included title, author information, year of publication, and full papers. With duplicates excluded (60 studies), 155 selected results adhered to specific criteria: age estimation utilizing dental or periodontal tissue, with a focus on human radiography specific to the dentition, with reviews and reports excluded. 84 studies were excluded due to the criteria, in total, 71 studies underwent thorough assessment.^(6,23,32,45,47,48,65-129) The publication count being at its highest in 2022 and following by in 2021 and 2020. Furthermore, the objective was to locate the most recent trend studies, which prompted the inclusion of studies up to 2023.

OPGs emerged as the most frequently used radiographic modality. Its popularity stems from its user-friendly nature, data collection simplicity, and ability to capture multiple teeth and anatomical changes within a single image. Consequently, numerous age estimation methods, such as the staging method, atlas, and assessment of open apices, rely greatly on OPG. Additionally, CBCT has proven valuable for assessing tooth volume, pulp cavities, and open apices. However, its applicability for evaluating developmental stages remains a topic of discussion. A study reported the use of MRI to examine pulp tissue areas and revealed the potential of MRI segmentation of tooth tissue volumes in predicting age for populations over 18 years old.⁽¹¹⁶⁾ In this context, 9.4 tesla ultra-short echo time (UTE)-MRI is considered a suitable option for both single-rooted and multiple-rooted teeth^(75,90), offering robust reliability and lower variation compared to CBCT. Nonetheless, manual segmentation is requisite for MRI due to the necessity for a detailed interior representation of the pulp cavity.⁽⁹⁰⁾ A study utilized periapical radiography for dental age estimation using the pulp and tooth ratio method with excellent results.⁽³²⁾

The distribution of age estimation methods is depicted in Figure 2, with further details available in Tables 1-3. The review denotes the continued prevalence of age estimation rooted in tooth development, accounting for 59% of all results. This preference arises from the method's precision in tracking developmental

timelines, thereby mitigating reliance on external factors. Within this category, the Demirjian staging method remains highly popular. However, certain studies have raised concerns about its potential for age overestimation^(10,45,71,83,92), while the Willems method, modified from Demirjian's, has demonstrated greater accuracy in some studies^(14,71,82,92,130) but yielded contrasting results in others.^(13,15) The assessment of open apices, as pioneered by Cameriere, is also extensively employed and has been reported to provide more accurate age estimations compared to Demirjian⁽¹⁰¹⁾ and Willems in some instances, although another has noted potential age underestimation.⁽⁷²⁾

The second choice for age determination (23.1%), employed when all teeth have fully developed, involves assessing anatomic changes. RPV by Olze *et al.*⁽⁶¹⁾ has proven valid for establishing a cutoff age at 21 years old. Moreover, pulp to tooth ratio is also popular in this aspect as many studies explored its potential in age estimation with promising results.^(32,68,75,76,84,90) This approach remains adequate for age estimation but leaves room for some error due to independence from various factors, such as individual oral hygiene and socio-economic conditions. Some studies have sought to compare the accuracy of different methodological groups to determine the most precise approach for major-minor identification. Specifically, a specific cutoff value of $I3M < 0.08$, proposed by Cameriere, has demonstrated superior accuracy, sensitivity, and specificity compared to Demirjian's Stage H (completed mineralization), Stage D of mandibular third molar eruption (full eruption) by Olze *et al.* and Stage 1 of RPV (root canal not visually observed to apex).⁽⁸⁵⁾ However, for establishing a legal age of 21 years old, Stage 2 of RPV has been found to be more reliable in differentiating individuals over 21 years old, exhibiting fewer false positives compared to a score $I3M < 0.02$.⁽¹⁰³⁾ Lastly, AI has gained prominence, comprising 17.9% of the studies. Researchers have shown increasing interest in AI, with promising results indicating its potential to reduce human workload and minimize human errors, thus augmenting traditional processes.^(23,108,110,117) Some studies have conducted comparisons between conventional AI-assisted models and traditional methods, with results indicating improved performance outcomes associated with AI.^(23,108,110) Nevertheless, it is important to note that Kumagai *et al.* reported a slight advantage for the tradi-

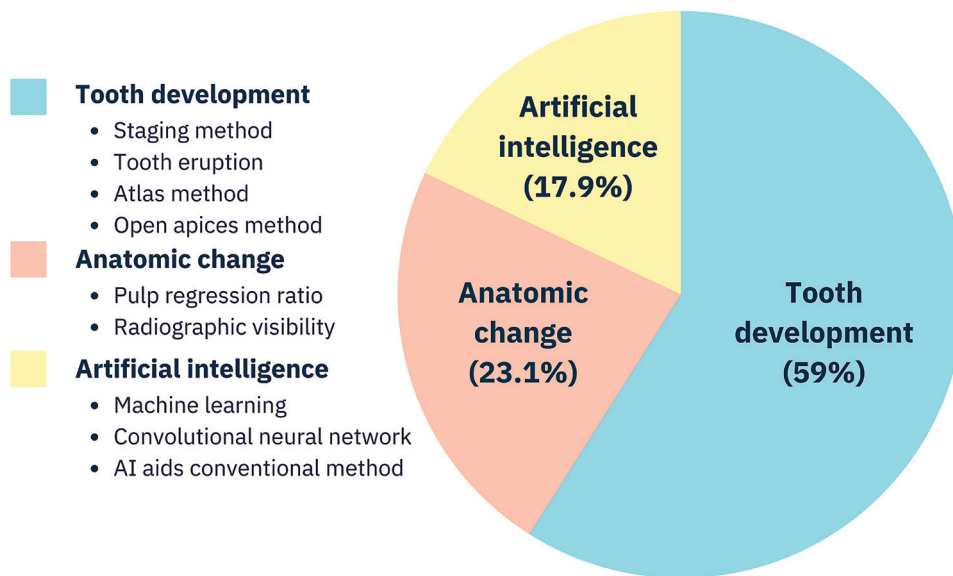


Figure 2: Percentage of age estimation methodologies in published articles included in this review.

tional (Demirjian) model over the AI model, although this was based on discussions with a relatively small number of participants.⁽¹²¹⁾

Conclusions

Age determination plays a pivotal role in forensics and legal contexts, and dental structures, renowned for their remarkable resilience, have emerged as an essential element in this pursuit. Dental radiography, notably OPG, stands as a non-invasive means to constantly contemplate age-related transformations in teeth. The radiological approach involves thoroughly examining diverse characteristics, facilitating the estimation of an individual's age, their grouping within specific age ranges, or determin-

ing whether they fall above or below designated thresholds. Age categorization opens through three distinctive phases: pre-natal, neo-natal, and post-natal; childhood and adolescence; and adulthood. While tooth development serves as generally used for age estimation in the initial phases, the observation of anatomical changes in adulthood takes priority. In recent times, there have been expanding explorations of AI as a robust tool in age estimation, yielding promising outcomes. AI holds the potential to enhance the precision of traditional methodologies, mitigating human errors and reducing associated workload, offering to produce ground for further development in coming years.

Table 1: Summary of findings in the articles assessing age estimation by tooth development methods. (see abbreviations in the footnote)

No.	Author (Year)	Method	Population	Age range (years)	Number of samples	Region of interest	Radiographic modality	Findings
1	Albermaz Neves <i>et al.</i> , 2020 ⁽⁶⁵⁾	I _{3M}	Portuguese	12-24	778	LL 8	OPG	Age ≥ 18: I _{3M} < 0.08: accuracy by AUC = 92.8, Se = 90.7%, Sp = 94.9%
2	Cameriere <i>et al.</i> , 2020 ⁽⁶⁶⁾	I _{3M}	Albanian, Australian, Chinese, Colombian, Dominican, Egyptian, French, Italian, Indian, Japanese, Polonian, Chileans, Serbian, Turkish, South African	14-24	3228	LL 8	OPG	Age ≥ 18: I _{3M} < 0.08: The minimum Se = 47% (French), the maximum Se = 93% (Colombian), Sp > 90% in all 15 countries
3	Gonçalves do Nascimento <i>et al.</i> , 2020 ⁽⁶⁷⁾	Cameriere (Open apices)	Brazilian	5-14.99	429	LL 1-7	OPG	Mean difference (DA-CA): males = -0.32 years; females = -0.30 years; Total = -0.31 years R ² : males = 80.06%; females = 78.95%; Total = 79.32%
5	Marrero-Ramos <i>et al.</i> , 2020 ⁽⁶⁹⁾	Demirjian	Spanish	15-30	180	L 8	OPG	Age ≥ 18: Demirjian stage H in L8 OR: Observer1 = 29.333, Observer2 = 23.250
6	Memorando <i>et al.</i> , 2020 ⁽⁷⁰⁾	Modified Demirjian	Filipino	9-23	384	LR 8	OPG	MAE: males = 1.05 years; females = 1.06 years, percentage error: males = 7.49; females = 7.43 Initial development of the third molars started around 9 years, and the root is completed around 19.
8	Paz Cortés <i>et al.</i> , 2020 ⁽⁷¹⁾	Willems, Demirjian, Nolla	Spanish	4-13	604	LL 1-7	OPG	Mean difference (DA-CA): Willems: males = -0.17 years; females = -0.35 years, Demirjian: males = -0.73 years; females = -0.68 years, Nolla: males = 0.82 years, females = 0.44 years
9	Rezende Machado <i>et al.</i> , 2020 ⁽⁷²⁾	Cameriere (Open apices), Willems	Brazilian	6-14	180	LL 1-7	OPG	Estimated difference: Cameriere: males = 0.03 years; females = 0.05 years, Willems: males = -0.39 years; females = -0.47 years, Cameriere+Willems: males = -0.18 years; females = -0.21 years
10	Scendoni <i>et al.</i> , 2020 ⁽⁷³⁾	I _{3M}	Russian	14-24	571	LL 8	OPG	Age < 18: I _{3M} > 0.08: males: PPV = 98.4%, NPV = 94.1 %, Se = 0.96, Sp = 0.98; females: PPV = 98.6%, NPV = 90.2%, Se = 0.93, Sp = 0.98
11	Sharma <i>et al.</i> , 2020 ⁽⁴⁸⁾	Cameriere (Open apices), London Atlas	Indian	5-15.99	335	LL 1-7 (Cameriere), UR/LR (London Atlas)	OPG	Mean error value: Cameriere = 0.59 years (SD = 1.32), London Atlas = -0.03 years (SD = 0.69)

Table 1: Summary of findings in the articles assessing age estimation by tooth development methods. (continued; see abbreviations in the footnote)

No.	Author (Year)	Method	Population	Age range (years)	Number of samples	Region of interest	Radiographic modality	Findings
12	Sheriff <i>et al.</i> , 2020 ⁽⁷⁴⁾	Willems, Bedek	Southern Indian	7-15	650	LL 1-7	OPG	MAE: Bedek's seven teeth: males = 0.85 years; females = 0.88 years; Total = 0.86 years, Willems: males = 1.02 years; females = 1.25 years, Total = 1.16 years
15	Yassin <i>et al.</i> , 2020 ⁽⁷⁷⁾	Nolla	Southern Saudi Arabian	5-11	458	LL 1-7	OPG	Mean age error range: males = -2.68 to -6 months; females = -2.17 to -4.24 months
16	Alqerban <i>et al.</i> , 2021 ⁽⁷⁸⁾	Willems, Saudi Arabian-specific model	Saudi Arabian	4-18	1146	LL 1-7	OPG	Overall, Willems MAE (1.37 years) is slightly higher than the Saudi Arabian-specific model MAE (1.33 years)
17	Franco <i>et al.</i> , 2021 ⁽⁷⁹⁾	Gleiser and Hunt modified by Kohler	Russian	8-23	918	U/L 8	OPG	AUC: males = 0.915; females = 0.904
20	Pan <i>et al.</i> , 2021 ⁽⁸²⁾	Demirjian, Willems, Chinese-specific Demirjian	Chinese	5-16	2367	LL 1-7	OPG	Accuracy (values within ± 1 year): Chinese-specific Demirjian: males = 83.7%; females = 79.6%, Demirjian: males = 73.9%; females = 70.2%, Willems: males = 75.0%; females = 75.9%
21	Pinchi <i>et al.</i> , 2021 ⁽⁸³⁾	Demirjian, Willems	Italian	3.3-15.99	752	LL 1-7	OPG	Willems' method underestimated age, while Demirjian's overestimated for both healthy and juvenile rheumatoid arthritis-affected children.
23	Pyata <i>et al.</i> , 2021 ⁽⁸⁵⁾	Demirjian, I_{3M} Olze (third molars eruption and RPV)	Southern Indian	14-30	1070	L 8	OPG	Age ≥ 18 : I_{3M} < 0.08 (most accurate): AUC: males = 0.95; females = 0.95, Se: males = 91.5%; females = 88.5%, Sp: males = 97.8%; females = 98.6%. Stage H of Demirjian: AUC: males = 0.94; females = 0.93, Se: males = 84.9%; females = 79.9%, Sp: males = 97.7%; females = 98.5%.
24	Rebouças <i>et al.</i> , 2021 ⁽⁸⁶⁾	Demirjian	Brazilian	9-15.5	113	L 3, 7	OPG	The calcification of L7 was a significant predictor of skeletal maturity indicators ($p = 0.003$), whereas this correlation was not observed for L3 ($p = 0.239$).
25	Saranya <i>et al.</i> , 2021 ⁽⁸⁷⁾	Demirjian	Southern Indian	12-20	640	LL 8	OPG	Age ≥ 16 : probability obtained by Stage F of Demirjian, males = 93.9%; females = 96.6%
26	Shen <i>et al.</i> , 2021 ⁽²³⁾	Machine learning: RF, SVM, L/R, Cameriere (Open apices)	Eastern Chinese	5-13.99	784	LL 1-7	OPG	MAE: SVM model = 0.489 years, traditional Cameriere = 0.846 years, Chinese Cameriere formula = 0.812 years

Table 1: Summary of findings in the articles assessing age estimation by tooth development methods. (continued; see abbreviations in the footnote)

No.	Author (Year)	Method	Population	Age range (years)	Number of samples	Region of interest	Radiographic modality	Findings
28	Thilak <i>et al.</i> , 2021 ⁽⁸⁹⁾	I _{3M}	Indian	14-24	542	LL 8	OPG	Age ≥ 18: I3M = 0.08; accuracy by AUC, males = 0.95; females = 0.93, Se, males = 0.899; females = 0.854, Sp, males = 0.90; females = 0.93.
30	Zirk <i>et al.</i> , 2021 ⁽⁹¹⁾	Demirjian, Nolla	European	13-21	312	L 8	OPG, CBCT	Staging results for 2D and 3D imaging differed significantly. Demirjian: 21% showed a one-stage difference, agreement range = 47.4% (stage E) - 87% (stage G), Nolla: stages 3-6 had discrepancies in staging for more than two categorical variables. Inconsistencies were observed in stages 4-8.
31	Bedeck <i>et al.</i> , 2022 ⁽⁹²⁾	Demirjian, Willems, Haavikko	Croatian	4-18	1996	LL 1-7	OPG	Mean error value: Demirjian: males = 0.80 years; females = 0.84 years, Willems: males = 0.41 years; females = 0.22 years, Haavikko: males = -0.61 years; females = -0.82 years
32	Boedi <i>et al.</i> , 2022 ⁽⁹³⁾	I _{3M}	Indonesian	8-23	222	U/L 8	OPG	Age ≥ 19: I3M ≤ 0.08 (males), 0.09 (females); accuracy = 80% for both sexes in the testing dataset.
33	Briem Stamm <i>et al.</i> , 2022 ⁽⁹⁴⁾	Demirjian	Argentine	5-16	508	LL 1-7	OPG	Mean error value: Demirjian: males = 1.04 years; females = 1.15 years; for both sexes = 1.09 years
34	Caggiano <i>et al.</i> , 2022 ⁽⁹⁵⁾	Demirjian	Southern Italian	3.3-15.99	460	U/L 8	OPG	Age > 18: accuracy of Stage H of the Demirjian method for at least one third molar if the other third molars reached a stage equal or superior to F = 90.2%; when all third molars reached stage H = 97.4%.
36	Kuremoto <i>et al.</i> , 2022 ⁽⁹⁷⁾	Development staging	Japanese	3-18	1024	FM	OPG	Cronbach's alpha coefficients: males = 0.987; females = 0.986. Females tended to form teeth faster than males until puberty, but males caught up with females after puberty.
38	Lin <i>et al.</i> , 2022 ⁽⁴⁷⁾	London Atlas, Willems	Chinese Uyghur	10-16.99	831	UL/LL 1-7	OPG	MAE: London atlas = 0.86±0.75 years, Willems = 1.17±0.89 years, quick method = 0.70±0.54 years
39	Melo <i>et al.</i> , 2022 ⁽⁹⁹⁾	Demirjian, I _{3M}	Spanish	10-26	1386	U/L 8	OPG	Age > 18: Stage H of Demirjian method: accuracy = 93%, I _{3M} = 0.08; accuracy = 88%, for both males and females
41	Milani <i>et al.</i> , 2022 ⁽¹⁰¹⁾	Demirjian, Cameriere (Open apices)	Iranian	6-10	212	LL 1-7	OPG	Mean error value: Demirjian: males = 0.93 years; females = 0.84 years, Cameriere: males = 0.04 years; females = -0.06 years
43	Mónico <i>et al.</i> , 2022 ⁽⁴⁵⁾	Demirjian	Portuguese, Spanish	6-14	574	LL 1-7	OPG	R ² : Demirjian global score = 0.651, tooth by tooth score = 0.717
44	Oh <i>et al.</i> , 2022 ⁽¹⁰²⁾	Demirjian, Lee's method	Japanese, Korean	15-23	2657	U/L 7 8	OPG	R2: Koreans: males = 0.834; females = 0.855, Japanese: males = 0.682; females = 0.585

Table 1: Summary of findings in the articles assessing age estimation by tooth development methods. (continued; see abbreviations in the footnote)

No.	Author (Year)	Method	Population	Age range (years)	Number of samples	Region of interest	Radiographic modality	Findings
45	Parvathala <i>et al.</i> , 2022 ⁽¹⁰³⁾	I _{3M} ^F Olze (RPV)	Southern Indian	16-30	910	L 8	OPG	Age ≥ 21: I _{3M} ^F cannot be used due to higher false positives. RPV stage 2: accuracy: males = 84.76%; female = 84.55%, Sp = 100% in both sexes
46	Prakoeswa <i>et al.</i> , 2022 ⁽¹⁰⁴⁾	London Atlas, Willems	Indonesian	6-17	150	FM	OPG	Mean age difference: Willems = -0.41±0.90 years for males and females, Al Qahtani = 0.33±0.61 years for males and females.
50	Shan <i>et al.</i> , 2022 ⁽¹⁰⁸⁾	Demirjian, Willem, Machine learning; SVR, BPNN, RF, AdaBoost, KNN, Light GBM, XGBoost, Extra trees, DT, GBDT, CatBoost	Southern Chinese	2-18	1477	FM	OPG	Chinese-specific Willem is the most accurate in the traditional method (MAE: males = 0.76; female = 0.77) The GBDT, CatBoost, XGBoost, LightGBM, DT, Extra tree model reduced the error in dental age estimation compared to the traditional mathematical method (MAE: GBDT: males = 0.495; females = 0.441, CatBoost: males = 0.545; females = 0.594, LightGBM: males = 0.648; females = 0.642, DT: males = 0.602; female = 0.643, Extra tree: males = 0.626; female = 0.682)
52	Shen <i>et al.</i> , 2022 ⁽¹¹⁰⁾	Demirjian, Machine learning; DT, BRR, KNN, Cameriere (Open apices)	Eastern Chinese	5-13	748	L 1-7	OPG	The highest accuracy is KNN model based on the Cameriere method. Demirjian: BRR: MAE = 0.510, R ² = 0.928, KNN: MAE = 0.517, R ² = 0.923, DT: MAE = 0.523, R ² = 0.892, Traditional: MAE = 0.982 years Cameriere: KNN: MAE = 0.473, R ² = 0.940, BRR: MAE = 0.535, R ² = 0.923, DT: MAE = 0.584, R ² = 0.893, Traditional: MAE = 0.846 years
53	Wang <i>et al.</i> , 2022 ⁽¹¹¹⁾	Willems	Eastern Chinese	11-16	1211	LL 1-7	OPG	MAE: Willems gender-specific method: males = 0.95 years; females = 1.00 years, Willems non-gender specific method: males = 1.02 years; females = 1.00 years
56	Abdul Rahim <i>et al.</i> , 2023 ⁽¹¹⁴⁾	Demirjian, Nolla, Moorrees	Malaysian, Chinese, Indian	6-15	200	UL/LL 1-7	OPG	Percentage agreement; Kappa values: Moorrees = 81%; 0.938, Nolla = 86 %; 0.922, Demirjian = 87%; 0.918
57	AlOtaibi <i>et al.</i> , 2023 ⁽¹¹⁵⁾	Demirjian, Moorrees, Fanning and Hunt, Gleiser and Hunt, Nolla, Chaillet, Nicodemo	Saudi Arabian	6-15.99	400	LL 1-7	OPG	Mean age difference: Demirjian = 0.15 years, Gleiser and Hunt = -1.00 years, Moorrees = -1.01 years, Fanning and Hunt = -1.01 years, Nolla = -1.29 years, Nicodemo = -1.72 years, Chaillet = -2.19 years

Table 1: Summary of findings in the articles assessing age estimation by tooth development methods. (continued; see abbreviations in the footnote)

No.	Author (Year)	Method	Population	Age range (years)	Number of samples	Region of interest	Radiographic modality	Findings
59	Bui <i>et al.</i> , 2023 ⁽¹¹⁷⁾	CNN; Mask R-CNN, U-Net with TDL or TDA-DL, I _{3M}	French, Ugandan	mean 17.9	456	L 8	OPG	The U-Net combined with TDL is the best approach for decision-making tools that replicated the I3M index for forensic experts with accuracy = 95% and MAE = 0.04±0.03 years.
60	El-Desouky <i>et al.</i> , 2023 ⁽¹¹⁸⁾	Cameriere (Open apices), Egyptian specific Cameriere	Egyptian	5-18	762	L 1-7	OPG	Mean age difference: Egyptian-specific Cameriere: males = -0.12 years; females = 0.1 years, Cameriere: males = -0.59 years; females = -0.53 years
62	Kuhnen <i>et al.</i> , 2023 ⁽¹²⁰⁾	Moorrees	Brazilian	2-25	1100	UL/LL 1-8	OPG	The numerical tables of the chronology of dental mineralization stages for Brazilian individuals were delivered using modified Moorrees <i>et al.</i> Only upper and lower canines differed between sexes.
63	Kumagai <i>et al.</i> , 2023 ⁽¹²¹⁾	Demirjian, Machine learning: KNN, SVM, L/R, DT, RF, XG-Boost, MLP	Korean, Japanese	15-23	2657	U/L 7 8	OPG	The accuracy of the conventional method was slightly higher than machine learning models, with MAE < 0.21 years, RMSE < 0.24 years. The highest different MAE and RMSE in the internal test set in the female group (MAE: KNN = 1.06, Conventional method = 0.85, RMSE: KNN = 1.32, Conventional method = 1.08)
64	Kwon <i>et al.</i> , 2023 ⁽¹²²⁾	Demirjian, Willem	Chinese	8-14.99	1259	L 1-7	OPG	Mean age difference in 2009-2011: Demirjian: males = 0.65±0.97 years; females = 0.48±1.04 years, Willem: males = 0.19 ± 1.00 years; females = -0.08±0.98 years Mean age difference in 2021: Demirjian: males = -0.51±0.73 years; females = -0.48±0.80 years, Willem: males = -0.80±0.71 years; females = -0.82±0.87 years Environmental factors and dietary habits affect dental development.
65	Lopatin <i>et al.</i> , 2023 ⁽¹²³⁾	Primary tooth development	Polish	3mo-14	58	Primary teeth	OPG	Tooth maturity stage 8 is reached earlier in males than females for all deciduous teeth except molars. Both sexes lose deciduous teeth after pre-puberty, with males losing at 3-9 years and females at 2-7 years.

Table 1: Summary of findings in the articles assessing age estimation by tooth development methods. (continued; see abbreviations in the footnote)

No.	Author (Year)	Method	Population	Age range (years)	Number of samples	Region of interest	Radiographic modality	Findings
68	Timme <i>et al.</i> , 2023 ⁽¹²⁶⁾	Olze (third molars eruption), Willmot, New model	German	15-25	211	L 8	OPG	Degree of correlation with Spearman's coefficients: Olze, new method: males= 0.58; females = 0.45
69	Topal <i>et al.</i> , 2023 ⁽¹²⁷⁾	Willems	Turkish	9-15	80	LL 1-97	OPG	Children with multiple persistent primary teeth can experience delayed dental development by 0.5-4 years. Willems method can assess their dental development.

Abbreviations: AUC (area under curve), BPNN (backpropagation neural network), BRR (Bayesian ridge regression), CA (chronological age), CBCT (cone-beam computed tomography), CNN (convolutional neural network), DA (dental age), DT (decision tree), FM (full mouth), GBDT (gradient boosting decision tree), GBM (gradient boosting machine), I3M (third molar maturity index, KNN (K-nearest neighbor), L (lower teeth), LL (lower left teeth), L/R (linear regression), LR (lower right teeth), MAE (mean absolute error), MLP (multilayer perceptron), NPV (negative predictive values), OPG (orthopantomography), OR (odd ratios), PPV (positive predictive values), RF (random forest), RMSE (root mean square error), RPV (root pulp visibility), SD (standard deviation), Se (sensitivity), Sp (specificity), SVM (support vector machine), SVR (support vector regression), TDA (topological data analysis), TDA-DL (topological data analysis with deep learning), U/L (upper and lower teeth, UR (upper right teeth), XGBoost (extreme gradient boosting)

Table 2: Summary of findings in the articles assessing age estimation by anatomic change method. (see abbreviations in the footnote)

No.	Author (Year)	Method	Population	Age range (years)	Number of samples	Region of interest	Radiographic modality	Findings
4	Helmy <i>et al.</i> , 2020 ⁽⁶⁸⁾	pulp/tooth volume ratio	Egyptian	21-50	505	U/L 7	CBCT	MAE: Upper teeth = 4.89 years, Lower teeth = 4.61 years
7	Miranda <i>et al.</i> , 2020 ⁽³²⁾	Kvaal, Cameriere (pulp/tooth ratio)	Brazilian	20-59	1280	U/L 3	Periapical	Kvaal was more accurate for the age groups of 20-29 (UR3: ME = 4.63) and 30-39 years (LL3: ME = 5.42), while Cameriere performed better for individuals over 40 years of age (UL3: ME = 6.08)
13	Timme <i>et al.</i> , 2020 ⁽⁷⁵⁾	pulp/tooth volume ratio	German	48-78	4	UR 1, 4 UL 3, 6	MRI	UTE-MRI at 9.4 T is a radiation-free procedure that allows for the determination of dental pulp volume at high spatial resolution, making it a valuable tool for forensic age assessment of living persons.
14	Yang <i>et al.</i> , 2020 ⁽⁷⁶⁾	pulp/tooth volume ratio	Eastern Chinese	8.18-19.92	230	UL 1, 3	CBCT	UL1: R2 = 0.44, SEE = 2.58, UL3: R2 = 0.69, SEE = 1.91
19	Manthapuri <i>et al.</i> , 2021 ⁽⁸¹⁾	Olze (RPV)	Indian	12-20	760	L 6	OPG	Age > 16: RPV stage 2; Se: males = 0.6; females = 0.65, Sp: males = 0.96; females = 0.97, accuracy: males = 0.77; females = 0.8, false negatives = 34.5% (both sexes)
22	Pires <i>et al.</i> , 2021 ⁽⁸⁴⁾	Kvaal	Portuguese	>=21	158	U/L Ant	CBCT	Mean error in age: coronal section = -21.4 years, sagittal section = -26.3 years
23	Pyata <i>et al.</i> , 2021 ⁽⁸⁵⁾	Demirjian, I _{3M} Olze (third molars eruption and RPV)	Southern Indian	14-30	1070	L 8	OPG	Age ≥ 18: RPV stage 1 or higher and stage D of third molars eruption were not recommended due to the higher incidence of incomplete mineralization in younger age groups and impaction.
27	Tantapanornkul <i>et al.</i> , 2021 ⁽⁸⁸⁾	Olze (PLV)	Thai	16-26	800	L 8	OPG	Periodontal ligament visibility stage 2 can be confirmed that the individual is at least 18 years of age according to the distribution table
29	Timme <i>et al.</i> , 2021 ⁽⁹⁰⁾	Pulp volume	German	18-78	13	FM	MRI, CBCT	UTE-MRI and CBCT are reliable methods for age estimation using pulp volume. MRI has a smaller variation in results but displays smaller pulp volume. Method-specific reference values are needed for practical age assessment with CBCT or MRI.
35	Gumacar <i>et al.</i> , 2022 ⁽⁹⁶⁾	Olze (RPV)	Turkish	16-68	290	L 8	OPG, CBCT	The presence of RPV Stage 3 can be used to identify individuals over 18. The use of CBCT for RPV evaluation is recommended for available cases.

Table 2: Summary of findings in the articles assessing age estimation by anatomic change method. (continued; see abbreviations in the footnote)

No.	Author (Year)	Method	Population	Age range (years)	Number of samples	Region of interest	Radiographic modality	Findings
40	Merdietio Boedi <i>et al.</i> , 2022 ⁽¹⁰⁰⁾	Regression change of crown and root	Indonesian	20-60	192	U Ant	CBCT	MAE: U2 = 5.3 years ($R^2 = 0.67$), U3 = 5.45 years ($R^2 = 0.66$), U1 = 6.19 years ($R^2 = 0.59$)
45	Parvathala <i>et al.</i> , 2022 ⁽¹⁰³⁾	I _{3M} -Olze (RPV)	Southern Indian	16-30	910	L 8	OPG	Age ≥ 21 : I _{3M} : cannot be used due to higher false positives. RPV stage 2: accuracy: males = 84.76%; female = 84.55%, Sp = 100% in both sexes
47	Santos <i>et al.</i> , 2022 ⁽¹⁰⁵⁾	Pulp volume, Multiple regression	Spanish	18-85	373	U 1	CBCT	SEE: axial linear measurements = ± 10.9 years ($R^2 = 0.49$), axial ratios = ± 10.8 years ($R^2 = 0.50$), multiplanar linear measurements = ± 10.9 years ($R^2 = 0.52$), multiplanar ratios = ± 10.7 years ($R^2 = 0.51$)
49	Shah <i>et al.</i> , 2022 ⁽¹⁰⁷⁾	TCI, Drusini	Western Indian	21-60	300	U/L 3, L 4-7	OPG	MAE < 10 years for all the teeth, with no statistically significant difference between the mean chronological age and mean calculated age for both pulp/tooth area ratios of U/L3 and TCI of L 4-7 (p-value > 0.05).
58	Björk <i>et al.</i> , 2023 ⁽¹¹⁶⁾	Tooth/tissue volume, Linear regression	Bayesian	14-24	67	U/L 8	MRI	MRI segmentation of tooth tissue volumes can be useful in predicting the age of sub-adults older than 18 years (p-value = 3.4×10^{-9}).
66	Merdietio Boedi <i>et al.</i> , 2023 ⁽¹²⁴⁾	Crown segment secondary dentine deposit regression	Indonesian	20-60	99	U Ant	CBCT	The highest R2 (0.6) was obtained from the U3, indicating a good model performance in anterior maxillary teeth. The enamel-to-dentine volume ratio and pulp-to-dentine volume ratio are related to chronological age.
67	Sharma <i>et al.</i> , 2023 ⁽¹²⁵⁾	TCI	Indian	20-70	700	L 4	OPG	Mean age difference: males = 1.48 ± 3.82 (SE = 0.76); females = 0.13 ± 17.65 (SE = 3.53)
70	Vangala <i>et al.</i> , 2023 ⁽¹²⁸⁾	Olze (RPV)	Southern Indian	15-30	930	L 6-8	OPG	RPV stage 3 in L6 were at least older than 21 years. RPV stage 2 and 3 in L7 were at least older than 21 years. RPV stage 1-3 in L8 were at least older than 21 years. Using these methods with other age estimation methods is recommended due to the higher percentage of false negatives with L 6-7.

Abbreviations: AUC (area under curve), Ant (anterior teeth), CBCT (cone-beam computed tomography), FM (full mouth), I3M (third molar maturity index), L (lower teeth), MAE (mean absolute error), ME (mean error), MRI (magnetic resonance imaging), OPG (orthopantomogram), PLV (periodontal ligament visibility), RPV (root pulp visibility), Se (sensitivity), SE (standard error), SEE (standard error of the estimate), Sp (specificity), TCI (tooth-coronal index), U/L (upper and Lower teeth), U (upper teeth), UTE-MRI (ultrashort echo time magnetic resonance imaging)

Table 3: Summary of findings in the articles assessing age estimation by artificial intelligence method. (see abbreviations in the footnote)

No.	Author (Year)	Method	Population	Age range (years)	Number of samples	Region of interest	Radiographic modality	Findings
18	Kim <i>et al.</i> , 2021 ⁽⁸⁰⁾	CNN; ResNet152, Tooth-wise age group prediction	Korean	0->60	1586	U/L 6	OPG	Accuracy range = 89.05-90.27%, AUC range = 0.94-0.98 for all age groups The CNNs focused on tooth pulp, alveolar bone level, or interdental space, depending on the age and location of the tooth.
26	Shen <i>et al.</i> , 2021 ⁽²³⁾	Machine learning; RF, SVM, L/R, Cameriere (Open apices)	Eastern Chinese	5-13.99	748	LL 1-7	OPG	MAE: SVM model = 0.489 years, traditional Cameriere = 0.846 years, Chinese Cameriere formula = 0.812 years
37	Lee <i>et al.</i> , 2022 ⁽⁹⁸⁾	Machine learning; LDA, L/R, MLP, SVM, XGBoost, 18 selected features	Korean	11-69	471	FM	OPG	Mean AUC range: 10-19 years group = 0.85-0.87, 60-69 years group = 0.80-0.90, which are the best scores. The L-Pulp Area was important for discriminating 10-49 years group, and L-Crown, U-Crown, L-Implant, U-Implant, and Periodontitis were for 50-69 years group.
42	Milošević <i>et al.</i> , 2022 ⁽⁶⁾	CNN; Dense Net201, InceptionResNetV2, ResNet50, VGG16, VGG19, Xception	Croatian	19-90	4035	FM	OPG	Whole OPG: MAE = 3.96 years, MEE = 2.95 years Individual teeth: L8 best score: MAE = 6.39 years, MEE = 4.68 years Dental variations, diseases, and missing teeth do not pose a problem to the proposed model.
48	Santosh <i>et al.</i> , 2022 ⁽¹⁰⁶⁾	Machine learning; MSVM, LIBSVM	Indian	1->60	1142	FM	OPG	MSVM and LIBSVM models: accuracy = 96% in age estimation and gender prediction.
50	Shan <i>et al.</i> , 2022 ⁽¹⁰⁸⁾	Demirjian, Willem, Machine learning; SVR, BPNN, RF, AdaBoost, KNN, Light GBM, XGBoost, Extra trees, DT, GBDT, CatBoost	Southern Chinese	2-18	1477	FM	OPG	Chinese-specific Willem is the most accurate in the traditional method (MAE: males = 0.76; female = 0.77) The GBDT, CatBoost, XGBoost, LightGBM, DT, Extra tree model reduced the error in dental age estimation compared to the traditional mathematical method (MAE: GBDT: males = 0.495; females = 0.441, CatBoost: males = 0.545; females = 0.594, LightGBM: males = 0.648; females = 0.642, DT: males = 0.602; female = 0.643, Extra tree: males = 0.626; female = 0.682)

Table 3: Summary of findings in the articles assessing age estimation by artificial intelligence method. (continued; see abbreviations in the footnote)

No.	Author (Year)	Method	Population	Age range (years)	Number of samples	Region of interest	Radiographic modality	Findings
51	Sharifonnasabi <i>et al.</i> , 2022 ⁽¹⁰⁹⁾	HCNN- KNN, CNN, ResNet, GoogLeNet Inception	Malaysian	1-17	1922	FM	OPG	HCNN-KNN: accuracy of 1 year = 99.98%, 6 months = 99.96%, 3 months = 99.87%, 1 month = 98.78%
52	Shen <i>et al.</i> , 2022 ⁽¹¹⁰⁾	Demirjian, Machine learning: DT, BRR, KNN, Cameriere (Open apices)	Eastern Chinese	5-13	748	L 1-7	OPG	The highest accuracy is KNN model based on the Cameriere method. Demirjian: BRR: MAE = 0.510, R ² = 0.928, KNN: MAE = 0.517, R ² = 0.923, DT: MAE = 0.523, R ² = 0.892, Traditional: MAE = 0.982 years Cameriere: KNN: MAE = 0.473, R ² = 0.940, BRR: MAE = 0.535, R ² = 0.923, DT: MAE = 0.584, R ² = 0.893, Traditional: MAE = 0.846 years
54	Wang <i>et al.</i> , 2022 ⁽¹¹²⁾	CNN: DENSEN (Based on SSR-Net), Bayesian CNNs Net, DANet	Chinese	3-85	1903	FM	OPG	MAE: DENSEN: 3-11 years group = 0.6885 years, 12-18 years group = 0.7615 years, 19-25 years group = 1.3502 years, and >25 years group = 2.8770 years
55	Zaborowicz <i>et al.</i> , 2022 ⁽¹¹³⁾	POD-GP, Tooth Geometry Indicators	Polish	4-18	619	U/L 3 5-7	OPG	Accuracy = 95%, MAE = ±7.5 months
59	Bui <i>et al.</i> , 2023 ⁽¹¹⁷⁾	CNN; Mask R-CNN, U-Net with and without TDA-DL), I3M	French, Ugandan	Mean 17.9	456	L 8	OPG	The U-Net combined with TDL is the best approach for decision-making tools that replicated the I3M index for forensic experts with accuracy = 95% and MAE = 0.04 ± 0.03 years.
61	Kim <i>et al.</i> , 2023 ⁽¹¹⁹⁾	CNN	Korean	10s-70s	10023	FM	OPG	Accuracy = 53.846%, with a tolerance of ±5 years
63	Kumagai <i>et al.</i> , 2023 ⁽¹²¹⁾	Demirjian, Machine learning: KNN, SVM, L/R, DT, RF, XGBoost, MLP	Korean, Japanese	15-23	2657	U/L 7 8	OPG	The accuracy of the conventional method was slightly higher than machine learning models, with MAE < 0.21 years, RMSE < 0.24 years. The highest different MAE and RMSE in the internal test set in the female group (MAE: KNN = 1.06, Conventional method = 0.85, RMSE: KNN = 1.32, Conventional method = 1.08)

Table 3: Summary of findings in the articles assessing age estimation by artificial intelligence method. (continued; see abbreviations in the footnote)

No.	Author (Year)	Method	Population	Age range (years)	Number of samples	Region of interest	Radiographic modality	Findings
71	Wang <i>et al.</i> , 2023 ⁽¹²⁹⁾	CNN; VGG16, ResNet101	Chinese	6-20	9586	LL 1-7	OPG	Accuracy: VGG16 model = 93.63%, ResNet101 = 88.73% in the 6-to-8-year-old group.

Abbreviations: AdaBoost (adaptive boosting), AUC (area under curve), BPNN (backpropagation neural network), BRR (Bayesian ridge regression), CNN (convolutional neural network), DT (decision tree), FM (full mouth), GBM (gradient boosting machine), GBDT (gradient boosting decision tree), HCNN-KNN (Hybrid HCNN-KNN), I3M (third molar maturity index), KNN (K-nearest neighbor), LDA (linear discriminant analysis), L (lower teeth), LL (lower left teeth), L/R (linear regression), LIBSVM (library for support vector machines), MAE (mean absolute error), MEE (median estimate error), MLP (multilayer perceptron), MSVM (multiclass support vector machine), OPG (orthopantomography), POD-GP (proper orthogonal decomposition and gaussian processes), RF (random forest), RMSE (root mean square error), SVM (support vector machine), SVR (support vector regression), TDA (topological data analysis), TDA-DL (topological data analysis with deep learning), U/L (upper and lower teeth), XGBoost (extreme gradient boosting)

References

- Hill AJ, Lain R, Hewson I. Preservation of dental evidence following exposure to high temperatures. *Forensic Sci Int.* 2011;205(1-3):40-3.
- Kieser J, de Feijter J, TeMoananui R. Automated dental aging for child victims of disasters. *Am J Disaster Med.* 2008;3(2):109-12.
- Pramod JB, Marya A, Sharma V. Role of forensic odontologist in post mortem person identification. *Dent Res J (Isfahan).* 2012;9(5):522-30.
- Yun JI, Lee JY, Chung JW, Kho HS, Kim YK. Age estimation of Korean adults by occlusal tooth wear. *J Forensic Sci.* 2007;52(3):678-83.
- Lu CK, Yee MCS, Ravi SB, Pandurangappa R. Forensic age estimation of Chinese Malaysian adults by evaluating occlusal tooth wear using modified Kim's index. *Int J Dent.* 2017;2017:4265753.
- Milošević D, Vodanović M, Galić I, Subašić M. Automated estimation of chronological age from panoramic dental x-ray images using deep learning. *Expert Syst Appl.* 2022; 189:116038.
- Helfman P BJ. Aspartic acid racemisation in dentine as a measure of ageing. *Nature.* 1976;262:279-81.
- Ohtani S. Estimation of age from dentin by using the racemization reaction of aspartic acid. *Am J Forensic Med Pathol.* 1995;16(2):158-61.
- Permsuwan R, Verochana K, Mahakkanukrauh P, Jaikang C, Srilesin C, Intui K, *et al.* Age estimation using aspartic acid racemization in various forensic samples: a preliminary study. *Chiang Mai. Med. J.* 2020;59(2):53-9.
- Duangto P, Janhom A, Prasitwattanaseree S, Mahakkanukrauh P, Iamaroon A. New prediction models for dental age estimation in Thai children and adolescents. *Forensic Sci Int.* 2016;266:583 e1-83 e5.
- Jayaraman J, Roberts GJ, Wong HM, King NM. Dental age estimation in southern Chinese population using panoramic radiographs: validation of three population specific reference datasets. *BMC Med Imaging.* 2018;18(1):5.
- Jayaraman J, Wong HM, Roberts GJ, King NM, Cardoso HFV, Velusamy P, *et al.* Age estimation in three distinct East Asian population groups using southern Han Chinese dental reference dataset. *BMC Oral Health.* 2019;19(1):242.
- Yang Z, Geng K, Liu Y, Sun S, Wen D, Xiao J, *et al.* Accuracy of the Demirjian and Willems methods of dental age estimation for children from central southern China. *Int J Legal Med.* 2019;133(2):593-601.
- Han MQ, Jia SX, Wang CX, Chu G, Chen T, Zhou H, *et al.* Accuracy of the Demirjian, Willems and Nolla methods for dental age estimation in a northern Chinese population. *Arch Oral Biol.* 2020;118:104875.
- Shen C, Pan J, Yang Z, Mou H, Tao J, Ji F. Applicability of 2 dental age estimation methods to Taiwanese population. *Am J Forensic Med Pathol.* 2020;41(4):269-75.
- Jayaraman J, Wong HM, King NM, Roberts GJ. Development of a reference data set (RDS) for dental age estimation (DAE) and testing of this with a separate validation set (VS) in a southern Chinese population. *J Forensic Leg Med.* 2016;43:26-33.
- Manjunatha BS, Soni NK. Estimation of age from development and eruption of teeth. *J Forensic Dent Sci.* 2014;6(2):73-6.
- AlQahtani SJ, Hector MP, Liversidge HM. Brief communication: The London atlas of human tooth development and eruption. *Am J Phys Anthropol.* 2010;142(3):481-90.
- Duangto P, Janhom A, Prasitwattanaseree S, Iamaroon A. New equations for age estimation using four permanent mandibular teeth in Thai children and adolescents. *Int J Legal Med.* 2018;132(6):1743-7.
- Kim S, Lee YH, Noh YK, Park FC, Auh QS. Author Correction: age-group determination of living individuals using first molar images based on artificial intelligence. *Sci Rep.* 2022;12(1):2332.
- Seyedashrafi M, Payahoo S, Noorizade A, Noruzi M. Relationship of morphological changes of the first molar pulp chamber and mineralization of developing third molar with cervical vertebral maturation on panoramic radiographs and lateral cephalograms. *Int J Clin Ski.* 2019;13(2):278-87.
- Someda H, Saka H, Matsunaga S, Ide Y, Nakahara K, Hirata S, *et al.* Age estimation based on three-dimensional measurement of mandibular central incisors in Japanese. *Forensic Sci Int.* 2009;185(1-3):110-4.
- Shen S, Liu Z, Wang J, Fan L, Ji F, Tao J. Machine learning assisted Cameriere method for dental age estimation. *BMC Oral Health.* 2021;21(1):641.
- Shah PH, Venkatesh R. Pulp/tooth ratio of mandibular first and second molars on panoramic radiographs: an aid for forensic age estimation. *J Forensic Dent Sci.* 2016;8(2):112.
- Li MJ, Chu G, Han MQ, Chen T, Zhou H, Guo YC. Application of the Kvaal method for age estimation using digital panoramic radiography of Chinese individuals. *Forensic Sci Int.* 2019;301:76-81.
- Marroquin TY, Karkhanis S, Kvaal SI, Vasudavan S, Kruger E, Tennant M. Age estimation in adults by dental imaging assessment systematic review. *Forensic Sci Int.* 2017; 275:203-11.
- Kvaal SI, Kolltveit KM, Thomsen IO, Solheim T. Age estimation of adults from dental radiographs. *Forensic Sci Int.* 1995;74(3):175-85.
- Joseph C, Reddy BH, Cherian N, Kannan S, George G. Intraoral digital radiography for adult age estimation: a reliable technique. *J Indian Acad Oral Med Radiol.* 2013; 25(4):287-90.
- Li M, Zhao J, Chen W, Chen X, Chu G, Chen T, *et al.* Can canines alone be used for age estimation in Chinese individuals when applying the Kvaal method? *Forensic Sci Res.* 2022;7(2):132-7.

30. Alharbi HS, Sr., Alharbi AM, Alenazi AO, Kolarkodi SH, Elmoazen R. Age estimation by Kvaal's method using digital panoramic radiographs in the Saudi population. *Cureus*. 2022;14(4):e23768.
31. Zdravkovic D, Jovanovic M, Papic M, Ristic V, Milojevic Samanovic A, Kocovic A, *et al*. Application of the Kvaal method in age estimation of the Serbian based on dental radiographs. *Diagnostics (Basel)*. 2022;12(4):911.
32. Miranda JC, Azevedo ACS, Rocha M, Michel-Crosato E, Biazevic MGH. Age estimation in Brazilian adults by Kvaal's and Cameriere's methods. *Braz Oral Res*. 2020;34:e051.
33. Mengjun Z, Xiaogang C, Lei S, Ting L, Fei F, Kui Z, *et al*. Age estimation in Western Chinese adults by pulp-tooth volume ratios using cone-beam computed tomography. *Aust J Forensic Sci*. 2021;53(6):681-92.
34. AlQarni S, Chandrashekar G, Bumann EE, Lee Y. Incremental learning for panoramic radiograph segmentation. *Annu Int Conf IEEE Eng Med Biol Soc*. 2022;2022:557-61.
35. Wallraff S, Vesal S, Syben C, Lutz R, Maier A. Age estimation on panoramic dental X-ray images using deep learning. In: Palm C, Deserno TM, Handels H, Maier A, Maier-Hein K, Tolxdorff T, editor(s). *Bildverarbeitung für die Medizin 2021. Informatik aktuell*. Springer Vieweg, Wiesbaden.;2021.p.186-91.
36. Vila-Blanco N, Varas-Quintana P, Aneiros-Ardao A, Tomas I, Carreira MJ. XAS: Automatic yet eXplainable age and sex determination by combining imprecise per-tooth predictions. *Comput Biol Med*. 2022;149:106072.
37. Pham CV, Lee SJ, Kim SY, Lee S, Kim SH, Kim HS. Age estimation based on 3D post-mortem computed tomography images of mandible and femur using convolutional neural networks. *PLoS One*. 2021;16(5):e0251388.
38. Stavrianos C, Mastagas D, Stavrianou I, Karaiskou O. Dental age estimation of adults: a review of methods and principals. *Res J Med Sci*. 2008; 2(5):258-68.
39. Nayyar A, Babu B, Krishnaveni B, Devi M, Gayitri HC. Age estimation: Current state and research challenges. *J Med Sci*. 2016;36(6):209-16.
40. Kraus BS, Jordan RE. *The human dentitionb birth*. Philadelphia: Lea and Febiger; 1965.
41. Nolla CM. The development of the permanent teeth. *J Dent Child*. 1960; 27:254-66.
42. Demirjian A, Goldstein H, Tanner JM. A new system of dental age assessment. *Hum Biol*. 1973;45(2):211-27.
43. Demirjian A, Goldstein H. New systems for dental maturity based on seven and four teeth. *Ann Hum Biol*. 1976;3(5):411-21.
44. Willems G, Van Olmen A, Spiessens B, Carels C. Dental age estimation in Belgian children: Demirjian's technique revisited. *J Forensic Sci*. 2001;46(4):893-5.
45. Mónico LS, Tomás LF, Tomás I, Varela-Patiño P, Martín-Biedma B. Adapting Demirjian standards for Portuguese and Spanish children and adolescents. *Int J Environ Res Public Health*. 2022;19(19):12706.
46. Duangto P, Janhom A, Iamaroon A. Age estimation using the London Atlas in a Thai population. *Aust J Forensic Sci*. 2023;55(6):700-7.
47. Lin Y, Maimaitiyiming N, Sui M, Abuduxiku N, Tao J. Performance of the London Atlas, Willems, and a new quick method for dental age estimation in Chinese Uyghur children. *BMC Oral Health*. 2022;22(1):624.
48. Sharma P, Wadhwan V. Comparison of accuracy of age estimation in Indian children by measurement of open apices in teeth with the London Atlas of tooth development. *J Forensic Odontostomatol*. 2020;38(1):39-47.
49. Cameriere R, Ferrante L, Cingolani M. Age estimation in children by measurement of open apices in teeth. *Int J Legal Med*. 2006;120(1):49-52.
50. Cameriere R, Ferrante L, De Angelis D, Scarpino F, Galli F. The comparison between measurement of open apices of third molars and Demirjian stages to test chronological age of over 18 year olds in living subjects. *Int J Legal Med*. 2008;122(6):493-7.
51. De Micco F, Martino F, Velandia Palacio LA, Cingolani M, Campobasso CP. Third molar maturity index and legal age in different ethnic populations: Accuracy of Cameriere's method. *Med Sci Law*. 2021;61(1 suppl):105-12.
52. Ivan G, Tomislav L, Hrvoje B, Marin V, Elizabeta G, Maria Gabriela Haye B, *et al*. Cameriere's third molar maturity index in assessing age of majority. *Forensic Sci Int*. 2015;252:191.e1-91.e5.
53. Zelic K, Galic I, Nedeljkovic N, Jakovljevic A, Milosevic O, Djuric M, *et al*. Accuracy of Cameriere's third molar maturity index in assessing legal adulthood on Serbian population. *Forensic Sci Int*. 2016;259:127-32.
54. Ikeda N, Umetsu K, Kashimura S, Suzuki T, Oumi M. Estimation of age from teeth with their soft X-ray findings. *Jpn J Leg Med*. 1985;39(3):244-50.
55. Gotmare SS, Shah T, Periera T, Waghmare MS, Shetty S, Sonawane S, *et al*. The coronal pulp cavity index: a forensic tool for age determination in adults. *Dent Res J (Isfahan)*. 2019;16(3):160-5.
56. Cameriere R, Ferrante L, Cingolani M. Variations in pulp/tooth area ratio as an indicator of age: a preliminary study. *J Forensic Sci*. 2004;49(2):317-9.
57. Yang F, Jacobs R, Willems G. Dental age estimation through volume matching of teeth imaged by cone-beam CT. *Forensic Sci Int*. 2006;159 (Suppl 1):S78-83.
58. Jagannathan N, Neelakantan P, Thiruvengadam C, Ramani P, Premkumar P, Natesan A, *et al*. Age estimation in an Indian population using pulp/tooth volume ratio of mandibular canines obtained from cone beam computed tomography. *J Forensic Odontostomatol*. 2011;29(1):1-6.

59. Biuki N, Razi T, Faramarzi M. Relationship between pulp-tooth volume ratios and chronological age in different anterior teeth on CBCT. *J Clin Exp Dent.* 2017;9(5):e688-e93.
60. Kazmi S, Mânica S, Revie G, Shepherd S, Hector M. Age estimation using canine pulp volumes in adults: a CBCT image analysis. *Int J Legal Med.* 2019;133(6):1967-76.
61. Olze A, Solheim T, Schulz R, Kupfer M, Schmeling A. Evaluation of the radiographic visibility of the root pulp in the lower third molars for the purpose of forensic age estimation in living individuals. *Int J Legal Med.* 2010;124(3):183-6.
62. Guo YC, Han M, Chi Y, Long H, Zhang D, Yang J, *et al.* Accurate age classification using manual method and deep convolutional neural network based on orthopantomogram images. *Int J Legal Med.* 2021;135(4):1589-97.
63. Vila-Blanco N, Varas-Quintana P, Tomás I, Carreira MJ. A systematic overview of dental methods for age assessment in living individuals: from traditional to artificial intelligence-based approaches. *Int J Legal Med.* 2023;137(4):1117-46.
64. Wang R, Chaudhari P, Davatzikos C. Embracing the disharmony in medical imaging: a simple and effective framework for domain adaptation. *Med Image Anal.* 2022;76:102309.
65. Albernaz Neves J, Antunes-Ferreira N, Machado V, Botelho J, Proença L, Quintas A, *et al.* Validation of the third molar maturation index (I3M) to assess the legal adult age in the Portuguese population. *Sci Rep.* 2020;10(1):18466.
66. Cameriere R, Velandia Palacio LA, Marchetti M, Baralla F, Cingolani M, Ferrante L. Child brides: the age estimation problem in young girls. *J Forensic Odontostomatol.* 2020;38(3):2-7.
67. Gonçalves do Nascimento L, Ribeiro Tinoco RL, Lacerda Protasio AP, Arrais Ribeiro IL, Marques Santiago B, Cameriere R. Age estimation in north east Brazilians by measurement of open apices. *J Forensic Odontostomatol.* 2020;38(2):2-11.
68. Helmy MA, Osama M, Elhindawy MM, Mowafey B. Volume analysis of second molar pulp chamber using cone beam computed tomography for age estimation in Egyptian adults. *J Forensic Odontostomatol.* 2020;38(3):25-34.
69. Marrero-Ramos MD, López-Urquía L, Suárez-Soto A, Sánchez-Villegas A, Vicente-Barrero M. Estimation of the age of majority through radiographic evaluation of the third molar maturation degree. *Med Oral Patol Oral Cir Bucal.* 2020;25(3):e359-e63.
70. Memorando JR. Evaluation of mandibular third molar for age estimation of Filipino population age 9-23 years. *J Forensic Odontostomatol.* 2020;38(1):26-33.
71. Paz Cortés MM, Rojo R, Alía García E, Mourelle Martínez MR. Accuracy assessment of dental age estimation with the Willems, Demirjian and Nolla methods in Spanish children: Comparative cross-sectional study. *BMC Pediatr.* 2020;20(1):361.
72. Rezende Machado AL, Borges BS, Cameriere R, Palhares Machado CE, Alves da Silva RE. Evaluation of Cameriere and Willems age estimation methods in panoramic radiographs of Brazilian children. *J Forensic Odontostomatol.* 2020;38(3):8-15.
73. Scendoni R, Zolotenkova GV, Vanin S, Pigolkin YI, Cameriere R. Forensic validity of the third molar maturity index (I3M) for age estimation in a Russian population. *Biomed Res Int.* 2020;2020:6670590.
74. Sheriff SO, Medapati RH, Ankiseti SA, Gurralla VR, Haritha K, Pulijala S, *et al.* Testing the accuracy of Bedek *et al's* new models based on 1-to-7 mandibular teeth for age estimation in 7-15 year old south Indian children. *J Forensic Odontostomatol.* 2020;38(2):22-39.
75. Timme M, Borkert J, Nagelmann N, Schmeling A. Evaluation of secondary dentin formation for forensic age assessment by means of semi-automatic segmented ultra-high field 9.4 T UTE MRI datasets. *Int J Legal Med.* 2020;134(6):2283-8.
76. Yang Z, Fan L, Kwon K, Pan J, Shen C, Tao J, *et al.* Age estimation for children and young adults by volumetric analysis of upper anterior teeth using cone-beam computed tomography data. *Folia Morphol (Warsz).* 2020;79(4):851-9.
77. Yassin SM, Alalmai BAM, Ali Huaylah SH, Althobati MK, Alhamdi FMA, Togoo RA. Accuracy of estimating chronological age from Nolla's method of dental age estimation in a population of Southern Saudi Arabian children. *Niger J Clin Pract.* 2020;23(12):1753-8.
78. Alqerban A, Alrashed M, Alaskar Z, Alqahtani K. Age estimation based on Willems method versus country specific model in Saudi Arabia children and adolescents. *BMC Oral Health.* 2021;21(1):341.
79. Franco R, Franco A, Turkina A, Arakelyan M, Arzukanyan A, Velenko P, *et al.* Radiographic assessment of third molar development in a Russian population to determine the age of majority. *Arch Oral Biol.* 2021;125:105102.
80. Kim S, Lee YH, Noh YK, Park FC, Auh QS. Age-group determination of living individuals using first molar images based on artificial intelligence. *Sci Rep.* 2021;11(1):1073.
81. Manthapuri S, Bheemanapalli SR, Namburu LP, Kunchala S, Vankdoth D, Balla SB, *et al.* Can root pulp visibility in mandibular first molars be used as an alternative age marker at the 16 year threshold in the absence of mandibular third molars: an orthopantomographic study in a South Indian sample. *J Forensic Odontostomatol.* 2021;39(2):21-31.
82. Pan J, Shen C, Yang Z, Fan L, Wang M, Shen S, *et al.* A modified dental age assessment method for 5- to 16-year-old eastern Chinese children. *Clin Oral Investig.* 2021;25(6):3463-74.
83. Pinchi V, Bianchi I, Pradella F, Vitale G, Focardi M, Tonni I, *et al.* Dental age estimation in children affected by juvenile rheumatoid arthritis. *Int J Legal Med.* 2021;135(2):619-29.

84. Pires AC, Vargas de Sousa Santos RF, Pereira CP. Dental age assessment by the pulp/tooth area proportion in cone beam computed tomography: is medico-legal application for age estimation reliable? *J Forensic Odontostomatol.* 2021;39(2):2-14.
85. Pyata JR, Kandukuri BA, Gangavarapu U, Anjum B, Chin-nala B, Bojji M, *et al.* Accuracy of four dental age estimation methods in determining the legal age threshold of 18 years among South Indian adolescents and young. *J Forensic Odontostomatol.* 2021;39(3):2-15.
86. Rebouças PRM, Alencar CRB, Arruda M, Lacerda RHW, Melo DP, Bernardino Í M, *et al.* Identification of dental calcification stages as a predictor of skeletal development phase. *Dental Press J Orthod.* 2021;26(4):e2119292.
87. Saranya K, Ponnada SR, Cheruvathoor JJ, Jacob S, Kandukuri G, Mudigonda M, *et al.* Assessing the probability of having attained 16 years of age in juveniles using third molar development in a sample of South Indian population. *J Forensic Odontostomatol.* 2021;39(1):16-23.
88. Tantanapornkul WB, Kaomongkolgit R, Tohnak S, Deepho C, Chansamat R. Dental age assessment based on the radiographic visibility of the periodontal ligament in lower third molars in a Thai sample. *J Forensic Odontostomatol.* 2021;39(2):32-7.
89. Thilak JT, Manisha KM, Sapna DR, Nivedita C. Evaluation of third molar maturity index (I3M) in assessing the legal age of subjects in an Indian Goan population. *J Forensic Odontostomatol.* 2021;39(3):16-24.
90. Timme M, Borkert J, Nagelmann N, Streeter A, Karch A, Schmeling A. Age-dependent decrease in dental pulp cavity volume as a feature for age assessment: a comparative in vitro study using 9.4-T UTE-MRI and CBCT 3D imaging. *Int J Legal Med.* 2021;135(4):1599-609.
91. Zirk M, Zoeller JE, Lentzen MP, Bergeest L, Buller J, Zinser M. Comparison of two established 2D staging techniques to their appliance in 3D cone beam computer-tomography for dental age estimation. *Sci Rep.* 2021;11(1):9024.
92. Bedek I, Dumančić J, Lauc T, Marušić M, Čuković-Bagić I. Applicability of the Demirjian, Willems and Haavikko methods in Croatian children. *J Forensic Odontostomatol.* 2022;40(2):21-30.
93. Boedi RM, Ermanto H, Skripsa TH, Prabowo YB. Application of third molar maturity index for Indonesia minimum legal age of marriage: a pilot study. *J Forensic Odontostomatol.* 2022;40(1):12-9.
94. Briem Stamm AD, Cariego MT, Vazquez DJ, Pujol MH, Saiegh J, Bielli MV, *et al.* Use of the Demirjian method to estimate dental age in panoramic radiographs of patients treated at the Buenos Aires University School of Dentistry. *Acta Odontol Latinoam.* 2022;35(1):25-30.
95. Caggiano M, Scelza G, Amato A, Orefice R, Belli S, Pagano S, *et al.* Estimating the 18-Year Threshold with third molars radiographs in the Southern Italy population: accuracy and reproducibility of Demirjian method. *Int J Environ Res Public Health.* 2022;19(16):10454.
96. Gunacar DN, Bayrak S, Sinanoglu EA. Three-dimensional verification of the radiographic visibility of the root pulp used for forensic age estimation in mandibular third molars. *Dentomaxillofac Radiol.* 2022;51(3):20210368.
97. Kuremoto K, Okawa R, Matayoshi S, Kokomoto K, Nakano K. Estimation of dental age based on the developmental stages of permanent teeth in Japanese children and adolescents. *Sci Rep.* 2022;12(1):3345.
98. Lee YH, Won JH, Auh QS, Noh YK. Age group prediction with panoramic radiomorphometric parameters using machine learning algorithms. *Sci Rep.* 2022;12(1):11703.
99. Melo M, Ata-Ali F, Ata-Ali J, Martinez Gonzalez JM, Cobo T. Demirjian and Cameriere methods for age estimation in a Spanish sample of 1386 living subjects. *Sci Rep.* 2022;12(1):2838.
100. Merdietio Boedi R, Shepherd S, Oscandar F, Mânica S, Franco A. Regressive changes of crown-root morphology and their volumetric segmentation for adult dental age estimation. *J Forensic Sci.* 2022;67(5):1890-8.
101. Milani S, Shahrabi M, H BF, Parvar S, Abdolhazadeh M. Accuracy of Demirjian's and Cameriere's methods for age estimation in 6- to 10-year-old Iranian children using panoramic radiographs. *Int J Dent.* 2022;2022:4948210.
102. Oh S, Kumagai A, Kim SY, Lee SS. Accuracy of age estimation and assessment of the 18-year threshold based on second and third molar maturity in Koreans and Japanese. *PLoS One.* 2022;17(7):e0271247.
103. Parvathala P, Chittamuru NR, Kakumanu NR, Yadav L, Hamid Ali S, Ali S, *et al.* Testing the maturation and the radiographic visibility of the root pulp of mandibular third molars for predicting 21 years. A digital panoramic radiographic study in emerging adults of South Indian origin. *J Forensic Odontostomatol.* 2022;40(3):22-33.
104. Prakoeswa B, Kurniawan A, Chusida A, Marini MI, Rizky BN, Margaretha MS, *et al.* Children and adolescent dental age estimation by the Willems and Al Qahtani methods in Surabaya, Indonesia. *Biomed Res Int.* 2022;2022:9692214.
105. Santos MA, Muinelo-Lorenzo J, Fernández-Alonso A, Cruz-Landeira A, Aroso C, Suárez-Cunqueiro MM. Age estimation using maxillary central incisor analysis on cone beam computed tomography human images. *Int J Environ Res Public Health.* 2022;19(20):13370.
106. Santosh KC, Pradeep N, Goel V, Ranjan R, Pandey E, Shukla PK, *et al.* Machine learning techniques for human age and gender identification based on teeth x-ray images. *J Healthc Eng.* 2022;2022:8302674.

107. Shah PH, Venkatesh R, More CB. Age estimation in Western Indian population by Cameriere's and Drusini's methods. *J Oral Maxillofac Pathol.* 2022;26(1):116-20.
108. Shan W, Sun Y, Hu L, Qiu J, Huo M, Zhang Z, *et al.* Boosting algorithm improves the accuracy of juvenile forensic dental age estimation in Southern China population. *Sci Rep.* 2022;12(1):15649.
109. Sharifonnasabi F, Jhanjhi NZ, John J, Obeidy P, Band SS, Alinejad-Rokny H, *et al.* Hybrid HCNN-KNN model enhances age estimation accuracy in orthopantomography. *Front Public Health.* 2022;10:879418.
110. Shen S, Yuan X, Wang J, Fan L, Zhao J, Tao J. Evaluation of a machine learning algorithms for predicting the dental age of adolescent based on different preprocessing methods. *Front Public Health.* 2022;10:1068253.
111. Wang J, Fan L, Shen S, Sui M, Zhou J, Yuan X, *et al.* Comparative assessment of the Willems dental age estimation methods: a Chinese population-based radiographic study. *BMC Oral Health.* 2022;22(1):373.
112. Wang X, Liu Y, Miao X, Chen Y, Cao X, Zhang Y, *et al.* DENSEN: a convolutional neural network for estimating chronological ages from panoramic radiographs. *BMC Bioinformatics.* 2022;23(Suppl 3):426.
113. Zaborowicz K, Garbowski T, Biedziak B, Zaborowicz M. Robust estimation of the chronological age of children and adolescents using tooth geometry indicators and POD-GP. *Int J Environ Res Public Health.* 2022;19(5):2952.
114. Abdul Rahim AH, Davies JA, Liversidge HM. Reliability and limitations of permanent tooth staging techniques. *Forensic Sci Int.* 2023;346:111654.
115. AlOtaibi NN, AlQahtani SJ. Performance of different dental age estimation methods on Saudi children. *J Forensic Odontostomatol.* 2023;41(1):27-46.
116. Bjørk MB, Kvaal SI, Bleka Ø, Sakinis T, Tuvnes FA, Haugland MA, *et al.* Age prediction in sub-adults based on MRI segmentation of 3rd molar tissue volumes. *Int J Legal Med.* 2023;137(3):753-63.
117. Bui R, Iozzino R, Richert R, Roy P, Bousset L, Tafrount C, *et al.* Artificial intelligence as a decision-making tool in forensic dentistry: a pilot study with I3M. *Int J Environ Res Public Health.* 2023;20(5):4620.
118. El-Desouky SS, Kabbash IA. Age estimation of children based on open apex measurement in the developing permanent dentition: an Egyptian formula. *Clin Oral Investig.* 2023;27(4):1529-39.
119. Kim YR, Choi JH, Ko J, Jung YJ, Kim B, Nam SH, *et al.* Age group classification of dental radiography without precise age information using convolutional neural networks. *Healthcare (Basel).* 2023;11(8):1068.
120. Kuhnen B, Fernandes C, Barros F, Scarso Filho J, Gonçalves M, Serra MDC. Chronology of permanent teeth mineralization in Brazilian individuals: age estimation tables. *BMC Oral Health.* 2023;23(1):165.
121. Kumagai A, Jeong S, Kim D, Kong HJ, Oh S, Lee SS. Validation of data mining models by comparing with conventional methods for dental age estimation in Korean juveniles and young adults. *Sci Rep.* 2023;13(1):726.
122. Kwon K, Pan J, Guo Y, Ren Q, Yang Z, Tao J, *et al.* Demirjian method and Willems method to study the dental age of adolescents in Shanghai before and after 10 years. *Folia Morphol (Warsz).* 2023;82(2):346-58.
123. Lopatin O, Barszcz M, Wozniak KJ. Skeletal and dental age estimation via postmortem computed tomography in Polish subadults group. *Int J Legal Med.* 2023;137(4):1147-59.
124. Merdietio Boedi R, Shepherd S, Oscandar F, Mânica S, Franco A. 3D segmentation of dental crown for volumetric age estimation with CBCT imaging. *Int J Legal Med.* 2023;137(1):123-30.
125. Sharma S, Karjodkar F, Sansare K, Mehra A, Sharma A, Saalim M. Age estimation using the tooth coronal index on mandibular first premolars on digital panoramic radiographs in an Indian population. *Front Dent.* 2023;20(6):1-7.
126. Timme M, Viktorov J, Steffens L, Streeter A, Karch A, Schmeling A. Third molar eruption in orthopantomograms as a feature for forensic age assessment—a comparison study of different classification systems. *Int J Legal Med.* 2023;137(3):765-72.
127. Topal BG, Tanrikulu A. Assessment of permanent teeth development in children with multiple persistent primary teeth. *J Clin Pediatr Dent.* 2023;47(2):50-7.
128. Vangala RM, Loshali A, Basa KS, Ch G, Masthan S, Ganachari BC, *et al.* Validation of radiographic visibility of root pulp in mandibular first, second and third molars in the prediction of 21 years in a sample of South Indian population: a digital panoramic radiographic study. *J Forensic Odontostomatol.* 2023;41(1):47-56.
129. Wang J, Dou J, Han J, Li G, Tao J. A population-based study to assess two convolutional neural networks for dental age estimation. *BMC Oral Health.* 2023;23(1):109.
130. Ye X, Jiang F, Sheng X, Huang H, Shen X. Dental age assessment in 7-14-year-old Chinese children: comparison of Demirjian and Willems methods. *Forensic Sci Int.* 2014;244:36-41.

Modern Trends in Oral Biology Research

Aetas Amponnawarat¹

¹Department of Family and Community Dentistry, Faculty of Dentistry, Chiang Mai University, Thailand

To the Editor:

Within mainstream oral biology, research is predominantly focused on the study of dental caries and periodontal diseases which are primarily influenced by complex interactions among oral microbes and between oral microbes and the host, respectively. Moreover, the maintenance of a homeostatic balance between oral microbes and host responses is of utmost importance for the preservation of both oral and systemic health due to their intricate comorbidities. A recent article review by Hajishengallis *et al.*⁽¹⁾, and Hajishengallis G⁽²⁾ meticulously explained these associations.

In the Cariology field, it has now become more evident that the complex interplay among the bacterial community as well as the inter-species interaction between fungi and bacteria have contributed significantly to the pathogenesis and severity of dental caries.^(3,4) It was previously believed that diverse microbial species within the oral cavity randomly established their habitats. However, recent evidence has demonstrated that the disease-causing microbial community, in fact, exhibits a unique and organized spatial structure where *Streptococcus mutans* aggregate as an inner core and are surrounded by other bacterial or fungal species. These corona-like arrangements not only aid in disease-causing processes for microbial communities but also protect from potentially harsh environments.⁽¹⁾

S. mutans is a keystone cariogenic bacterium that has been clinically associated with dental caries. Other bacterial species including *Streptococcus gordonii* and *Streptococcus oralis* have also been shown to contribute to disease progress and severity. However, a more recent report⁽⁴⁾ analyzed comprehensive taxonomic association in metagenomics and metatranscriptomics data obtained from the supragingival plaque of 300 children, and discovered several new bacterial species with strong association with dental caries. The leading species were *Selenomonas sputigena*, *Prevotella salivae*, and *Leptotrichia wadei*. Among these bacteria, *S. sputigena* is a flagellated anaerobic bacterium found in subgingival microbiota and has no prior reports on the involvement in dental caries biofilm. This study demonstrated, for the first time, the unrecognized role of *S. sputigena* in dental caries pathogenesis which involves an interaction with *S. mutans* as a pathobiont that enhances biofilm virulence, thus exacerbating dental caries severity *in vivo*.⁽⁴⁾

The research into dental caries management and prevention has progressively advanced to date. The studies cover a range of topics from enhancing the efficacy of existing methods to developing entirely new strategies. Fluoride application has been widely acknowledged as an effective prevention for dental caries. For example, stannous fluoride (SnF₂) is a commonly used anticaries agent due to its antibacterial and antibiofilm activities. However, one major limitation of SnF₂ is that it is susceptible to degradation in aqueous solution requiring chemical additives which, in turn, reduce the fluoride bioavailability. Ferumoxytol is a Food and Drug Administration (FDA)-approved iron oxide nanoparticle solution used for the treat-



Editor:
Anak Iamaroon,
Chiang Mai University, Thailand.

Received: December 11, 2023
Revised: December 13, 2023
Accepted: December 18, 2023

Corresponding Author:
Dr. Aetas Amponnawarat,
Department of Family and Community
Dentistry, Faculty of Dentistry,
Chiang Mai University, Chiang Mai
50200, Thailand.
E-mail: aetas.a@cmu.ac.th

ment of iron deficiency. Interestingly, Ferumoxytol has recently been shown to effectively eradicate cariogenic biofilm from tooth surfaces *in vitro* and *in vivo*. While Ferumoxytol is a very promising antibiofilm agent, it does not prevent or revert the demineralization process on tooth enamel. Surprisingly, a recent finding by Huang *et al.*⁽⁵⁾ discovered a notable synergistic effect of SnF₂ and Ferumoxytol where a progression of dental caries is completely immobilized following the use of SnF₂ and Ferumoxytol combination. The authors revealed that the combination helps stabilize the SnF₂ as well as enhance enamel resistance against the demineralization process without affecting oral microbiota or other surrounding tissues.⁽⁵⁾ Nevertheless, the removal of biofilm in extremely small or hard-to-reach areas remains challenging due to their inaccessibility. Microrobotics which operates at scales from micrometers to millimeters has recently been designed for biofilm removal in such areas. Microrobotics is a highly advanced and efficient technology that enables precise control and navigation of microrobots to the biofilm-infected site. These microrobots are equipped with magnetic nanoparticles called ferrofluids, which can be manipulated to provide physical disruption of the biofilm.^(6,7) Furthermore, microrobotics also allows for the delivery of catalytic nanoparticles known as nanozymes, which can further enhance antimicrobial activity chemically.^(7,8) This groundbreaking technology has the potential to improve the standard of care for biofilm-related infections.

Periodontology, on the other hand, is driven by the collective interconnections between polymicrobial dysbiosis and exaggerated host inflammatory responses. Whether the dysbiotic microbiome caused periodontal inflammation or if the breakdown of periodontal tissues favored pathogenic microbes leading to dysbiosis, is controversial. However, findings by Payne *et al.*⁽⁹⁾ demonstrated using mouse models of vertical and horizontal transmissions of dysbiotic microbiome that a dysbiotic microbiome precedes periodontal disease. Further corroborating this notion, a recent report showed that bacteria exploiting the altered environment to flourish do not necessarily exacerbate the disease. According to Chipashvili *et al.*,⁽¹⁰⁾ the epibiont species *Saccharibacteria*, which is commonly found in the microbiome of periodontitis patients, thrives in an inflammatory environment. However, this bacterium offers protection to the mammalian host by

reducing the pathogenicity of other bacteria in the vicinity, thereby reducing inflammatory alveolar bone loss.

While the current therapeutic strategy for periodontitis emphasizes the physical and chemical removal of bacterial plaque, numerous reports on immunomodulation are emerging. Complement activation has long been implicated in periodontitis and it is believed that targeting complement activation could ameliorate periodontal disease severity.^(11,12) Remarkably, a myriad of complement-targeting inhibitors has been investigated in clinical trials. Among these, a C3-targeting compound known as AMY-101 was investigated in a phase II clinical trial and showed sustainable resolution of gingival inflammation in patients with periodontal inflammation.⁽¹³⁾ This study suggests that using immunomodulation as an adjunct to traditional periodontal treatment is a promising strategy.

Oral biology research has made notable strides in recent years. In addition to cariology and periodontology, various other oral biology disciplines have also made substantial progress in the field. These advancements can broaden our perspectives not only in terms of research methodology, but also in how discoveries are made. Nonetheless, the ultimate goal remains to enhance our understanding of oral health and diseases, which can pave the way for improved prevention, diagnosis, and treatment strategies.

References

1. Hajishengallis G, Lamont RJ, Koo H. Oral polymicrobial communities: assembly, function, and impact on diseases. *Cell Host Microbe*. 2023;31(4):528-38.
2. Hajishengallis G. Interconnection of periodontal disease and comorbidities: Evidence, mechanisms, and implications. *Periodontol* 2000. 2022;89(1):9-18.
3. Sadiq FA, Burmølle M, Heyndrickx M, Flint S, Lu W, Chen W, *et al.* Community-wide changes reflecting bacterial interspecific interactions in multispecies biofilms. *Crit Rev Microbiol*. 2021;47(3):338-58.
4. Cho H, Ren Z, Divaris K, Roach J, Lin BM, Liu C, *et al.* *Selenomonas sputigena* acts as a pathobiont mediating spatial structure and biofilm virulence in early childhood caries. *Nat Commun*. 2023;14(1):2919.
5. Huang Y, Liu Y, Pandey NK, Shah S, Simon-Soro A, Hsu JC, *et al.* Iron oxide nanozymes stabilize stannous fluoride for targeted biofilm killing and synergistic oral disease prevention. *Nat Commun*. 2023;14(1):6087.
6. Hwang G, Paula AJ, Hunter EE, Liu Y, Babeer A, Karabucak B, *et al.* Catalytic antimicrobial robots for biofilm eradication. *Sci Robot*. 2019;4(29).

7. Tran HH, Watkins A, Oh MJ, Babeer A, Schaer TP, Steager E, *et al.* Targeting biofilm infections in humans using small scale robotics. *Trends Biotechnol.* Forthcoming 2024.
8. Oh MJ, Yoon S, Babeer A, Liu Y, Ren Z, Xiang Z, *et al.* Nanozyme-based robotics approach for targeting fungal infection. *Adv Mater.* 2023:e2300320.
9. Payne MA, Hashim A, Alsam A, Joseph S, Aduse-Opoku J, Wade WG, *et al.* Horizontal and vertical transfer of oral microbial dysbiosis and periodontal disease. *J Dent Res.* 2019;98(13):1503-10.
10. Chipashvili O, Utter DR, Bedree JK, Ma Y, Schulte F, Mascarin G, *et al.* Episymbiotic *Saccharibacteria* suppresses gingival inflammation and bone loss in mice through host bacterial modulation. *Cell Host Microbe.* 2021;29(11):1649-62. e7.
11. Mastellos DC, Hajishengallis G, Lambris JD. A guide to complement biology, pathology and therapeutic opportunity. *Nat Rev Immunol.* Forthcoming 2024.
12. Wang H, Ideguchi H, Kajikawa T, Mastellos DC, Lambris JD, Hajishengallis G. Complement is required for microbe-driven Induction of Th17 and periodontitis. *J Immunol.* 2022;209(7):1370-8.
13. Hasturk H, Hajishengallis G, Lambris JD, Mastellos DC, Yancopoulou D. Phase IIa clinical trial of complement C3 inhibitor AMY-101 in adults with periodontal inflammation. *J Clin Invest.* 2021;131(23).